ANALYSIS FOR DESIGN OF EHV AND UHV 3-PHASE AND 6-PHASE LINES BASED ON ELECTROSTATIC FIELD, AUDIBLE NOISE AND RADIO NOISE

A thesis submitted

in Partial Fulfilment of the Requirements

for the degree of

MASTER OF TECHNOLOGY

by

J. SENTHIL

to the

DEPARTMENT OF ELECTRICAL ENGINEERING
INDIAN INSTITUTE OF TECHNOLOGY, KANPUR

JUNE, 1984

To my

Parents

CERTIFICATE

This work entitled 'ANALYSIS FOR DESIGN OF EHV AND UHV 3-PHASE AND 6-PHASE LINES BASED ON ELECTROSTATIC FIELD, AUDIBLE NOISE AND RADIO NOISE' by Shri J. Senthil has been carried out under our supervision and this has not been submitted elsewhere for a degree.

Dr. Ravindra Arora
Assistant Professor

Dr. Rakosh Das Begamudre
Visiting Professor

Department of Electrical Engineering
Indian Institute of Technology
Kanpur 208016.

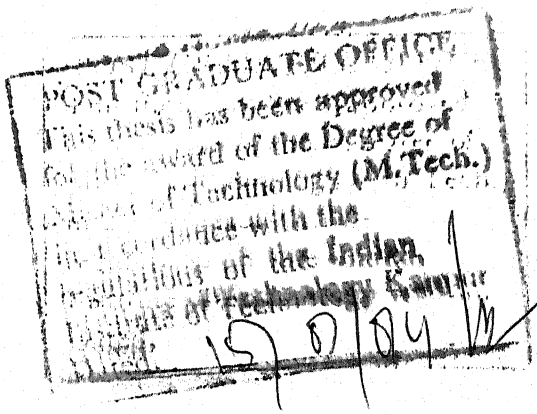

ACKNOWLEDGEMENTS

I wish to take this opportunity to express my deepest sense of gratitude to my thesis supervisors Dr. Rakosh Das Begamudre and Dr. Ravindra Arora who initiated me into the problem and provided the necessary guidance for carrying out the work. Without their help, this project would never have reached a completion.

I am grateful to Professor L.P. Singh for his constant encouragement during the course of this work. To Dr. Sachchidanand I am very much indebted for his advice, his suggestions and for his readiness to help me.

I am extremely thankful to Ashish and Bharati for their help in bringing the thesis to its final shape. To my other classmates, Sanjiv, Pradeep and Khairul, I am highly obliged for their cooperation rendered to me at all stages of the work.

Finally, a special word of thanks to my friend Shri Nalini Kant Ratha, for his help and encouragement throughout my stay at I.I.T. Kanpur and to Mr. C.M. Abraham for his efficient typing.

SENTHIL
JUNE, 1984

CONTENTS

LIST OF FIGURES

LIST OF TABLES

ABSTRACT

High voltages in the EHV and UHV ranges are being adopted for transmitting power over long distances. The impact of such high voltages on the environment are the strong electrostatic (ES) field, Audible Noise (AN) and Radio Noise (RN) interferences. In this thesis, lateral profiles of ES field, AN and RN have been calculated for transmission lines of voltages ranging from 400 kV to 1300 kV. Both single and multi-circuit lines have been considered. Advantage of adopting a 400 kV, 4-circuit configuration for India, instead of the proposed 750 kV configuration has been pointed out. Empirical relations for predicting the maximum electrostatic ground gradients have been suggested. Method of extrapolation of 1-phase AN test results to 3-phase case has been indicated.

CHAPTER 1

INTRODUCTION

1.1 GENERAL

With the increasing demand for transmitting large amount of power over long distances, transmission voltages in the EHV and UHV levels are being adopted. Some of the important impacts of such high voltages on the environment are, corona effects and high electrostatic (ES) fields in the space surrounding the lines. The two principal corona effects that have been considered in this thesis are, the audible noise (AN) and the radio interference (RI). The quality of radio-reception, especially in the amplitude modulated broadcast frequency range, in the vicinity of a transmission line is greatly influenced by the corona generated RI. The ES field which surrounds a high voltage line may have adverse effects on living organisms and hence design consideration for EHV and UHV lines should, in addition to the AN and RI limits take into effect the ES field effects also.

Limits for AN are specified depending on the subjective analysis of annoyance experienced, while those of RI depends on the desired quality of radio reception. Limits for the ES fields are specified from the point of view of safety considera tions for living organisms in the vicinity of transmission

lines. However, in order to specify the limits, lateral profiles of AN, RI and the ES field must be known.

In this thesis, an attempt is made to calculate the AN, RI and ES field with respect to the lateral distance from the center of the tower for transmission lines of voltages ranging from 400 kV to 1300 kV. Both single and multi-circuit lines have been considered.Audible noise profile has been computed using the empirical relation of Bonneville Power Administration (BPA) [10], while that of RI has been computed using the CIGRE formula [19] and the excitation function for the EHV and UHV lines respectively. Calculations for the ES fields have been done by applying the Gauss's theorem.

1.2 OUTLINE OF THE THESIS

The chapterwise summary of the thesis is as follows :

i) Chapter 2 deals with the ES field calculations. Nature of the variation of horizontal, vertical and the total component of the field intensity have been shown against the normalised horizontal distance from the tower centre (horizontal distance/ line height). The possibility of using a 400 kV, 4-circuit configuration instead of one single circuit 750 kV line for India has been explored.

ii) The transmission line audible noise profiles at ground levels have been calculated in Chapter 3. Method of extending

CHAPTER 2

ELECTROSTATIC FIELDS

With the advent of long distance transmission, high voltages in the EHV and UHV ranges are being adopted. Electric fields under such high voltage transmission lines can have adverse effects on living organisms (including humans).

In this chapter, electric field intensities of transmission lines of voltages ranging from 138 kV to 1300 kV have been calculated. Both single as well as multi-circuit lines have been considered. Results of these calculations have been shown graphically. Dimensions of the different lines, for which the electric field intensities have been calculated, are given in the form of a table. Limits for these fields have also been specified from the safety considerations to living organisms such as plants, human beings and animals.

2.1 SIGNIFICANCE OF ELECTROSTATIC (ES) FIELD

The power handling capacity for ac lines is inversely proportional to the line length and directly proportional to the square of the line-to-line voltage. Hence, for long distance power transmission, transmission voltages in the EHV and UHV ranges are preferred.

It is well known that strong electric fields are set up in the space surrounding a high voltage line and such fields

may have adverse biological effects on living organisms. Before any investigations can be carried out into such biological effects, the nature of the electric fields created by these high voltage EHV and UHV lines will have to be determined. This includes the determination of the lateral profile of the maximum Horizontal, Vertical and Total components of the voltage gradient at ground level and also at an elevation from the ground. A large number of meters for measuring the ES field are available, but these can be used only after a line is built and not at the design stage.

2.2 LIMITS FOR ELECTROSTATIC FIELDS

The effects of high ES field due to the EHV and UHV line is important on (a) plant life (b) animals (c) humans and (d) vehicles. For investigating the dangers present due to the high ES fields, the objects, on which the investigations are to be carried out, will have to be placed under the line. However, the introduction of the object modifies the field. In order to provide some standardization in the reporting procedure, EPRI has specified that the reported field intensities in these studies should be the undisturbed field strength [4]; that is, the uniform field strength prior to the introduction of any object.

(a) Plant Life :

Investigations into the effects of ES fields is of

importance to plants such as wheat, rice or sugarcane which have sharp pointed upper parts.

Sharp edges of wheat go into corona when exposed to undisturbed field greater than 20 kV/m (RMS) [5,6]. The resistive current which flows leads to the death of a layer of cells. Corona gives Ozone and N_2O as by-products which damages the grain-bearing parts.

Below 20 kV/m, the plant is unaffected. Hence, for plants which have sharp pointed upper parts, this can be taken as the limiting value. Rounded, blunt or fleshy parts are not damaged even when exposed to 50 kV/m for several days.

(b) Birds and Animals :

It has been reported in [5] that the growth of hens and pigeons gets affected when exposed to fields of 30 kV/m because of enormous spillage of grains when picking with their beaks.

(c) Human Beings :

With a normal human impedance to ground of 1500 ohms, the limits of let-go currents of 9 mA is not exceeded even when exposed to ground-level gradients of 12 kV/m. However, it has been reported in [4] that ground gradients greater than 15 kV/m causes unpleasant sensation for majority of cases.

(d) Vehicles :

Rubber tyres being good insulators, vehicles parked under a live line act as a capacitance to ground and accumulates electric charge. When a human being comes in contact with the metallic chassis, the capacitor discharges and the discharge current through the body may exceed the let-go value. Apart from shock, the other hazard is due to the ignition of fuel vapors. The severity of these problems depends on the size of the vehicle and its proximity to the lines. Grounding strips are used to reduce this hazard.

2.3 METHOD OF CALCULATION

The calculation of the electric field intensity is done in two stages :

(1) Calculation of charges per unit length.

(2) Calculation of electric field produced by these charges.

2.3.1 Calculation of Charges per Unit Length

The first step in the calculation of charges per unit length is the determination of the matrix of potential coefficients [P] defined in equation (2.1),

$$[V] = [P]\,[Q]/2\pi\epsilon_o \qquad (2.1)$$

[Q] is the column matrix of the charge per unit length.

[V] is the column matrix of the complex potential of each phase, in the case of ground wires, potential V = 0.

ϵ_o is the permittivity of free space equal to 8.854×10^{-12} farads/meter.

The elements of [P] can be obtained by using the theory of images with reference to a perfectly conducting earth plane.

For bundle conductors, which are used in EHV and UHV lines to reduce the conductor surface voltage gradient, the bundle is represented by an equivalent conductor with radius γ_{eq} given by;

$$\gamma_{eq} = R \times (nxr/R)^{1/n} \qquad (2.2)$$

where

r = Radius of subconductor

R - Radius of the bundle

n - number of subconductors in a bundle.

The matrix [P] for an N-conductor configuration can be written as ;

$$[P] = \begin{bmatrix} P(1,1) & \cdots & P(1,N) \\ \vdots & & \vdots \\ P(N,1) & \cdots & P(N,N) \end{bmatrix} \qquad (2.3)$$

The diagonal elements are ;

$$P(i,i) = \text{Log}_e[2y_i/(\gamma_{eq})_i] \qquad (2.4)$$

and the off-diagonal elements are

$$P(i,j) = P(j,i) = \text{Log}_e[D'_{ij}/D_{ij}] \qquad (2.5)$$

y_i - Height of ith conductor above the ground.

$(\gamma_{eq})_i$ - equivalent radius of the ith line-conductor.

D'_{ij} - Aerial distance between conductor i and the image of the jth conductor

D_{ij} - Distance between the conductor i and conductor j.

Once matrix P is evaluated, the charges per unit length can be found out by inverting P. The resulting equations are,

$$[Q]/2\pi\epsilon_o = [P]^{-1}\,[V] \qquad (2.6)$$

or

$$[Q]/2\pi\epsilon_o = [M]\,[V] \qquad (2.7)$$

where $[M] = [P]^{-1}$.

2.3.2 Calculation of Electric Field Intensity

The electric field intensity vector at a distance 'S' from a charge Q is from Gauss's theorem,

$$E = Q/(2\pi\epsilon_o s) \qquad (2.8)$$

Using the equation (2.8), the maximum Horizontal, Vertical and Total components of electric field can be calculated.

(a) Calculation of Horizontal Component

Figure 2.1 shows a conductor with a charge Q_i and its image with a charge $-Q_i$. Coordinates of the conductor are (x_i, y_i) and of its image are $(x_i, -y_i)$. The electric field E at a point (x,y) in space has been indicated in the figure figure 2.1.

If there are N-line conductors, the horizontal component of the field due to the ith conductor at the point (x,y) is ;

$$E_{Hi} = \frac{Q_i}{2\pi \epsilon_o} \left[\frac{x-x_i}{(x-x_i)^2+(y-y_i)^2} - \frac{x-x_i}{(x-x_i)^2+(y+y_i)^2}\right] \qquad (2.9)$$

The derivation of equation (2.9) is given in Appendix A.

Equation (2.9) can be written in a compact way as;

$$E_{Hi} = \frac{Q_i}{2\pi \epsilon_o} K_{Hi} \qquad (2.10a)$$

where

$$K_{Hi} = \left[\frac{x-x_i}{(x-x_i)^2+(y-y_i)^2} - \frac{x-x_i}{(x-x_i)^2+(y+y_i)^2}\right] \qquad (2.10b)$$

From equation (2.9) it can be seen that the horizontal component at ground level (y=o) is zero.

Substituting for $(Q_i/2\pi\epsilon_o)$ from equation (2.7) into equation (2.10a),

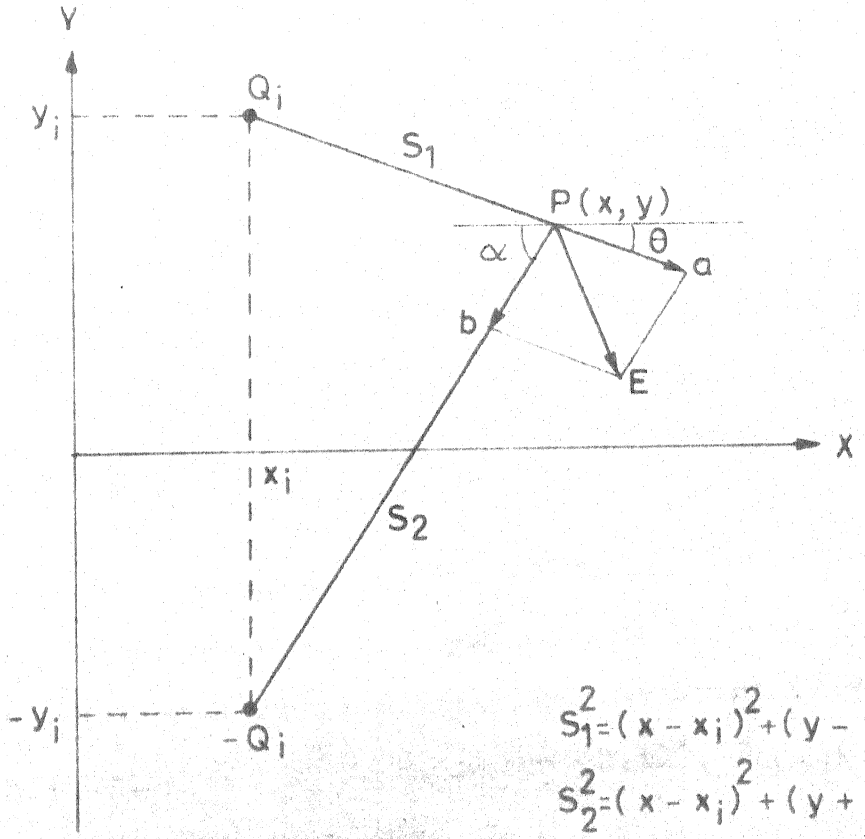

FIG. 2·1 DIAGRAM RELATED TO THE CALCULATI
OF FIELD UNDER A LINE

$$E_{Hi} = \sum_{j=1}^{N} M(i,j)\ V_j\ K_{Hi} \qquad (2.11)$$

Voltage V_j is the root mean square (rms) line to ground voltage of the jth conductor.

The horizontal component of the electric field at the point (x,y) due to all the N-conductors is ;

$$E_H = \sum_{i=1}^{N} E_{Hi} = \sum_{i=1}^{N}\sum_{j=1}^{N} M(i,j)\ V_j\ K_{Hi} \qquad (2.12)$$

Voltage V_j's are sinusoidal functions of time. Differentiating E_H with respect to θ (= ωt) and setting it equal to zero gives θ_{max} at which E_H becomes maximum at the point (x,y). Substituting this value of 'θ' in equation (2.12), E_{Hmax}, the maximum value of E_H can be obtained.

(b) Calculation of Vertical Component

Referring to Fig. 2.1, the vertical component of the electric field due to the ith conductor at the point (x,y) is,

$$E_{Vi} = \frac{Q_i}{2\pi\epsilon_o}\left[\frac{y-y_i}{(x-x_i)^2+(y-y_i)^2} - \frac{y+y_i}{(x-x_i)^2+(y+y_i)^2}\right] \qquad (2.13)$$

Derivation of equation (2.13) has been given in Appendix-A.

$$\text{Define } K_{vi} = \left[\frac{y-y_i}{(x-x_i)^2+(y-y_i)^2} - \frac{y+y_i}{(x-x_i)^2+(y-y_i)^2}\right]$$

Thus,

$$E_{vi} = \frac{Q_i}{2\pi\epsilon_o} K_{vi} \qquad (2.14)$$

Substituting equation (2.7) into equation (2.14) and taking summation for all N-conductors; the net vertical component is,

$$E_v = \sum_{i=1}^{N} E_{vi} = \sum_{i=1}^{N} \sum_{j=1}^{N} M(i,j)\ V_j\ K_{vi} \qquad (2.15)$$

Again differentiating E_v with respect to θ ($= \omega t$) and setting it equal to zero gives the value of θ at which E_v becomes maximum. Substituting this value of 'θ' in equation (2.15) gives E_{vmax}, the maximum value of E_v.

(c) Calculation of Total Component

The total component E_T due to all N-conductors at a given point is,

$$E_T^2 = E_H^2 + E_v^2 \qquad (2.16)$$

Substituting for E_H and E_v from equations (2.12) and (2.15) in equation (2.16),

$$E_T^2 = \left[\sum_{i=1}^{N} \sum_{j=1}^{N} M(i,j)\ V_j\ K_{Hi}\right]^2 + \left[\sum_{i=j}^{N} \sum_{j=1}^{N} M(i,j)\ V_j\ K_{vi}\right]^2 \qquad (2.17)$$

By a similar procedure as outlined above, E_{Tmax}, the maximum value of E_T can be found out.

Detailed derivations of E_{Hmax}, E_{Vmax} and E_{Tmax} for 3-phase

(single, double and four-circuit) lines and for 6-phase lines have been given in Appendices B,C and D respectively.

2.4 DIMENSIONS USED

The ac line geometries for which calculations were made are tabulated in Table I. The geometries have been classified as Types I,II, III or IV in correspondence with the configurations shown in Figure 2.2. The dimensions of the German four circuit line and that of the proposed Indian four-circuit line have been shown in Figure 2.3a, while the dimensions of the 138 kV, 6-phase configuration has been shown in Figure 2.3(b).

These dimensions have been collected by a study of the existing literature.

2.5 RESULTS

The results of the calculation of field intensity, based on the dimensions given in Table I, have been shown graphically.

Graphs indicating the nature of variation of E_{Hmax}, E_{Vmax} and E_{Tmax} with respect to normalised horizontal distance from tower centre (i.e., horizontal distance/line height), for ground level and also at an elevation of 4m from the ground have been shown in Figures 2.5 to 2.23. From these graphs, the maximum ground gradient for each line was noted these maximum ground gradient values have been indicated in Table II.

Data for calculations

CONFIGURATION			LINE VOLTAGE		CONDUCTOR GEOMETRY				LINE DIMENSION			
					n (1)	d (2)	BS (3)	BD (4)	D_1	D_2	H_1 (5)	H_2 (5)
S.no	Type	Line	Nominal kV	Max. kV		cm	cm	cm	m	m	m	m
1	I	Hydro-quebec	735	750	4	3·02	45·72		15·24		13·72	
2	I	Hydro-quebec	735	750	4	4·03	45·72		15·24		13·72	
3	I	Canada	1200	1200	6	4·63		120	18·0		21·0	
4	I	Canada	1200	1200	6	5·08		120	18·0		21·0	
5	I	Canada	1200	1200	8	4·14		120	18·0		21·0	
6	I	Canada	1200	1200	8	4·63		120	18·0		21·0	
7	I	Swedish	800	800	4	4·07	60		15·0		18·0	
8	I	Europe	765	765	4	3·8	45·6		13·0		12·0	
9	I	Europe	1000	1050	4	4·4	52·8		17·0		14·8	
10	I	Europe	1000	1050	4	4·7	56·4		17·0		14·8	
11	I	Europe	1000	1050	6	3·8	45·6		17·0		14·8	
12	I	Europe	1300	1300	4	5·2	62·4		20·5		17·3	
13	I	Europe	1300	1300	6	4·4	52·8		20·5		17·3	
14	I	Europe	1300	1300	8	3·8	45·6		20·5		17·3	
15	I	USSR	1150	1200	8	2·4	40		23·5		14·5	
16	I	USSR	1150	1200	8	2·4	40		23·5		18·5	
17	I	USSR	1150	1200	8	2·4	40		23·5		21·0	
18	II	BPA USA	1150	1200	8	4·1		107	24·0		26·0	44·0
19	I	UP	400	420	2	3·18	45·72		11·3		8·85	
20	IV	Bhakra beas	400	420	2	3·18	45·72		13·0		9·05	16·75
21	III	Andhra 2 circuit	400	420	2	3·18	45·72		7·7	14·5	9·0	18·24

NOTES:

1 n: Number of subconductors
2 d: Subconductor diameter
3 BS: Bundle spacing or subconductor spacing
4 BD: Bundle diameter
5 Clearances specified are the minimum line to ground clearances

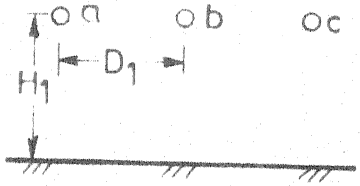

TYPE I

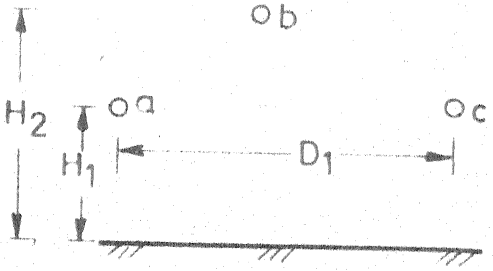

$D_2 = D_1/2$

TYPE II

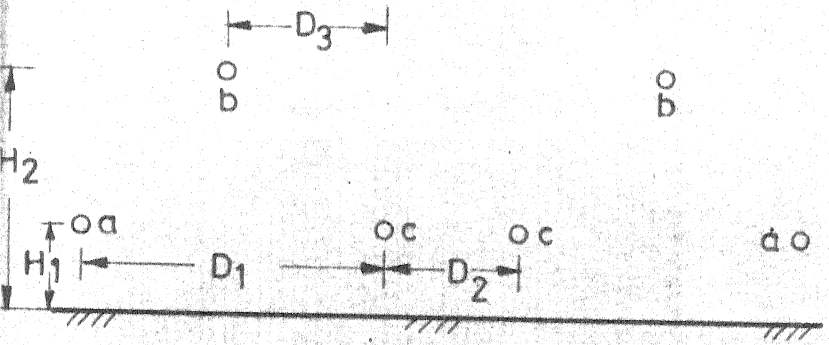

$D_3 = D_1/2$

TYPE III

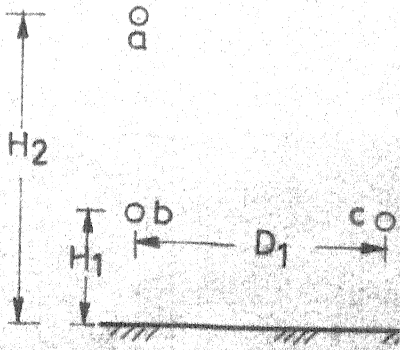

TYPE IV

FIG. 2-2 LINE CONFIGURATIONS REFERENCED BY TABLE I

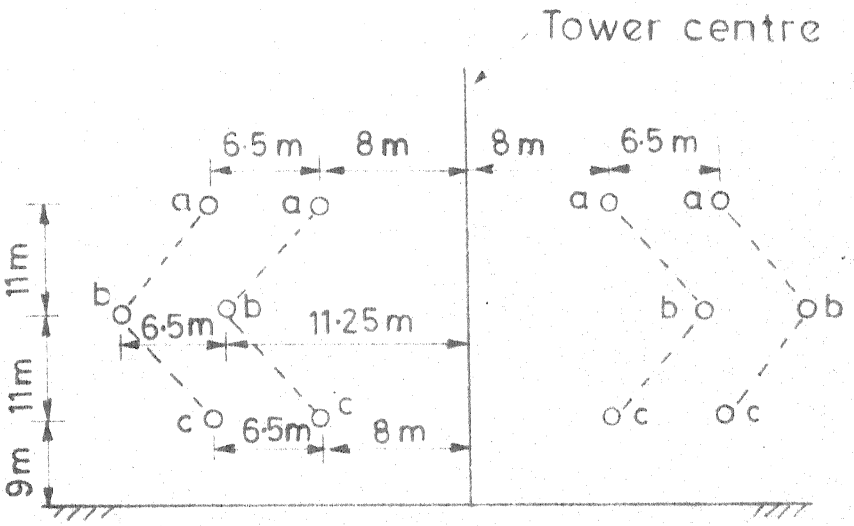

German 4 Circuit
n=4, d=2·17cm, BS=40cm

Indian 4-Circuit
n=2, d=3·18cm

BS=45·72 cm

n: no. of subconductors in a bundle

d: Subconductor diameter

BS: Subconductor spacing

(a) 400 kV, 4-Circuit configuration

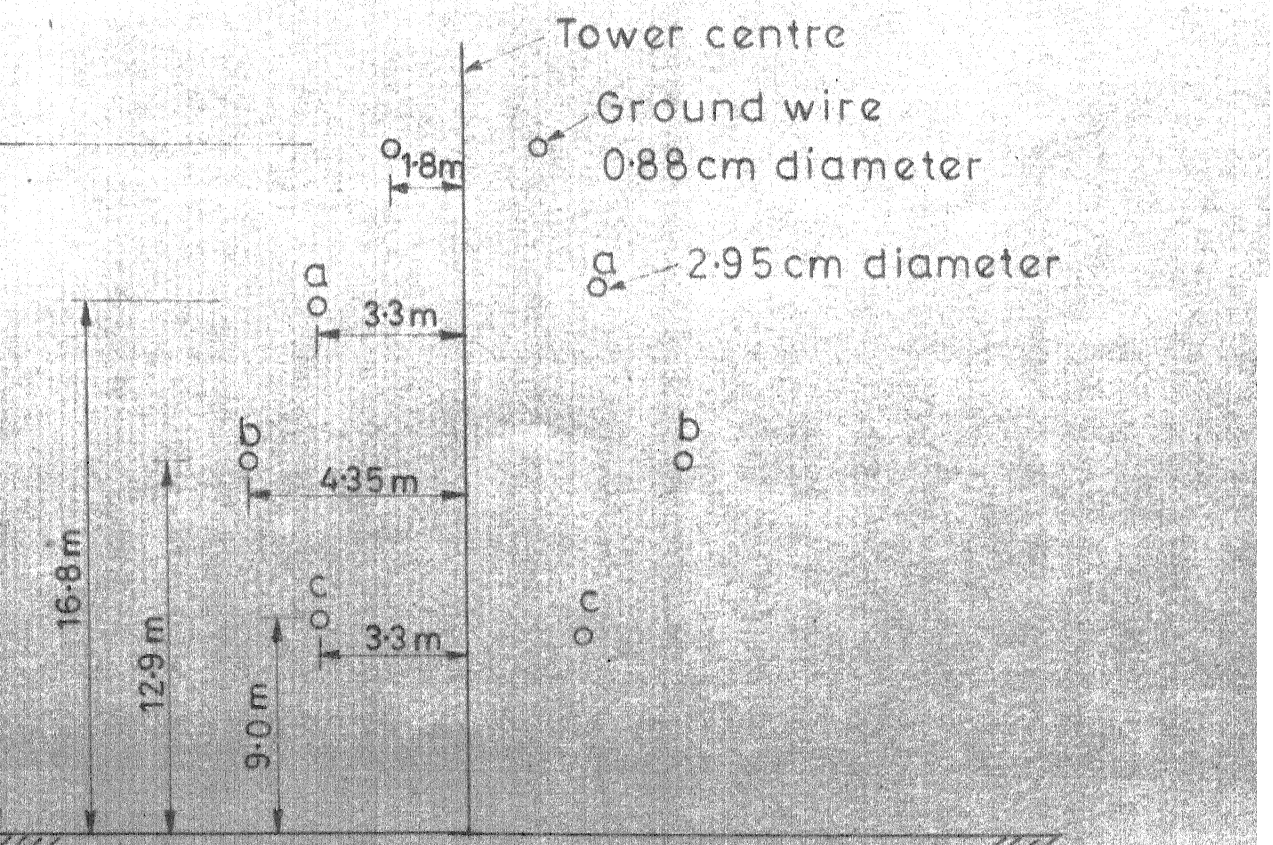

(b) 138 kV 6-Phase configuration

TABLE II

Maximum ground gradients

CONFIG.	138 kV			800 kV			400 kV			735-765kV			1000 kV			1200 kV			1300 kV		
	E_{Hmax}	E_{Vmax}	E_{Tmax}	E_{Hmax}	E_{Vmax}	E_{Tmax}	E_{Hmax}	E_{Vmax}	E_{Tmax}	E_{Hmax}	E_{Vmax}	E_{Tmax}	E_{Hmax}	E_{Vmax}	E_{Tmax}	E_{Hmax}	E_{Vmax}	E_{Tmax}	E_{Hmax}	E_{Vmax}	E_{Tmax}
6 Phase	0·0	3·6	3·6																		
[illegible] ckt																					
E-Type							0·0	7·2	7·2												
Double ckt							0·0	7·6	7·6												
4-ckt German							0·0	15·0	15·0												
4-ckt Indian							0·0	13·0	13·0												
				0·0	7·8	7·8	0·0	8·6	8·6	0·0	*10·6	10·6	0·0	14·2	14·2	0·0	11·0	11·0	0·0	15·2	15·2
Single ckt Horizontal Config.										0·0	*10·8	10·8	0·0	14·4	14·4	0·0	11·0	11·0	0·0	16·4	16·4
										0·0	**12·6	12·6	0·0	15·4	15·4	0·0	11·2	11·2	0·0	17·0	17·0
																0·0	11·2	11·2			
																0·0	20·0	20·0			
																0·0	14·2	14·2			
																0·0	11·6	11·6			
BPA Delta																0·0	9·0	9·0			

*735 kV **765 kV

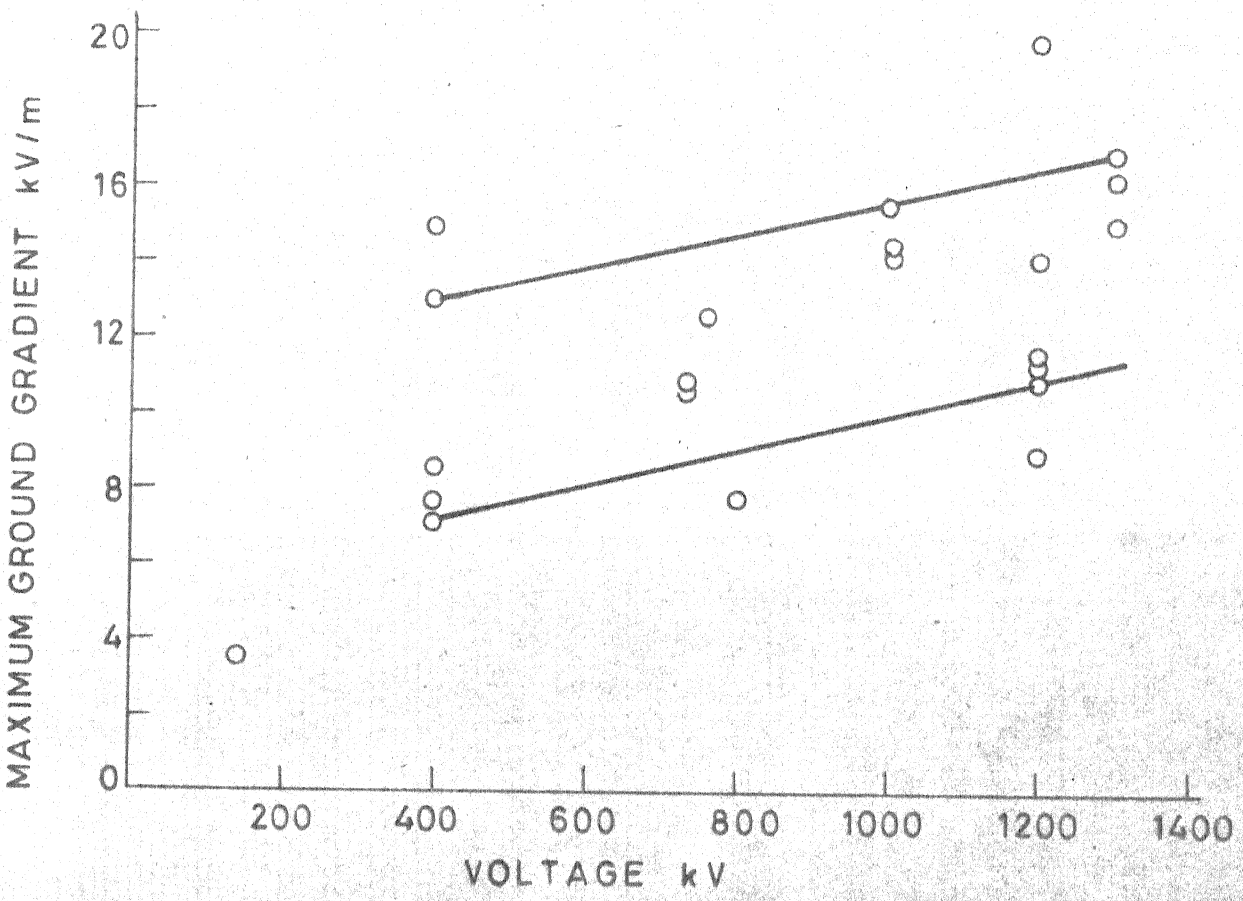

FIG. 2·4 MAXIMUM GROUND GRADIENTS AT DIFFERENT LINE VOLTAGES

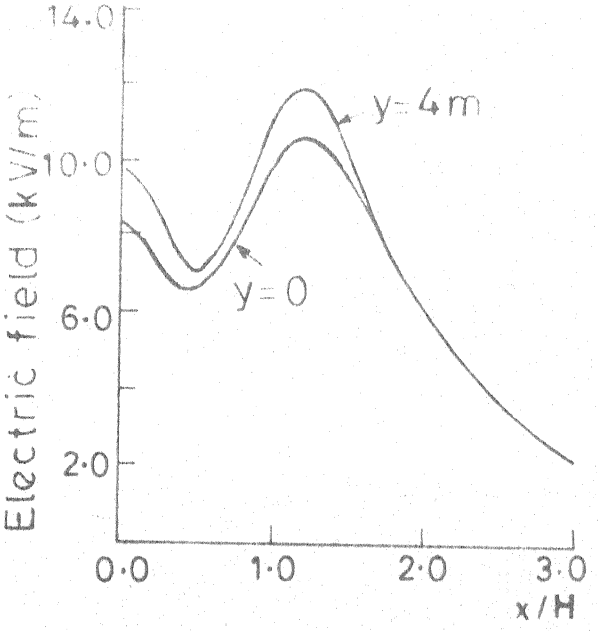

(a) Hydro-Quebec 735kV
4×0·0302m

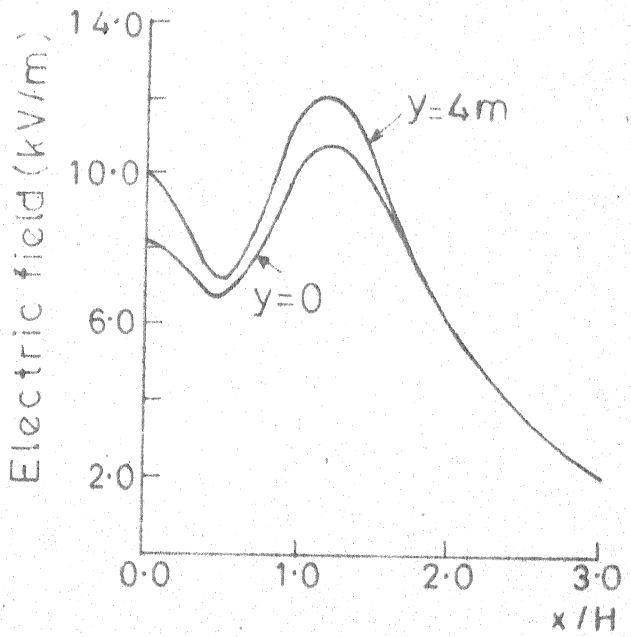

(b) Hydro-Quebec 735kV
4×0·0403m

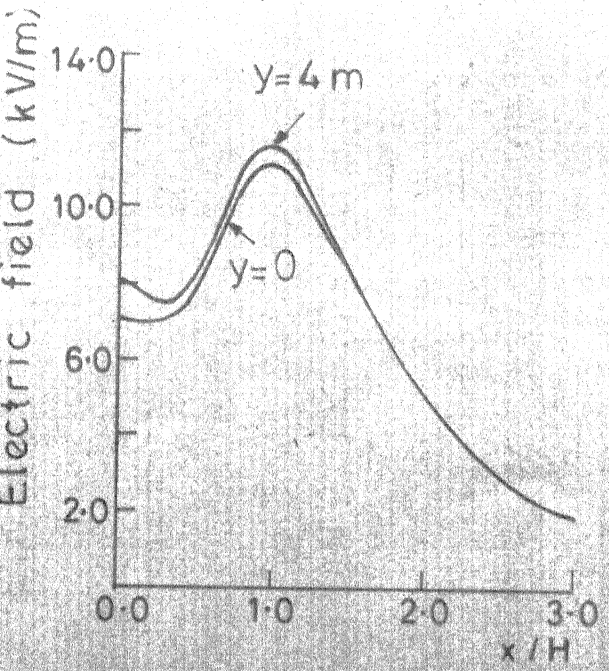

(c) Canadian 1200kV
6×0·0463m

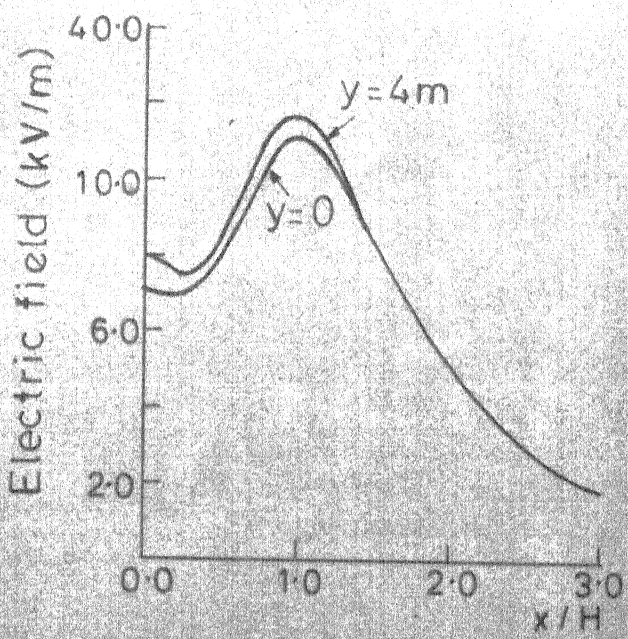

(d) Canadian 1200kV
6×0·058m

FIG·2·5 VERTICAL COMPONENT OF ES FIELD

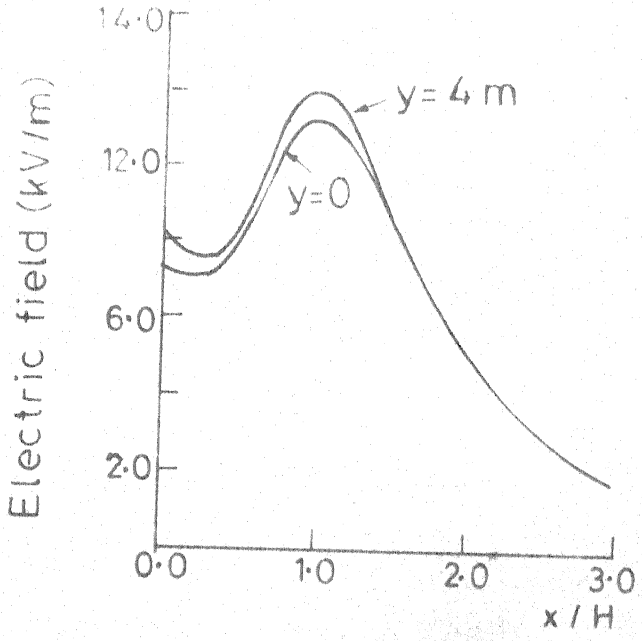

(a) Canadian 1200 kV
8×0·0414m

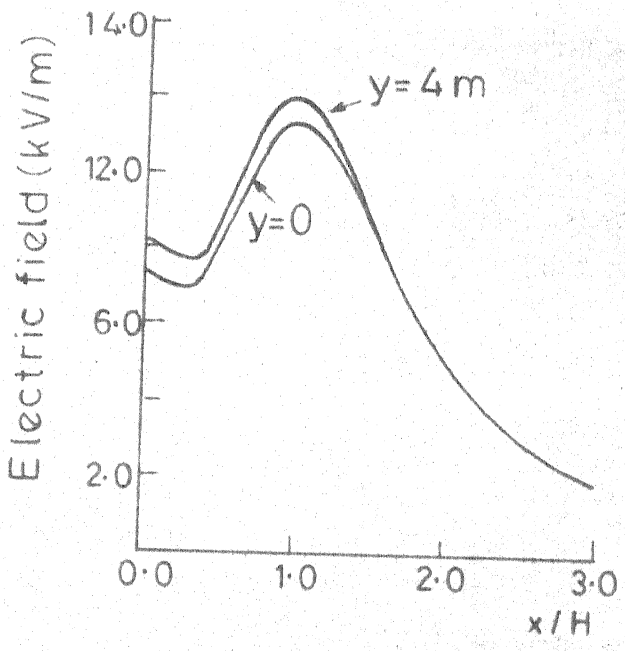

(b) Canadian 1200kV
8×0·0463m

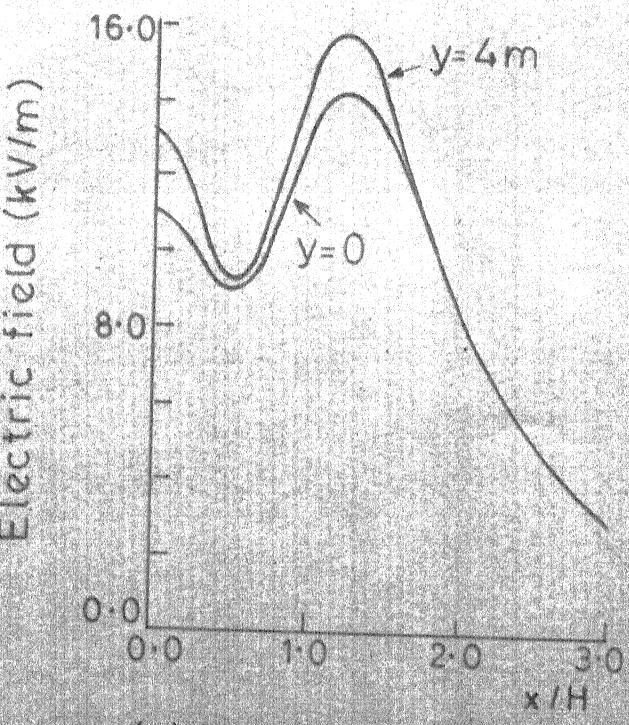

(c) Europian 1000kV
4×0·044m

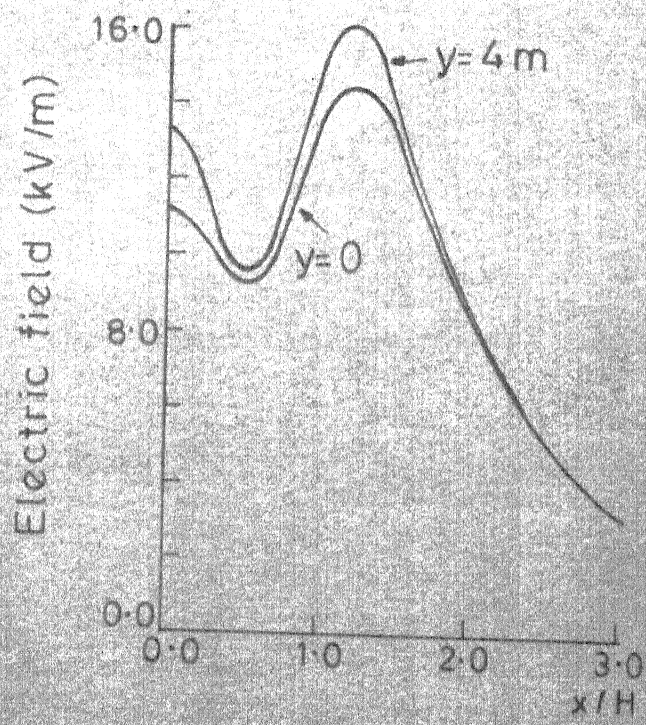

(d) Europian 1000 kV
4×0·047m

FIG·2·6 VERTICAL COMPONENT OF ES FIELD

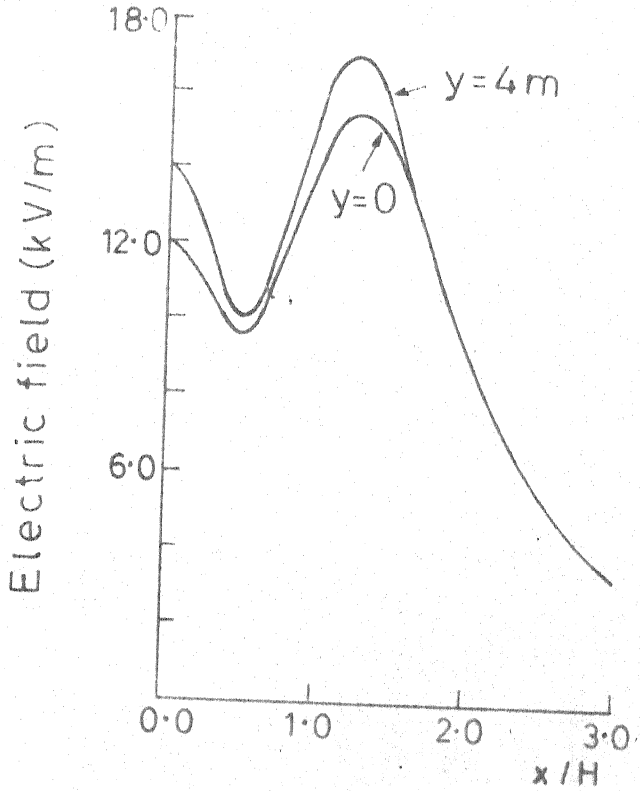

(a) Europian 1000 kV
6x0·038m

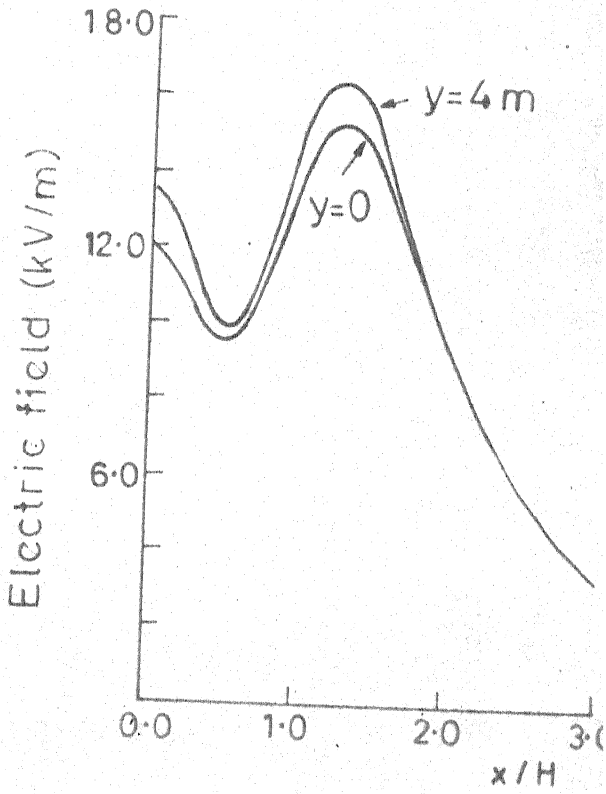

(b) Europian 1300 kV
4x0·052m

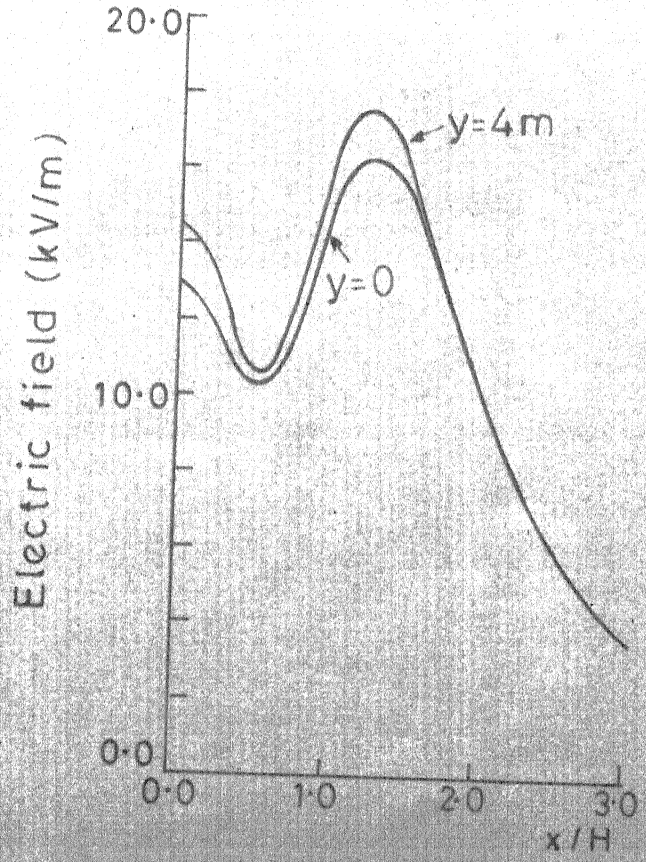

(c) Europian 1300 kV
6x0·0044m

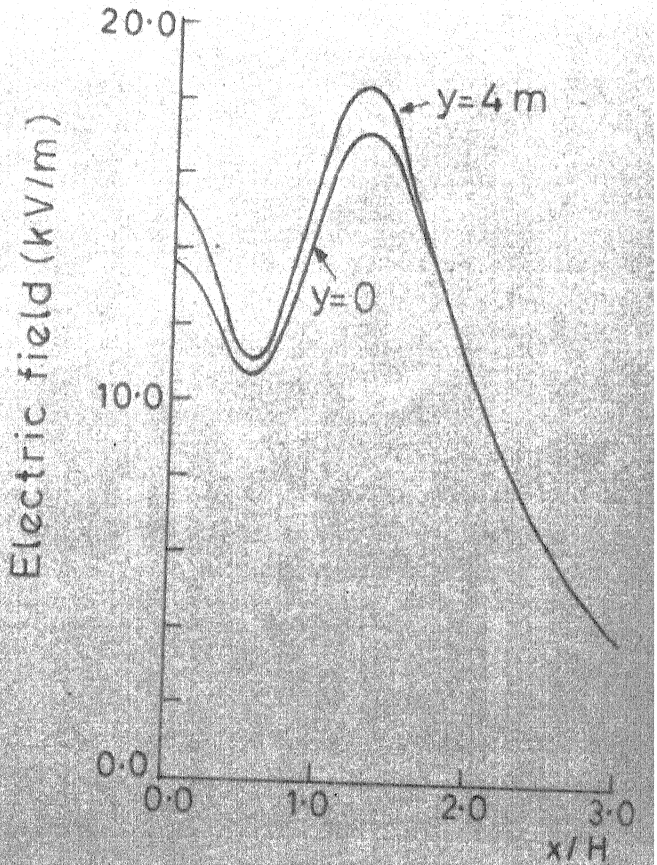

(d) Europian 1300 kV
8x0·038

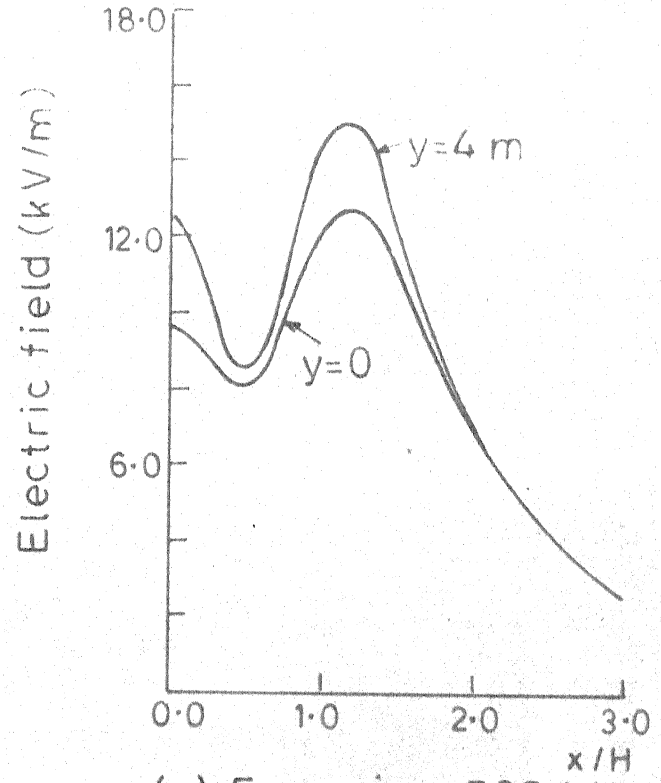

(a) Europian 765 kV

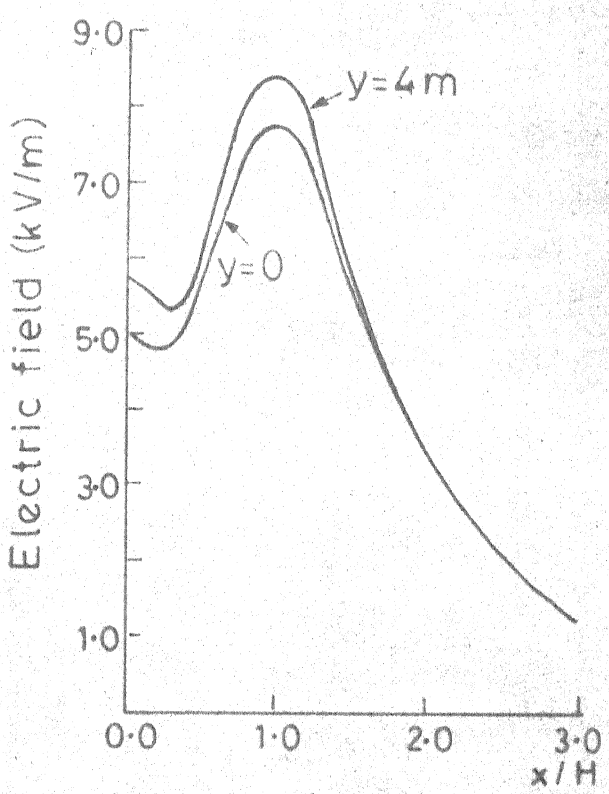

(b) Swedish 800 kV

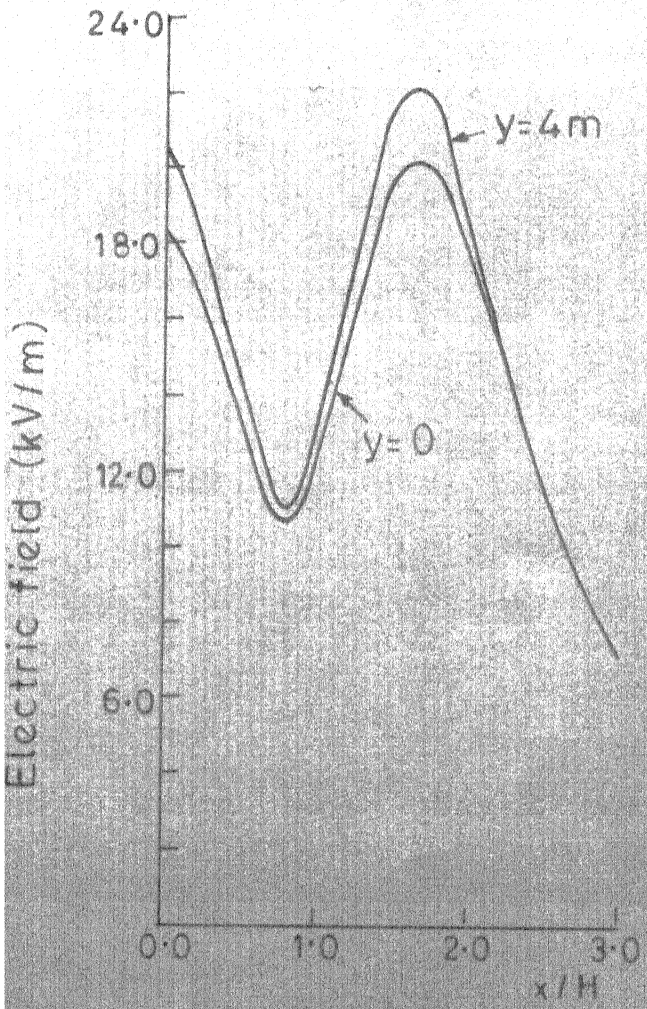

(c) USSR 1150 kV

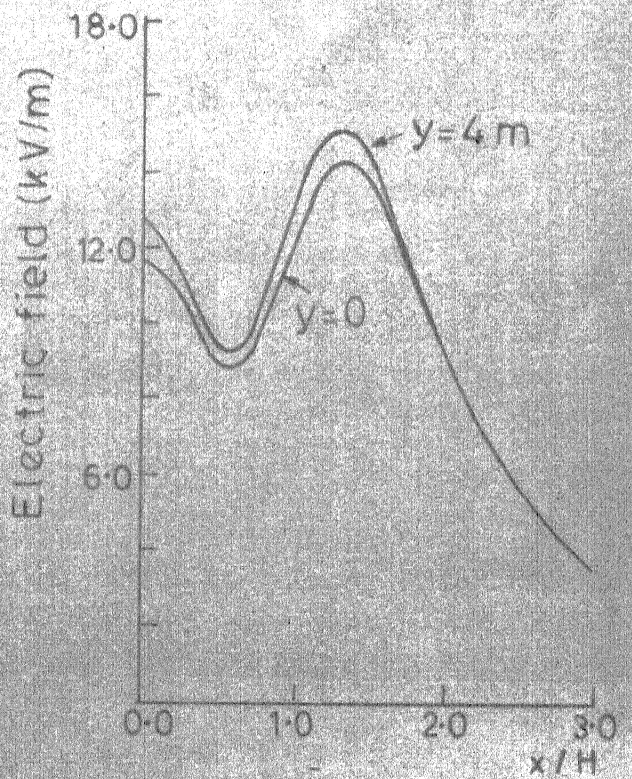

(d) USSR 1150 kV

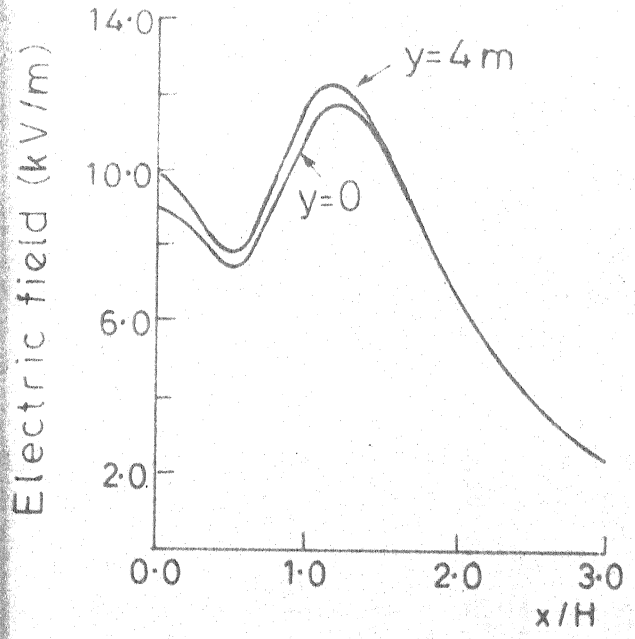

(a) USSR 1150 kV
21·0 m clearance

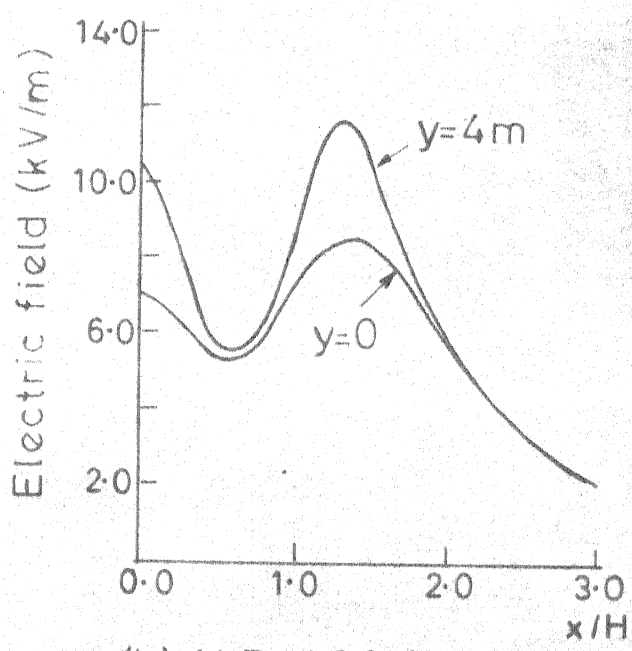

(b) U P 400 kV

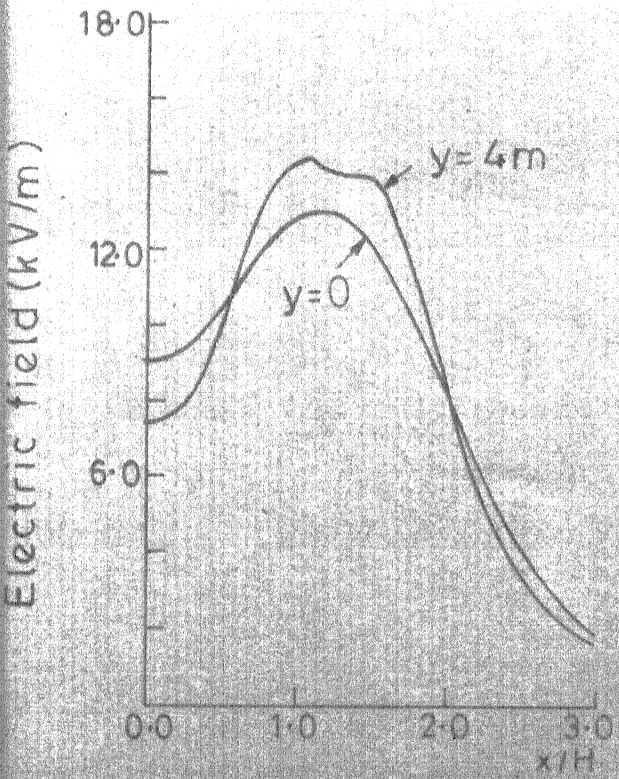

(c) Indian 400 kV
4-Circuit

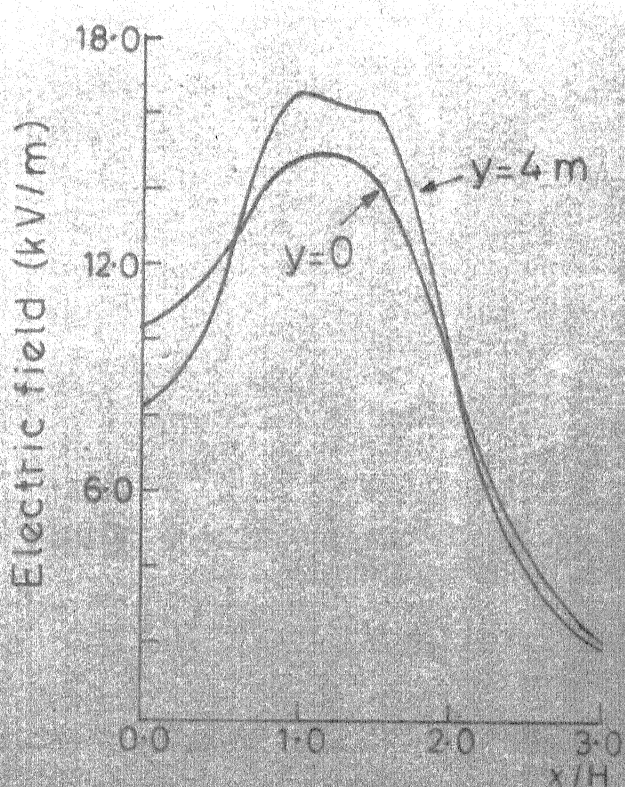

(d) German 400 kV
4-Circuit

FIG·2·9 VERTICAL COMPONENT OF ES FIELD

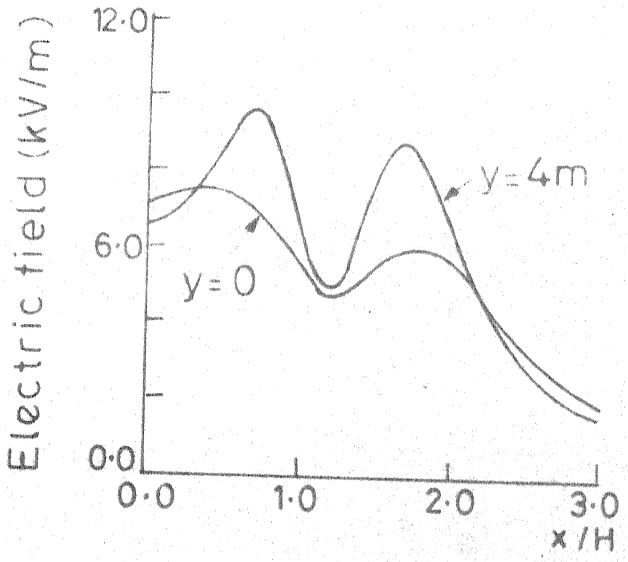

(a) Andhra 400 kV

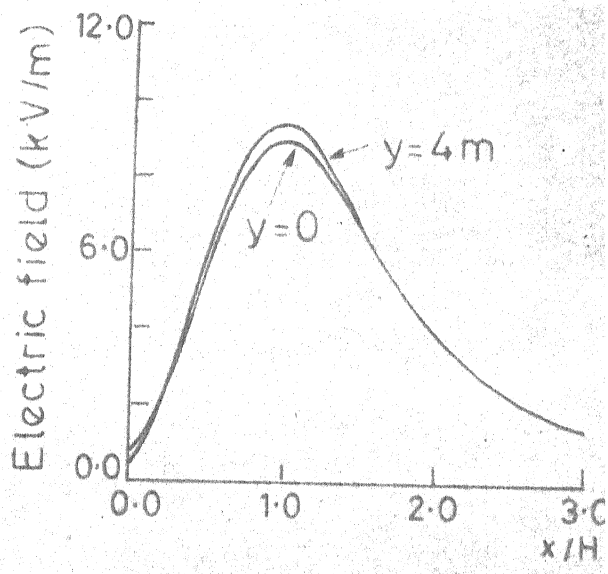

(b) BPA 1200 kV

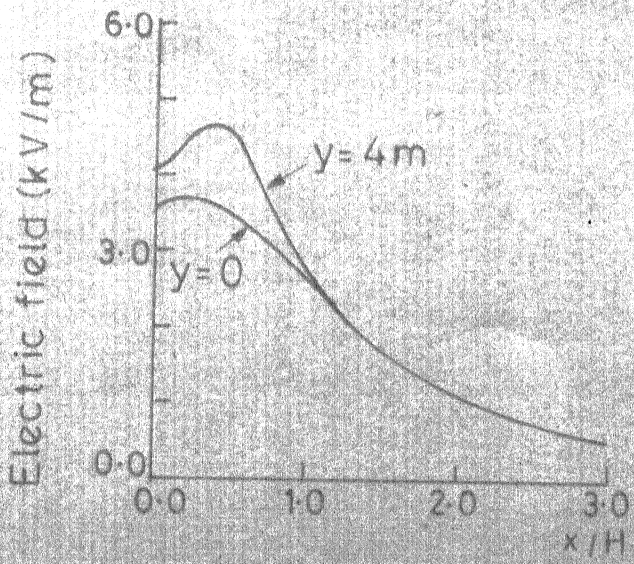

(c) 6 Phase 138 kV
with no ground wire

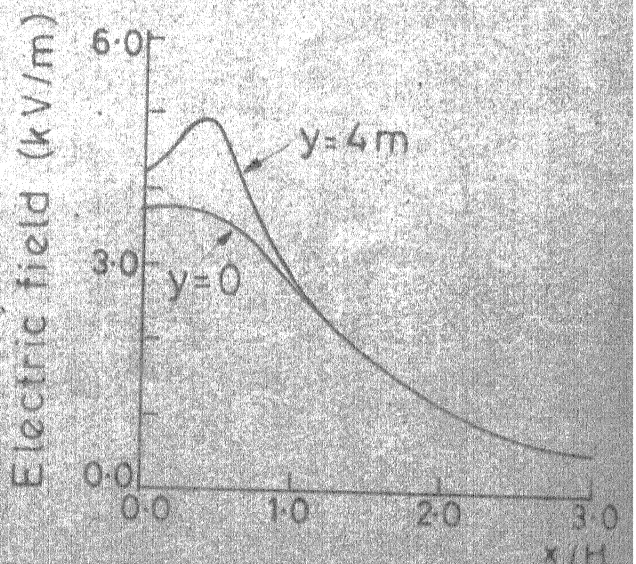

(d) 6 Phase 138 kV
with ground wire

FIG·2·10 VERTICAL COMPONENT OF ES FIELD

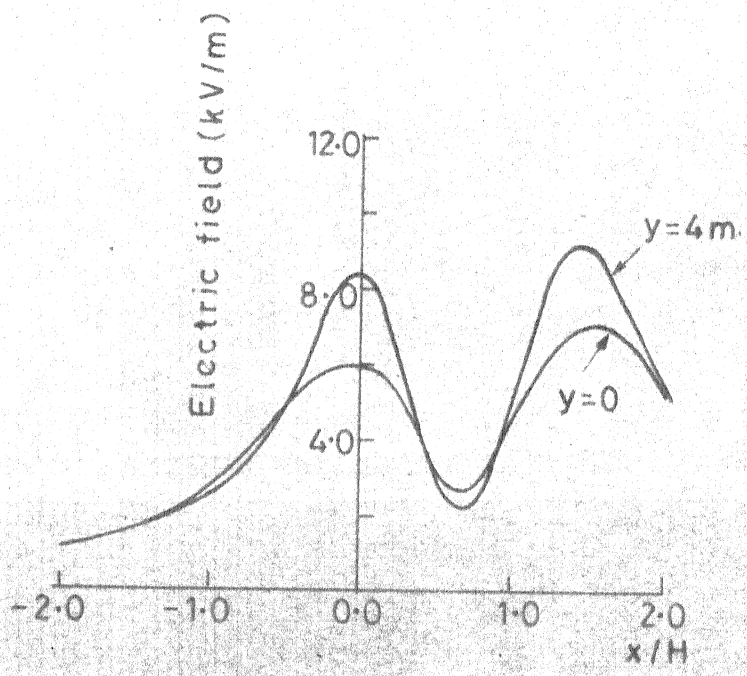

FIG.2.11 VERTICAL COMPONENT OF ES FIELD OF L-TYPE 400 kV LINE

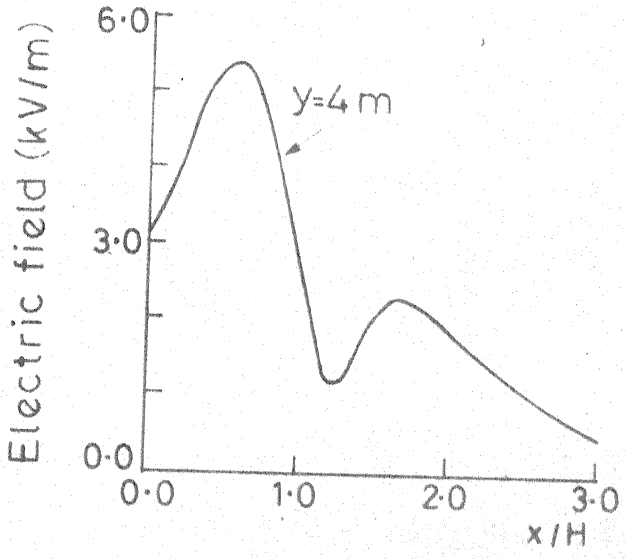

(a) Hydro-Quebec 735 kV
4x0·0302m

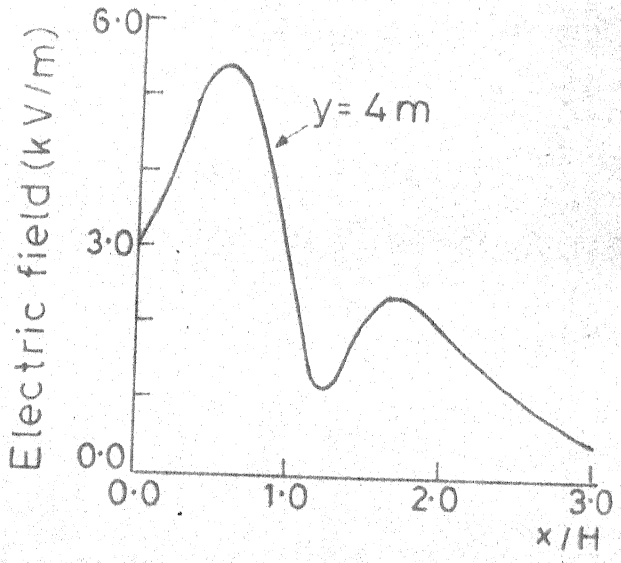

(b) Hydro-Quebec 735 k
4x0·0403 m

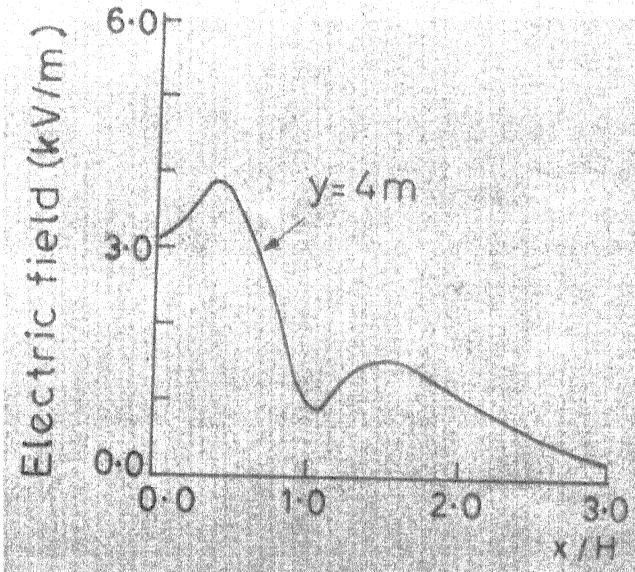

(c) Canadian 1200 kV
6 x 0·0463m

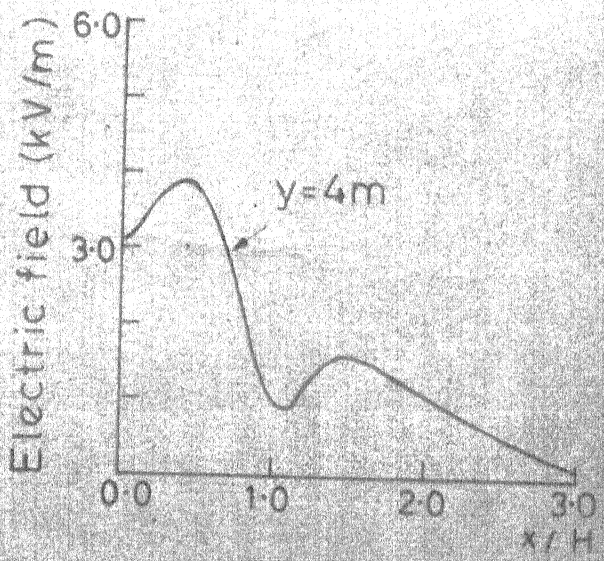

(d) Canadian 1200 kV
6x0·0508m

FIG. 2·12 HORIZONTAL COMPONENT OF ES FIELD

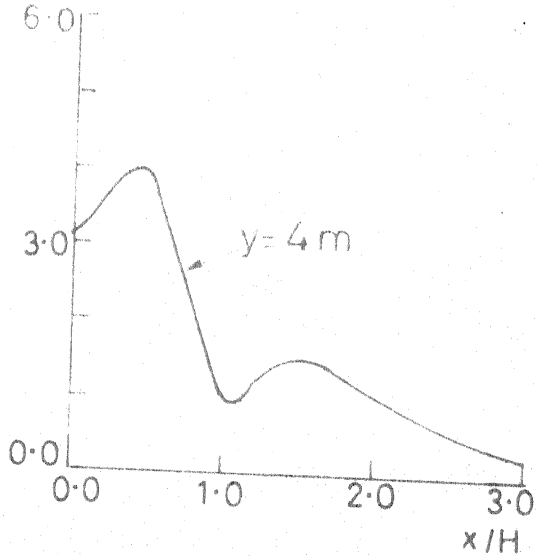

(a) Canadian 1200 kV
8x0·0414 m

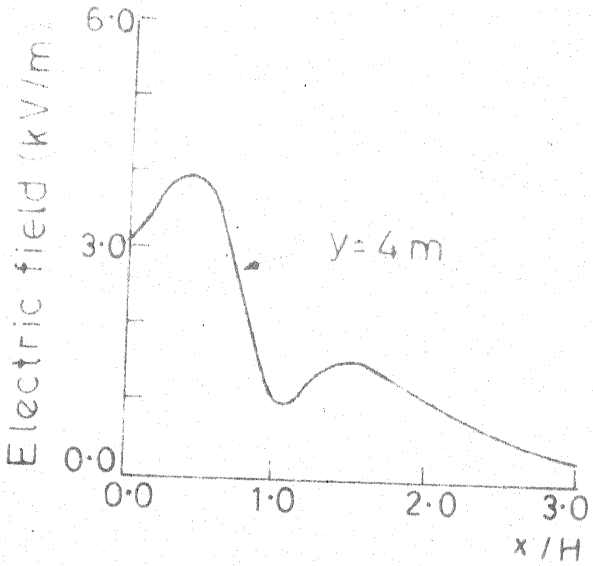

(b) Canadian 1200 kV
8x0·046 m

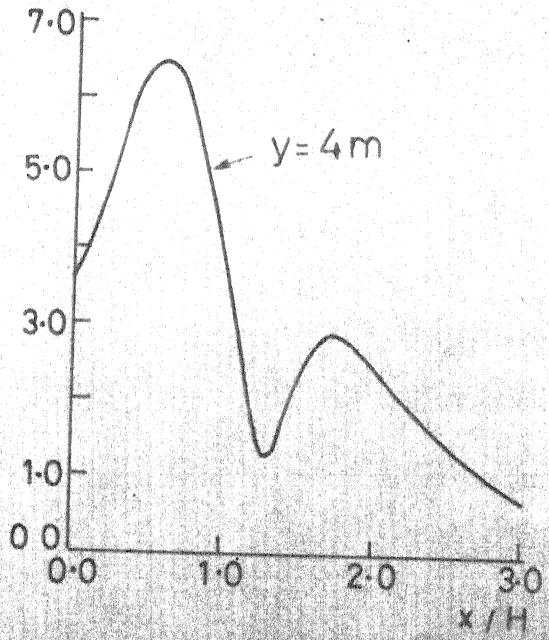

(c) Europian 1000 kV
4x0·044m

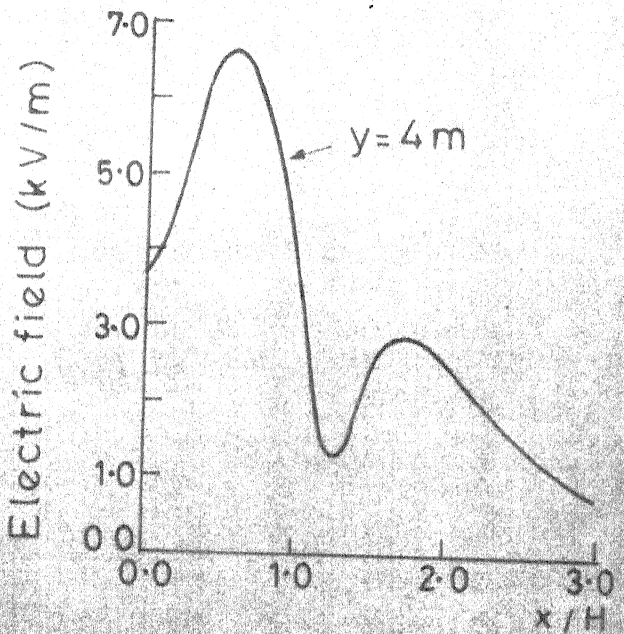

(d) Europian 1000 kV
4x0·047m

FIG. 2·13 HORIZONTAL COMPONENT OF ES FIELD

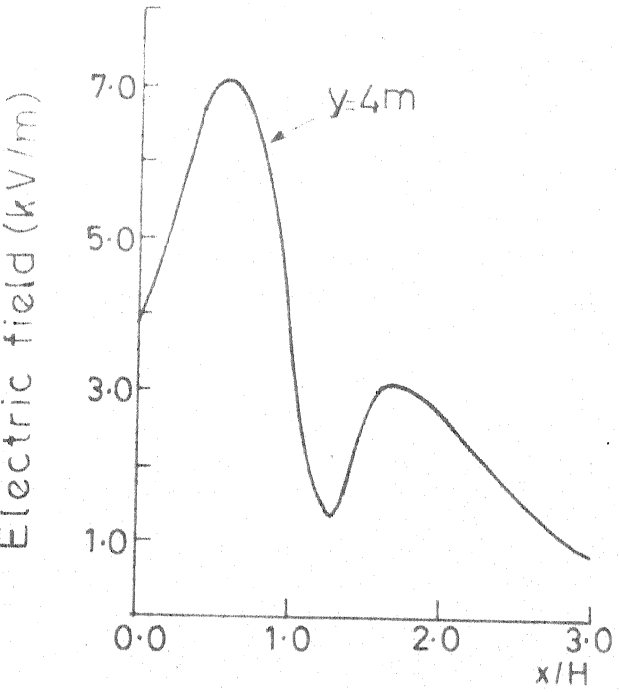

(a) Europian 1000 kV
6x0·038 m.

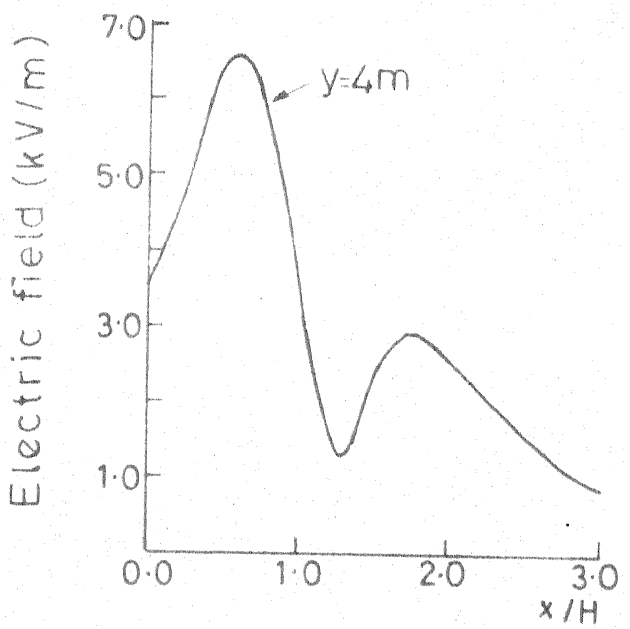

(b) Europian 1300 kV
8x0·038m

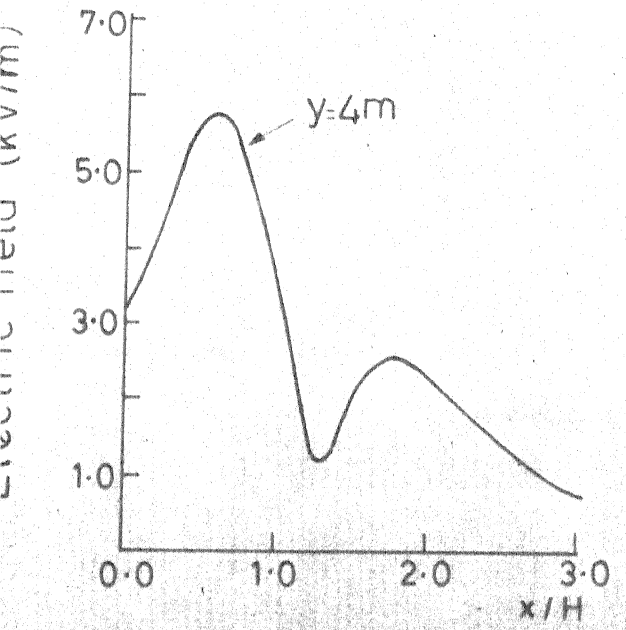

(c) Europian 1300 kV
4x0·052m

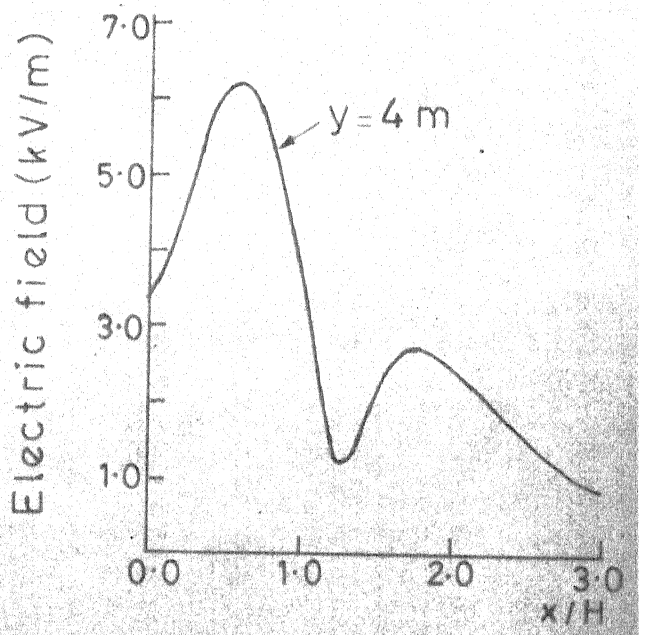

(d) Europian 1300 kV
6x0·044m

FIG.2·14 HORIZONTAL COMPONENT OF ES FIELD

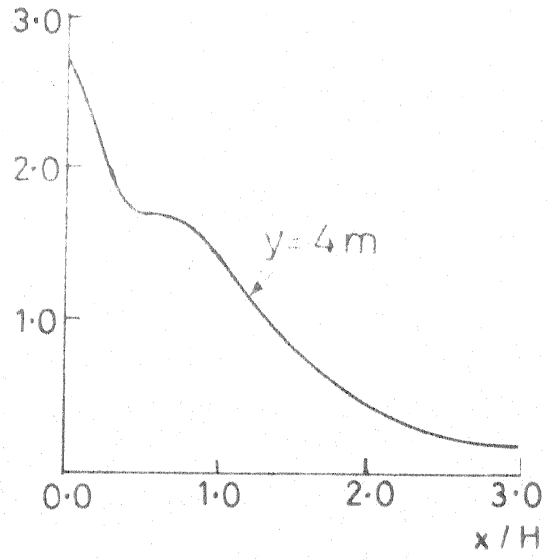

(a) 6-Phase 138 kV

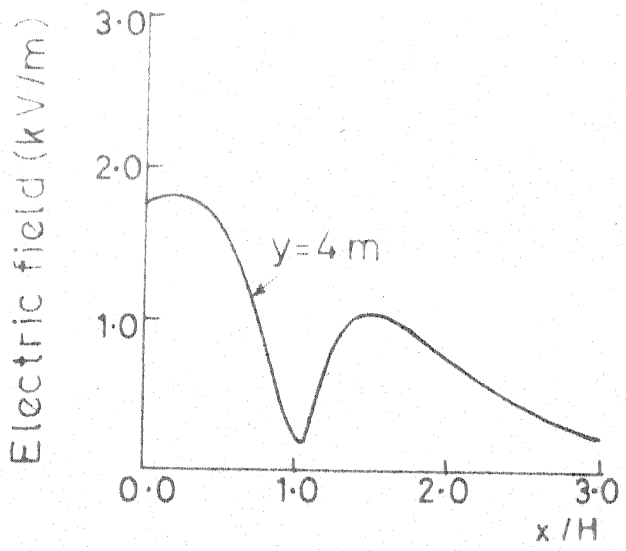

(b) BPA-1150 kV

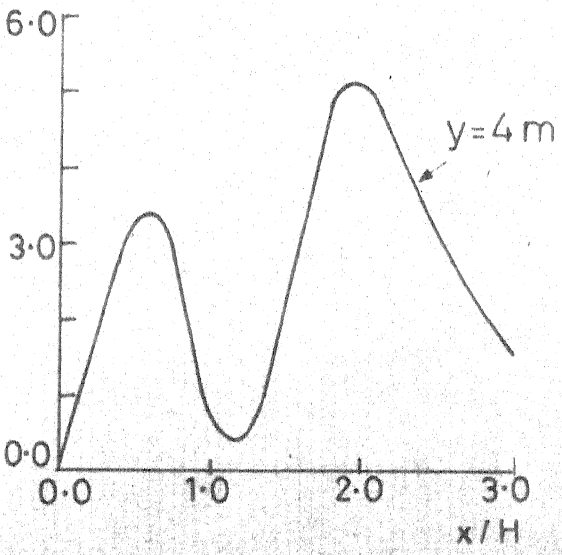

(c) Indian 400 kV
4-Circuit

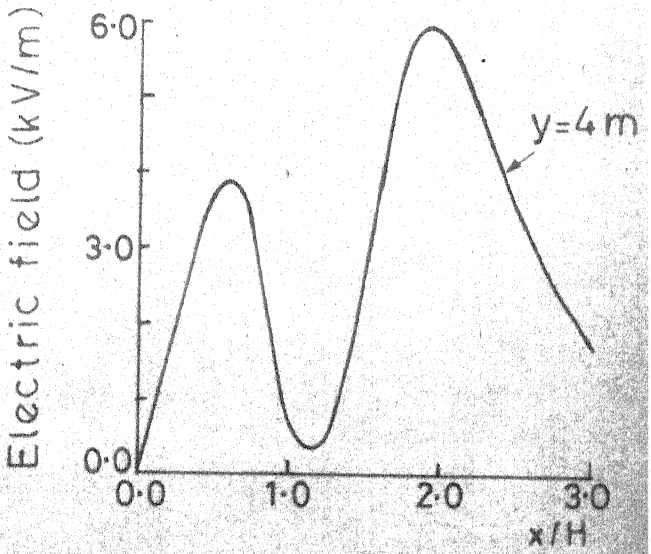

(d) German 400 kV
4-circuit

FIG. 2·15 HORIZONTAL COMPONENT OF ES FIELD

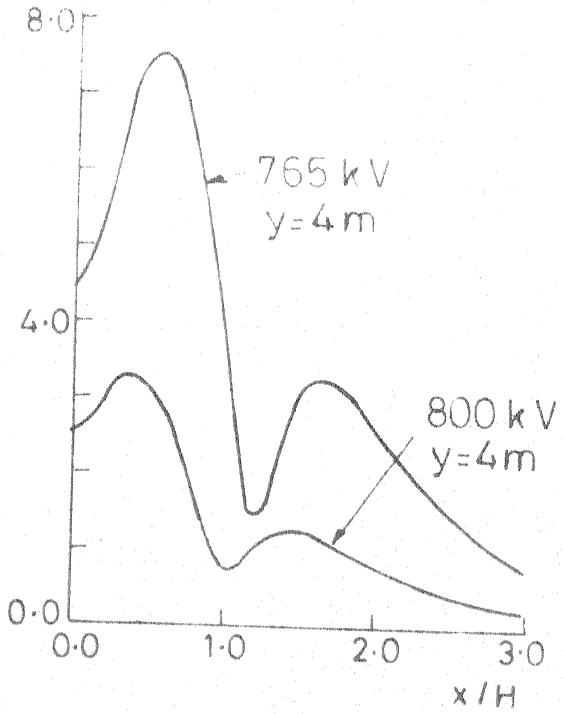

(a) Europe 765 kV

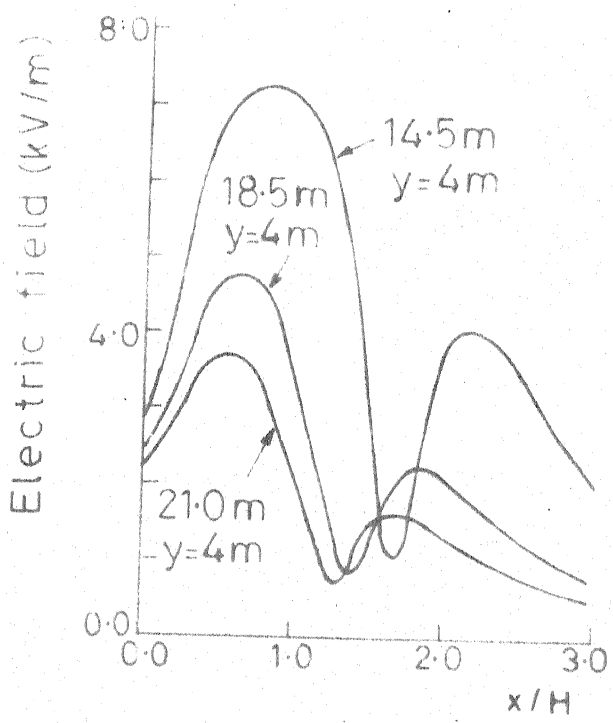

(b) USSR 1150 kV

14·5m, 18·5m and 21·0m clearance

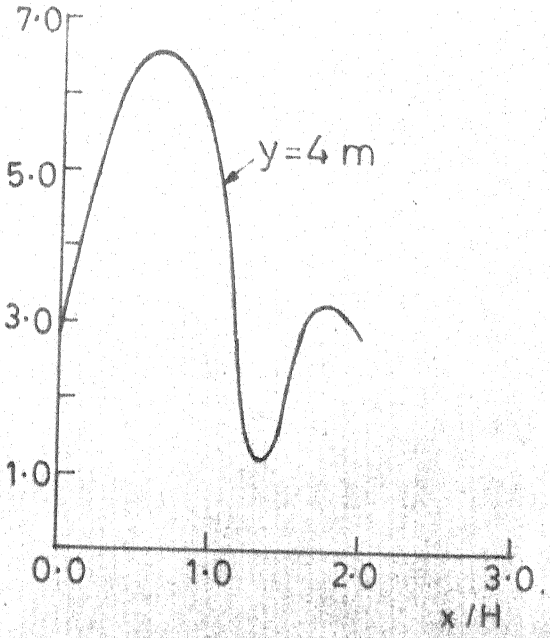

(c) UP 400 kV

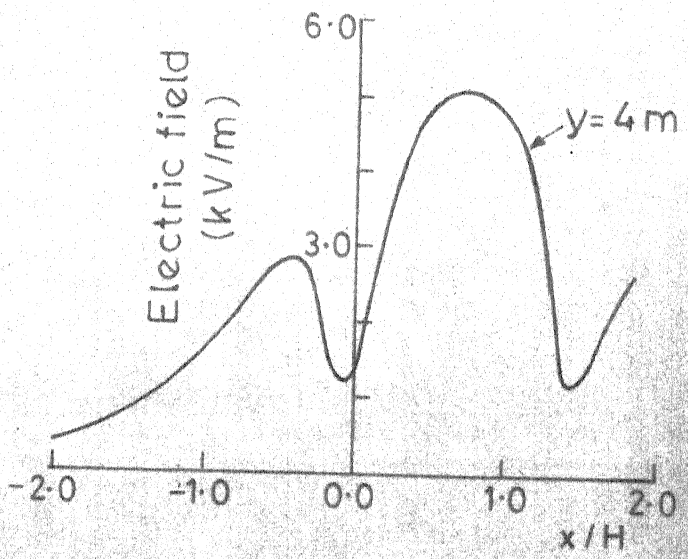

(d) L-Type 400 kV

FIG.2·16 HORIZONTAL COMPONENT OF ES FIELD

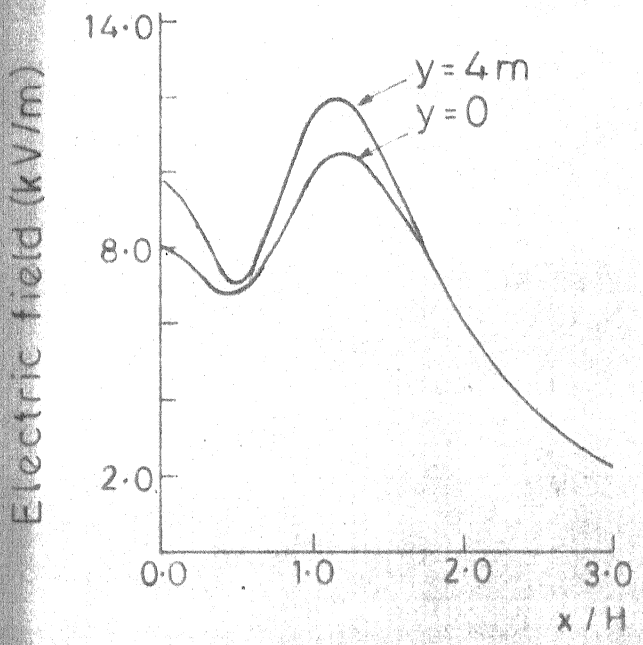

(a) Hydro-Quebec 735 kV
4x0·0302m

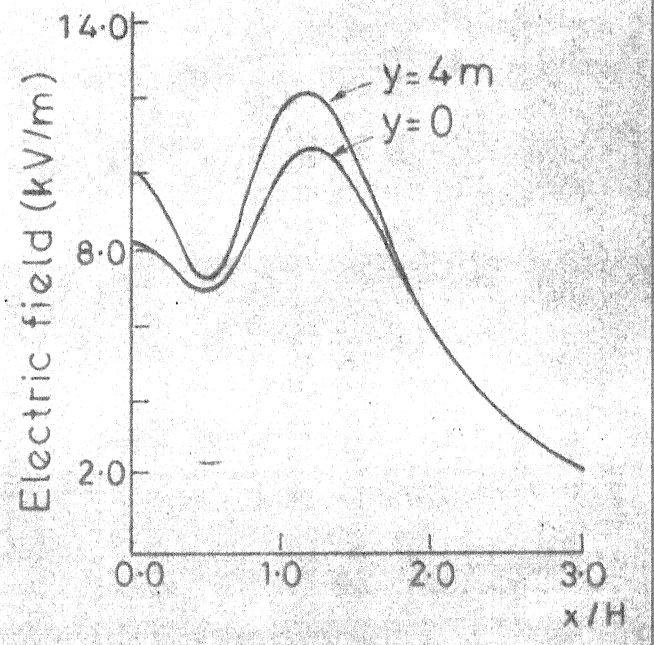

(b) Hydro-Quebec 735 kV
4x0·0403m

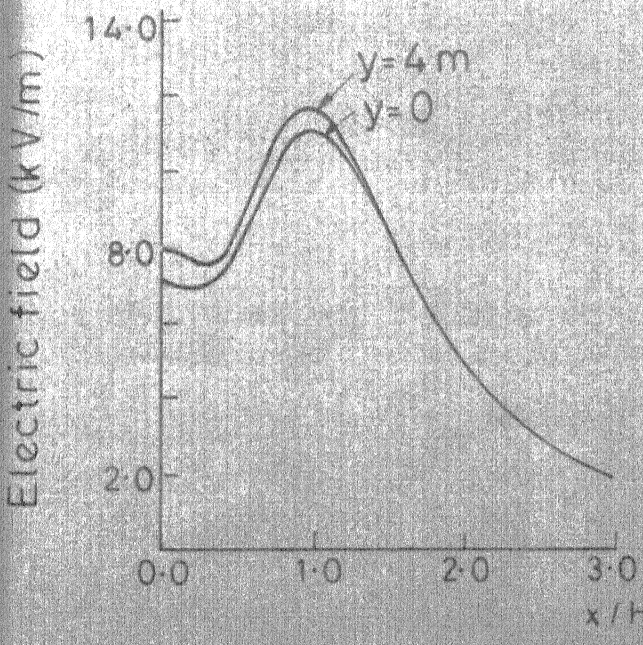

(c) Canadian 1200 kV
6 x 0·0463m

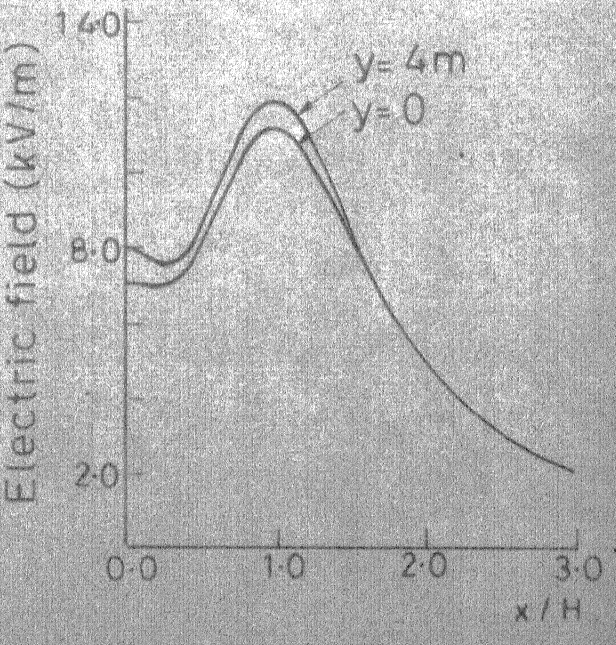

(d) Canadian 1200 kV
6x0·058m

FIG·2·17 TOTAL COMPONENT OF ES FIELD

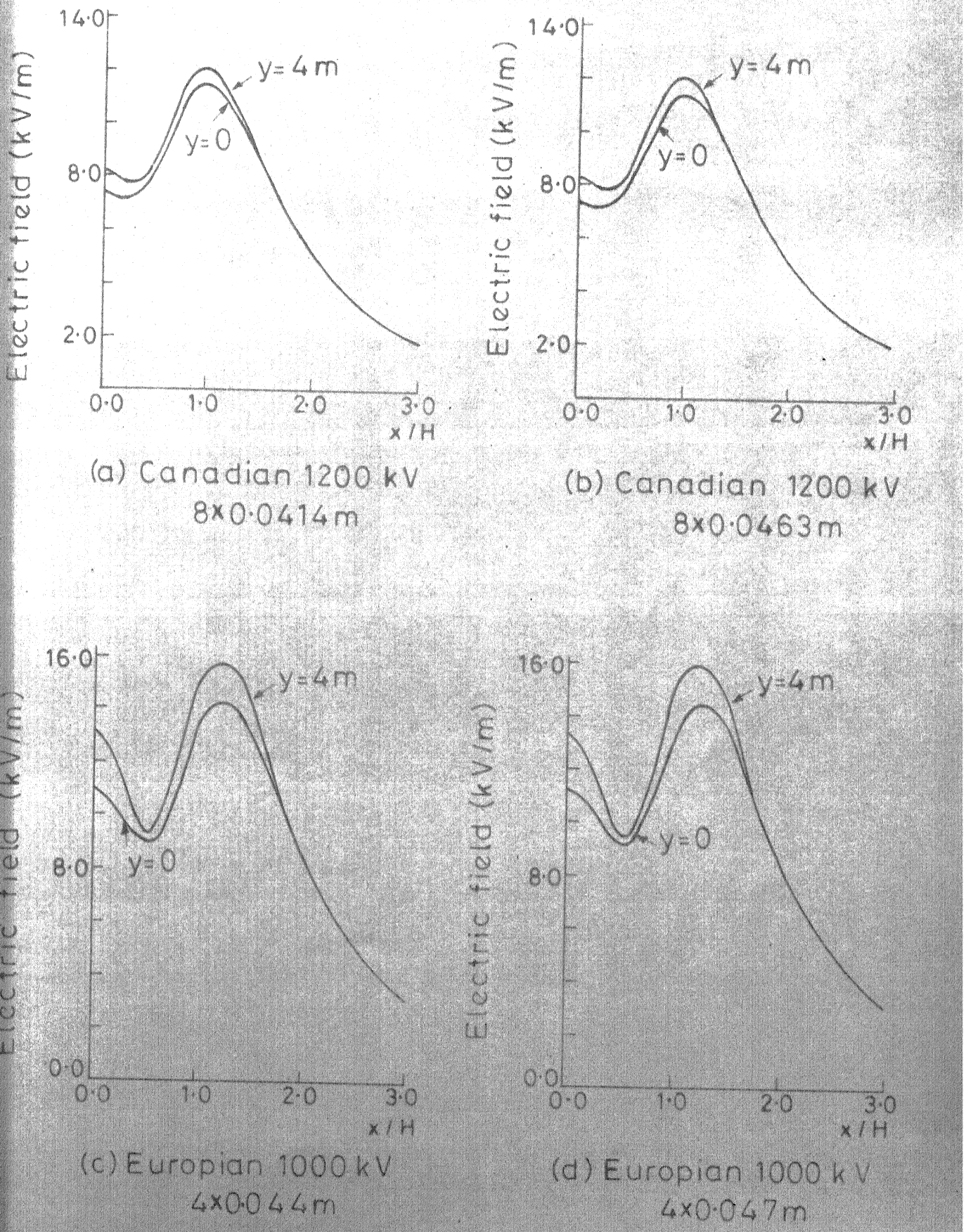

FIG. 2·18 TOTAL COMPONENT OF ES FIELD

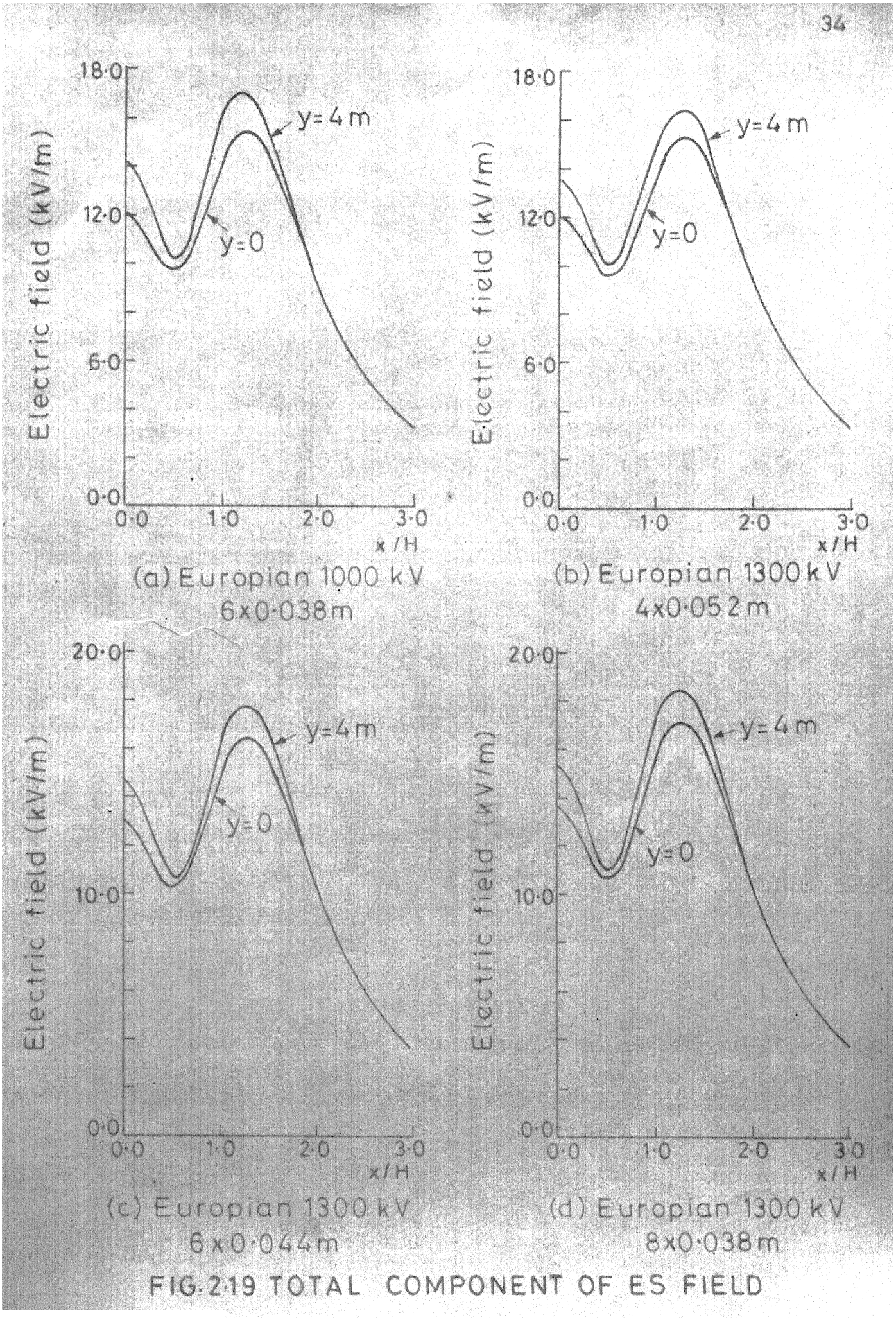

FIG. 2·19 TOTAL COMPONENT OF ES FIELD

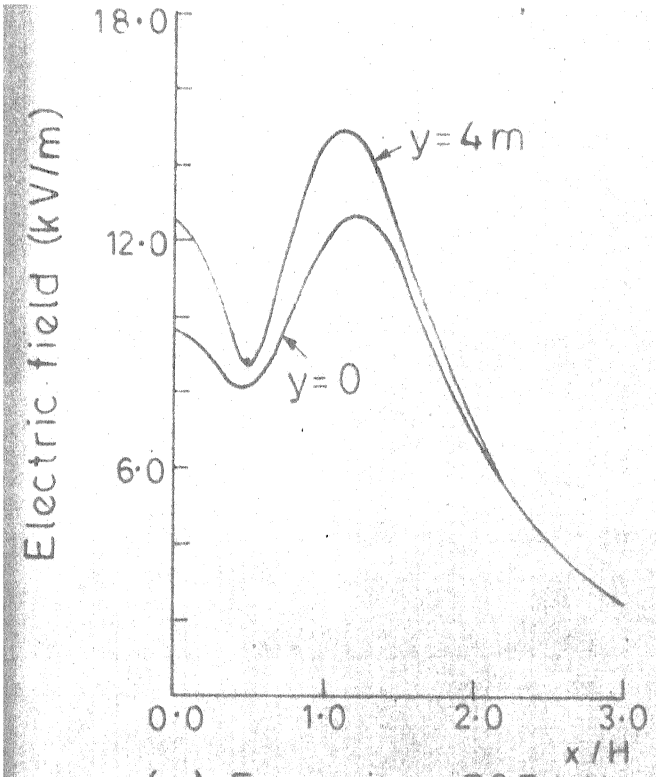

(a) Europian 765 kV

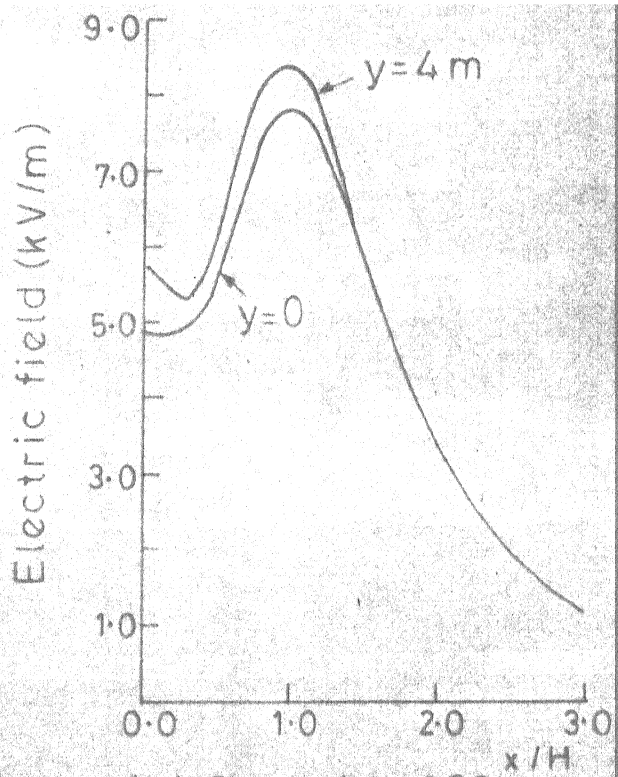

(b) Swedish 800kV

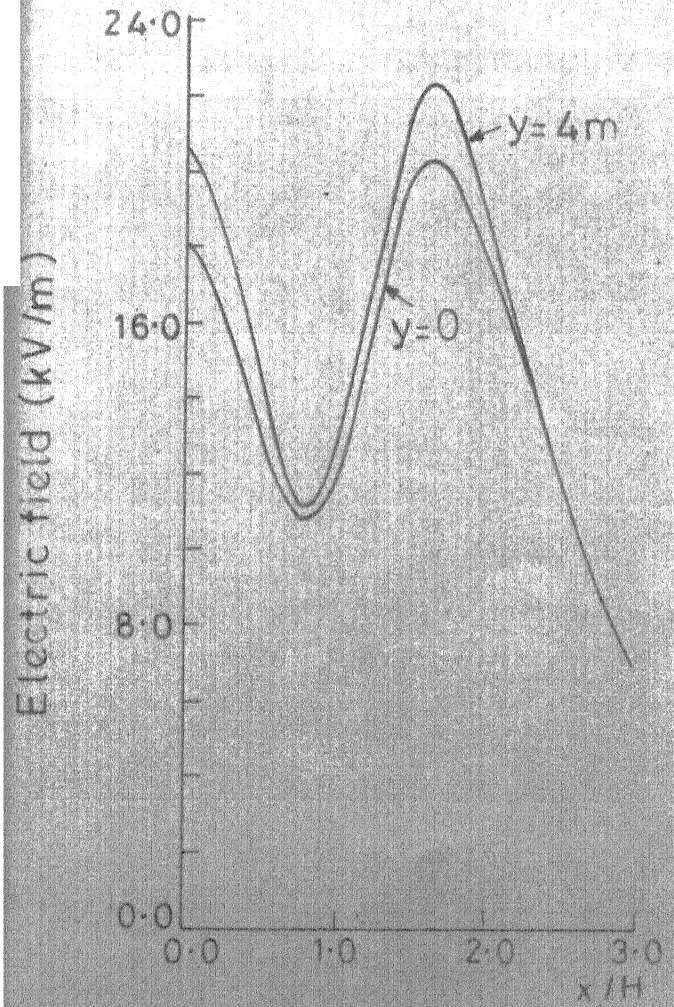

(c) USSR 1150 kV

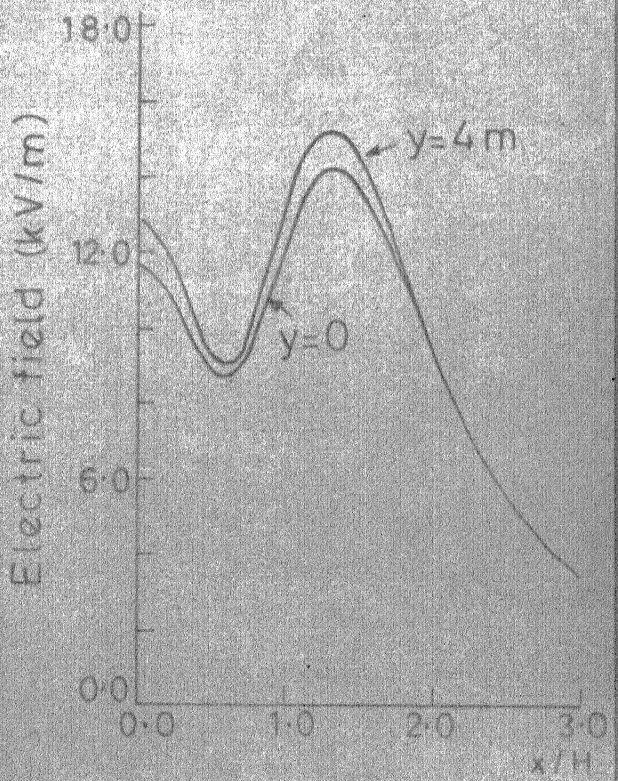

(d) USSR 1150 kV

FIG. 2·21 TOTAL COMPONENT OF ES FIELD

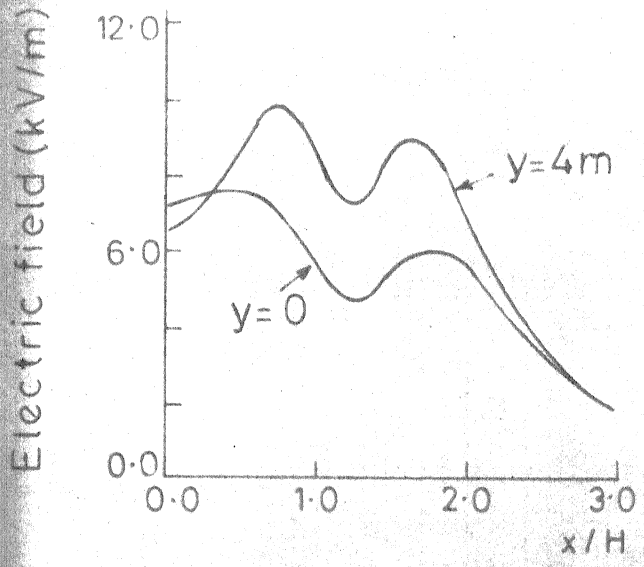

(a) Andhra 400 kV
2-Circuit

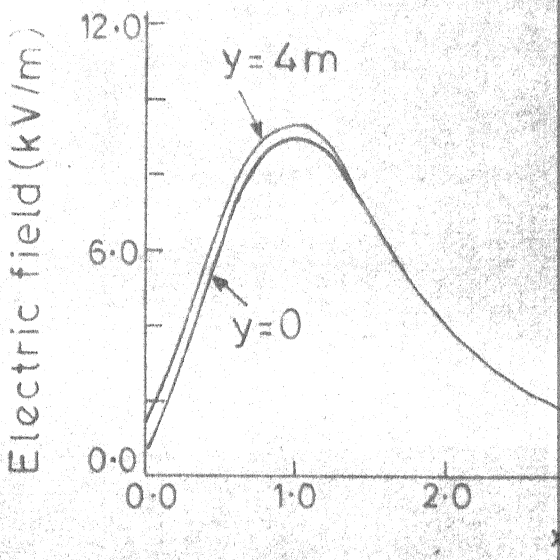

(b) BPA 1200 kV

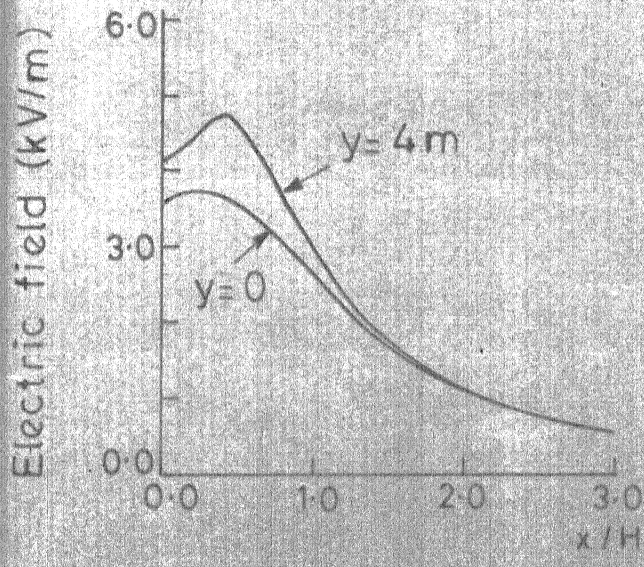

(c) 6-Phase 138kV
With no ground wire

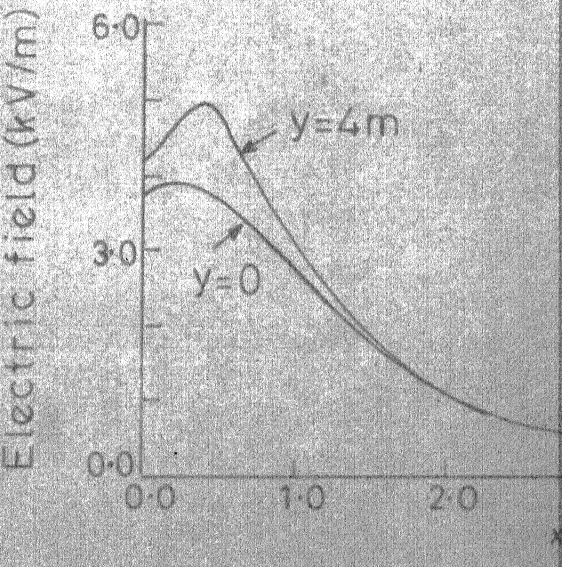

(d) 6-Phase 138 kV
with ground wi

FIG. 2·22 TOTAL COMPONENT OF ES FIELD

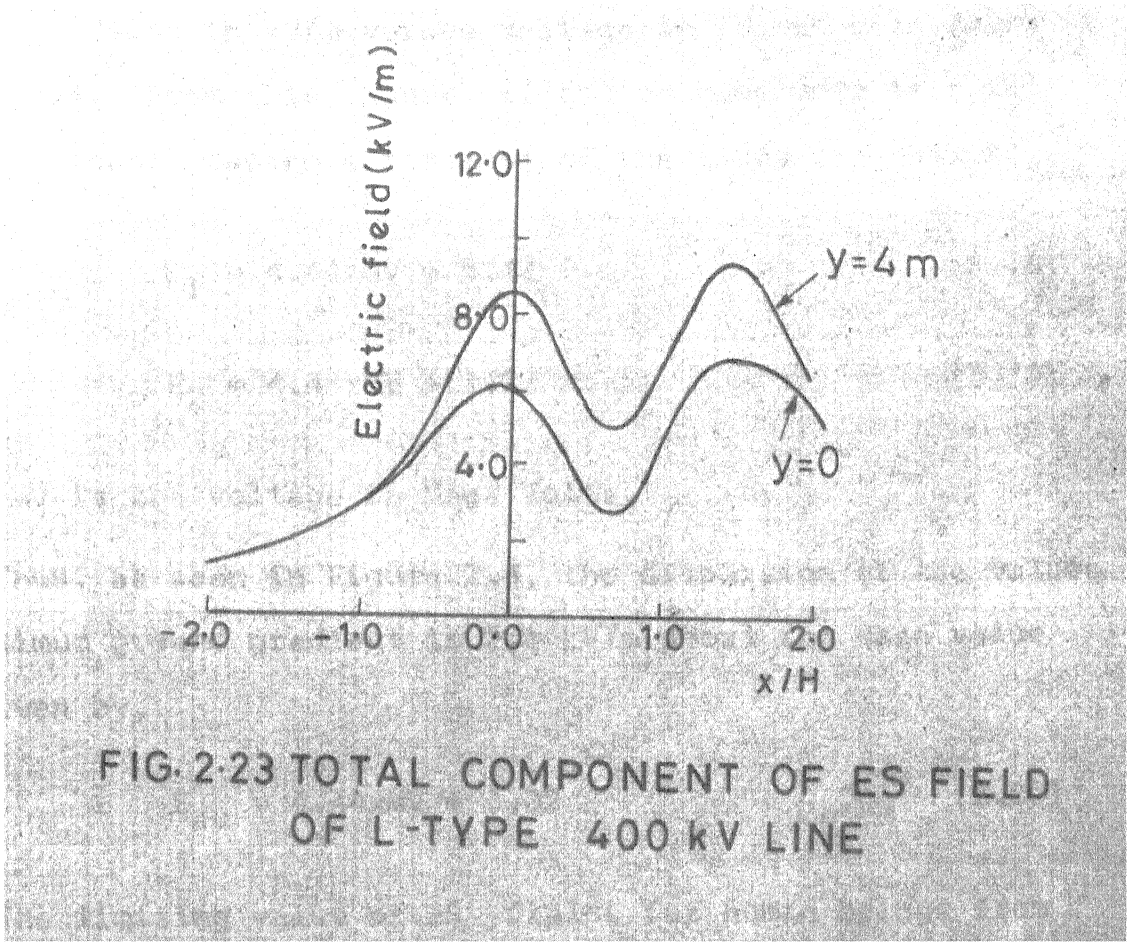

FIG. 2·23 TOTAL COMPONENT OF ES FIELD OF L-TYPE 400 kV LINE

2.6 CONCLUSIONS

Using the values listed in Table II, a graph of maximum ground gradient in kV/m versus voltage in kV has been drawn in Figure 2.4. From this figure, it can be concluded that the maximum ground gradients for most of the lines lie between,

$$E_1 = 4.44 \times MV + 5.42 \qquad (2.18)$$

and

$$E_2 = 4.44 \times MV + 11.22 \qquad (2.19)$$

where MV is the voltage in Mega Volts.

Thus, as seen in Figure 2.4, the dispersion of the values of maximum ground gradient is 2.5 kV/m about the mean value E_{av} given by,

$$E_{av} = 4.44 \times MV + 8.32 \qquad (2.20)$$

The limiting value of ES fields for human beings from safety considerations can be taken to be 15 kV/m. Since, for most of the line dimensions given in this document, the ES field is below the suggested limiting value, the line designs may be treated as acceptable. However, certain extraordinary circumstances might arise where taller than normal objects might have a chance of being present under the lines. Contingencies can be provided for these extraneous circumstances by increasing the minimum clearance. But this will have to be

3. In India at present, the highest voltage for transmission is 400 kV, 3-phase ac. However, once the National Grid becomes a reality, there will be need for higher transmission voltage. The next higher transmission voltage which can be adopted is 750 kV ac. Since a 400 kV, 4-circuit line has the same power carrying capacity as one single circuit 750 kV line, it is suggested that the 400 kV, 4-circuit configuration can be adopted as an alternative to 750 kV line. The maximum ground gradient for a 400 kV, 4-circuit configuration, calculated based on conductor diameter of 3.18 cm is found to be about 13 kV/m which is less than the value specified for safe limit.

CHAPTER 3

AUDIBLE NOISE

One of the important aspects of corona is the audible noise (AN) from EHV and UHV transmission lines. The audible noise is most noticeable in foul weather and the highest levels are obtained during heavy rains [11].

The audible noise created by transmission lines have two characteristic components of noise namely i) broadband white noise, resembling a crackling sound and ii) pure tone components which are harmonics of fundamental frequency. The most predominant component is the 100 Hz hum. Pure tone components are superimposed on the broadband noise.

3.1 AUDIBLE NOISE GENERATION

Atmospheric air contains free electrons and ions as a result of various effects, such as, u-v radiations from sun, cosmic rays etc. Under the influence of the alternating electric field, these positive and negative ions are continuously attracted to and repelled away from the conductors. This motion establishes a sound pressure having a frequency twice that of power-frequency voltage (i.e., 100 Hz for a 50 Hz system).

Audible noise during fair weather is due to the roughness of the conductor and pollution in the atmosphere. During foul weather (i.e., during rain and snow), rain drops under the effect of the alternating electric field are alternately attracted to and repelled away from the conductor. This to and fro motion of the water droplets produces the characteristic hum.

3.2 NOISE MEASUREMENT

Noise measurement essentially involves the determination of air pressure fluctuations. A microphone is used to convert the air pressure fluctuations into corresponding electric voltage variations and is placed at the point of sound measurement. This voltage is calibrated to read the sound pressure level (SPL) in decibels (dB).

Human ear is most sensitive to frequencies in the range of 20 Hz to 20KHz. Sound level meters which are employed to measure SPL should therefore, reject those frequencies which are not within the audible range. This is done using weighting circuits. The A-weighting circuit, which has a flat band-pass characteristics from 500 Hz to 8000 Hz, is used for transmission line noise measurement.

Sound Pressure Levels which are measured using the A-weighting network are accordingly known as the A-weighted sound levels (SLA) and the unit for this is dB (A).

3.3 LIMITS FOR AUDIBLE NOISE

Basis for calculating the limits of AN have been discussed in [5]. As pointed out in this paper, these limits are established based on the following two criteria :

i) Perry's criterion

ii) The day night equivalent noise level.

The Perry's criterion is based on the analysis of annoyance experienced by groups of human beings living close to the transmission lines. The limits as specified by this criterion are :

i) High noise level, greater than 59 dB(A).

ii) Moderate noise level, 52.5 to 59 dB(A).

iii) Low noise, less than 52.5 dB(A).

The values specified are the L_{50} levels or, the noise levels that will be present for more than 50% of the time in foul weather.

The second criterion identifies the fact that a certain sound level which may be acceptable during the day time may be found to be objectionable during the night time when the ambient noise level is comparatively lower. Hence, the equivalent sound level is found by increasing the night time sound level by a factor of 10 dB(A) [12]. Suppose, the L_{50} noise level of a transmission line is 50 dB(A) and suppose the day is assumed to

extend for 17 hours and the night for 7 hours, then the equivalent noise level is,

$$L_{dn} = 10 \text{ Log}_{10} \frac{1}{24} [17 \times 10^{(50/10)} + 7 \times 10^{(50+10)/10}]$$

$$= 55.6 \text{ dB(A)}$$

This calculation assumes that rain is present for the entire 24 hours. However, if the rain is present only for a certain percentage of time during the day, say for 15 percent of the time during the day and for 40 percent of time during night, then the equivalent noise is given as following :

$$L_{dn} = 10 \text{ Log}_{10} \frac{1}{24} [17 \times 0.15 \times 10^{(5.0)} + 7 \times 0.4 \times 10^{(6.0)}]$$

$$= 51.0 \text{ dB(A)}$$

3.4 METHODS FOR CALCULATING AUDIBLE NOISE

Calculation of AN is important as it aids the designer in selecting a suitable conductor size, number of subconductors and the phase spacing. A number of methods, developed by different power companies are available for calculation of AN. All these empirical relations have been formulated to have a close relation with the measured data. However, there is no absolute guarantee that the reported measurements are fully reliable. The errors in the measured values may be due to incorrect calibration procedures or due to high ambient noise levels.

A total of nine methods for AN measurement on ac lines have been reported in [9]. Of these, only four methods have been indicated in Table III, because these are more general than the remaining ones. These can be applied both to single and multi-circuit lines of any configuration-horizontal, vertical or triangular. All these methods predict the noise levels in terms of A-weighted sound level, dB(A) i.e., the level which gives more weight to mid-frequencies for which the human ear is most sensitive.

The noise level of each phase, as given by any of these four methods can be written in a generalized form as following :

$$AN = K_1 f_1(g) + K_2 f_2(n) + K_3 f_3(d) + K_4 f_4(D) + AN_0 + K \qquad (3.1)$$

where,

n - number of subconductors in a bundle

d(cm) - diameter of subconductors

D(m) - radial distance from the line conductors to the point at which noise is to be calculated

AN(dB(A))- 'A' - weighted sound level of the noise produced by one phase of the line

AN_0(dB(A))- reference A-weighted sound level

g(kV/cm) - conductor surface gradient

$f_1(g), f_2(n), f_3(d), f_4(D)$ - functions of the parameters g,n,d,D

Using the formulas given in Table III, the AN due to each phase can be found. Once the noise level of each phase is calculated, the total noise level of the line can be found by the following summation :

$$SL = 10 \text{ Log}_{10} \left[\sum_{i=1}^{p} \text{Antilog}_{10}(AN_i/10) \right] \qquad (3.2)$$

where p is total number of line conductors (for example; 6 for a double circuit 3-phase line) and AN_i - noise level of conductor i calculated from equation (3.1).

3.5 EXTENSION OF SINGLE PHASE RESULTS TO 3-PHASE CASE

In order to investigate the high voltage phenomena relating to line design, outdoor experiments with a full scale three-phase configuration are thought to be essential. However, if experiments can be performed on a single-phase line and the results extended to a 3-phase case, a considerable economy may result. The possibility of such an extrapolation has been investigated in this work.

The AN due to ith conductor can be written as

$$AN_i = K_1 f_1(g_i) + K_2 f_2(n) + K_3 f_3(d) + K_4 f_4(D_i) + AN_o + K \qquad (3.3)$$

g_i - conductor surface gradient of the ith conductor

D_i - radial distance between the ith conductor and the point where noise is being calculated.

Table III.

Formulas for calculating the Audible Noise of Transmission Lines

Power Company	Formula (for each phase)	Application	Noise measure	Range of validity
BPA, USA	$AN=120\ \mathrm{Log}(g)+K\ \mathrm{log}(n)+55\ \mathrm{Log}(d)-11.4\ \mathrm{Log}(D)+AN_o$ $K=26.4$ for $n \geq 3$ $=0$ for $n < 3$ $AN_o = -128.4$ for $n \geq 3$ $= -115.4$ for $n < 3$	all line geometries	L_{50}	230-1500kV $n \leq 16$ $2 \leq d \leq 6.5$
ENEL, ITALY	$AN=85\ \mathrm{Log}(g)+18\ \mathrm{Log}(n)+45\ \mathrm{Log}(d)-10\ \mathrm{Log}(D)-71+K$ $K = 3$ for $n = 1$ $= 0$ for $n \geq 2$	all line geometries	maximum rain	400-1200kV $n \leq 10$ $2 \leq d \leq 5$
FGH, GERMANY	$AN=2g+18\ \mathrm{Log}(n)+45\ \mathrm{Log}(d)-10\ \mathrm{Log}(D)-0.3$	all line geometries	maximum rain	$n \leq 6$ $2 \leq d \leq 6$
HYDRO-QUEBEC	$AN=72\ \mathrm{Log}(g)+22.7\mathrm{Log}(n)+45.8\ \mathrm{Log}(d)-11.4\mathrm{Log}(D)-57.6$	all line geometries	maximum rain	345-1500kV $n \geq 2$

Based on the fact that gradient on conductors do not vary much, we can replace the gradients by average gradient g_{av}, where

$$g_{av} = [\sum_{i=1}^{p} g_i]/p$$

p is the number of line conductors.

Equation (3.3) can now be written as,

$$AN_i = [K_1 f_1(g_{av}) + K_2 f_2(n) + K_3 f_3(d) + AN_o + K] + K_4 f_4(D_i) \quad (3.4)$$

The quantities within the square brackets in equation (3.4) are constant for each phase and can be replaced by 'M'. Thus equation (3.4) can now be rewritten as

$$AN_i = M + K_4 f_4(D_i)$$

The total noise level due to all the p-conductors is,

$$SL_T = 10 \text{ Log}_{10}[\sum_{i=1}^{p} 10^{(AN_i/10)}]$$

or

$$SL_T = 10 \text{ Log}_{10} \sum_{i=1}^{p} [10^{(M+K_4 f_4(D_i))/10}]$$

i.e. $$SL_T = M+10 \text{ Log}_{10} \sum_{i=1}^{p} [10^{K_4 f_4(D_i)/10}] \quad (3.5)$$

If now, a single phase line of the same dimension is considered, the AN at a radial distance D due to this line is,

$$SL = M + 10 \text{ Log}_{10}[10^{K_4 f_4(D)/10}] \qquad (3.6)$$

Combining equations (3.5) and (3.6) we get

$$SL_T = SL + 10 \text{ Log}_{10} \sum_{i=1}^{p} \left[\frac{10^{K_4 f_4(D_i)/10}}{10^{K_4 f_4(D)/10}}\right] \qquad (3.7)$$

Equation (3.7) gives a relation between the noise level (SL_T) of a p-conductor configuration and the noise level (SL) of a single phase line.

The values of the constant K_4 and function f_4 will depend upon the respective formula considered. For the BPA formula, which is listed in Table III. , the values are

$$f_4(D) = \text{Log}_{10}(D)$$

and

$$K_4 = -11.4$$

If a 3-phase single circuit line is considered, i.e., p = 3, for the BPA formula, equation (3.7) can be written as follows :

$$SL_T = SL + 10\text{Log}_{10}\left[\frac{10^{-1.14\text{Log}_{10}(D_1)} + 10^{-1.14\text{Log}_{10}(D_2)} + 10^{-1.14\text{Log}_{10}(D_3)}}{10^{-1.14\text{Log}_{10}(D)}}\right]$$

$$\text{or} \quad SL_T = SL + 10 \text{ Log}_{10}\left[\frac{D_1^{-1.14} + D_2^{-1.14} + D_3^{-1.14}}{D^{-1.14}}\right]$$

$$= SL + 10 \text{ Log}_{10}\left[\left(\frac{D}{D_1}\right)^{1.14} + \left(\frac{D}{D_2}\right)^{1.14} + \left(\frac{D}{D_3}\right)^{1.14}\right] \qquad (3.8)$$

Here, D_1,D_2 and D_3 are the radial distances of the three conductors from the point where the noise is being calculated.

Using equation (3.8), suitable decibel adders are found in order to extrapolate single-phase results to 3-phase case.

3.6 RESULTS AND DISCUSSION

Using the BPA formula given in Table III, lateral profiles of AN at ground level have been calculated for transmission lines of voltages varying from 400 kV to 1300 kV. All these calculations are based on the dimensions given in Table I. The results of the calculation have been shown in Figures 3.1 to 3.3.

Assuming the edge of right-of-way (R-O-W)to be 15m from the outer conductor, the noise level at this point for the proposed Indian 400 kV, 4 circuit configuration, whose dimensions are given in Figure 2.3a,is 46 dB(A). This is less than the limit specified by the Perry's criterion for no complaints.

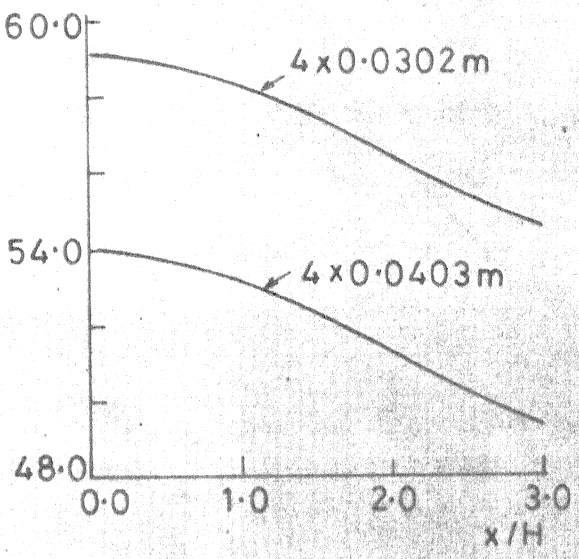

(a) Hydro-Quebec 735 kV

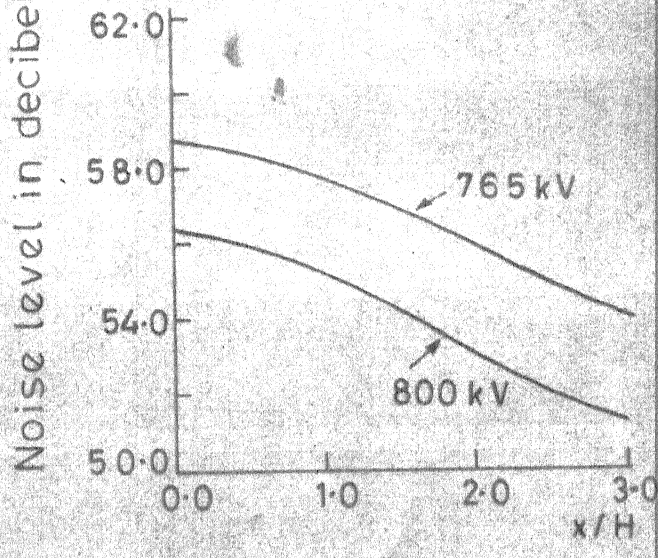

(b) Swedish 800 kV and Europe 765 kV

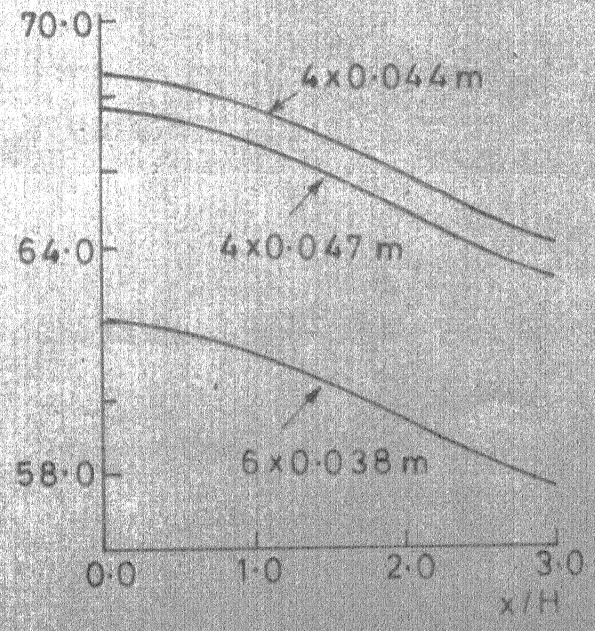

(c) Europe 1000 kV

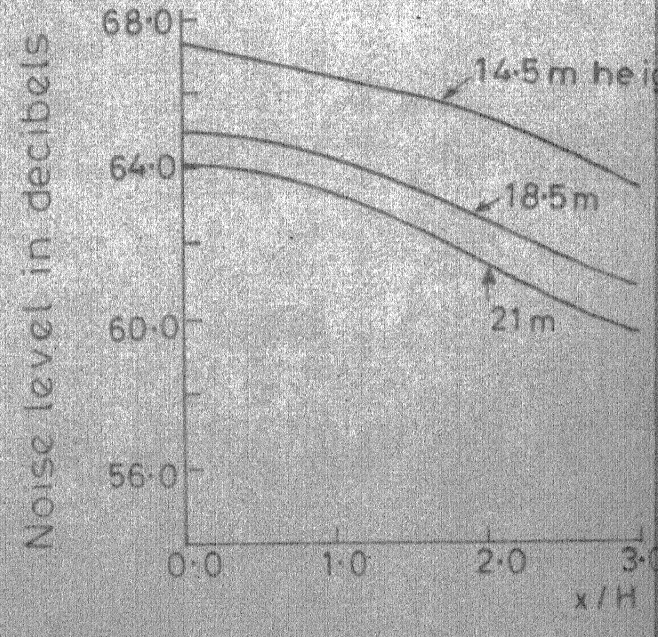

(d) USSR 1150 kV

FIG.3·1 AUDIO NOISE PROFILES AT GROUND LEVEL

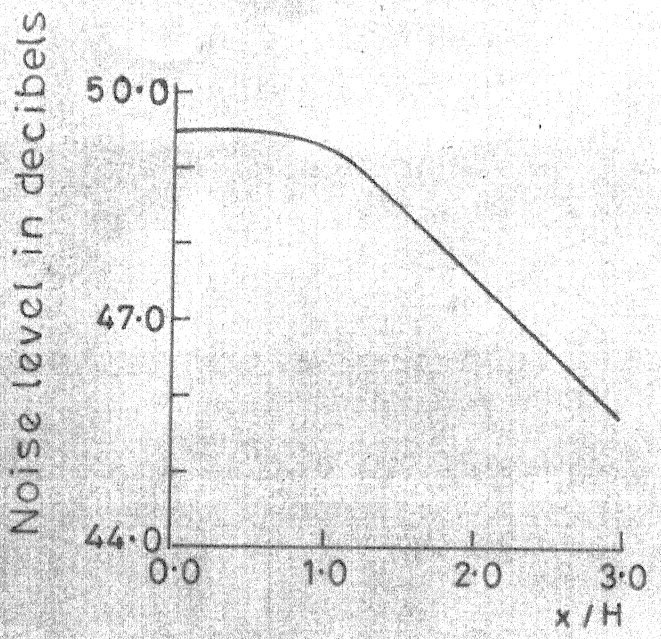

(a) BPA 1150 kV

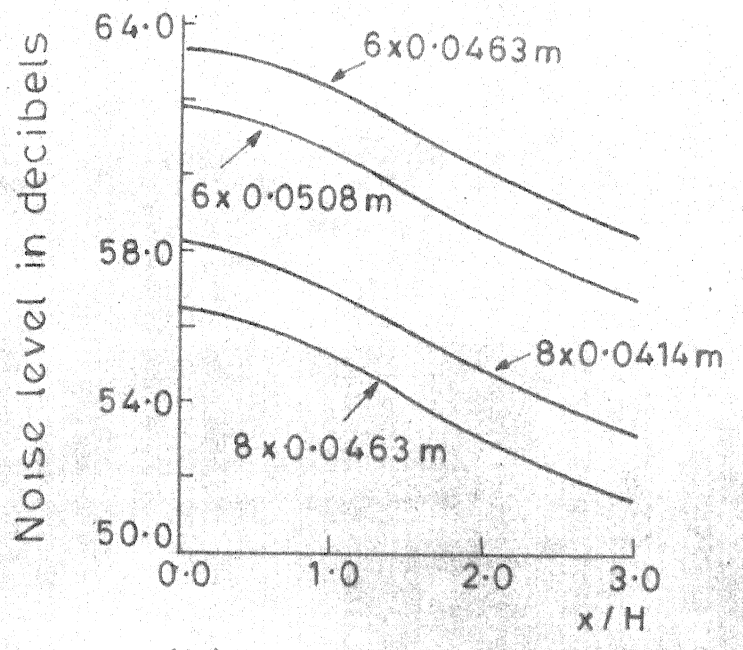

(b) Canadian 1200 kV

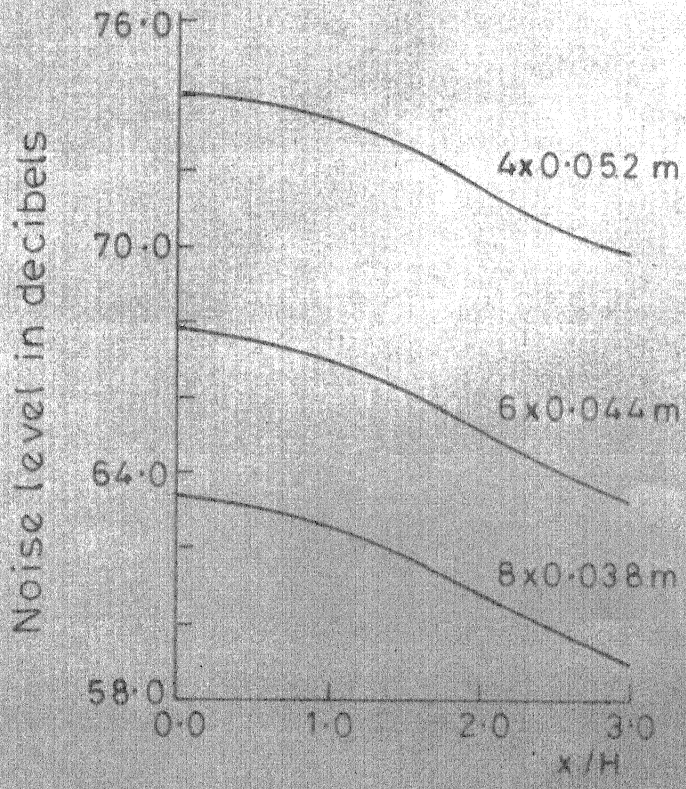

(c) Europe 1300 kV

FIG·3·2 AUDIO NOISE PROFILE
AT GROUND LEVEL

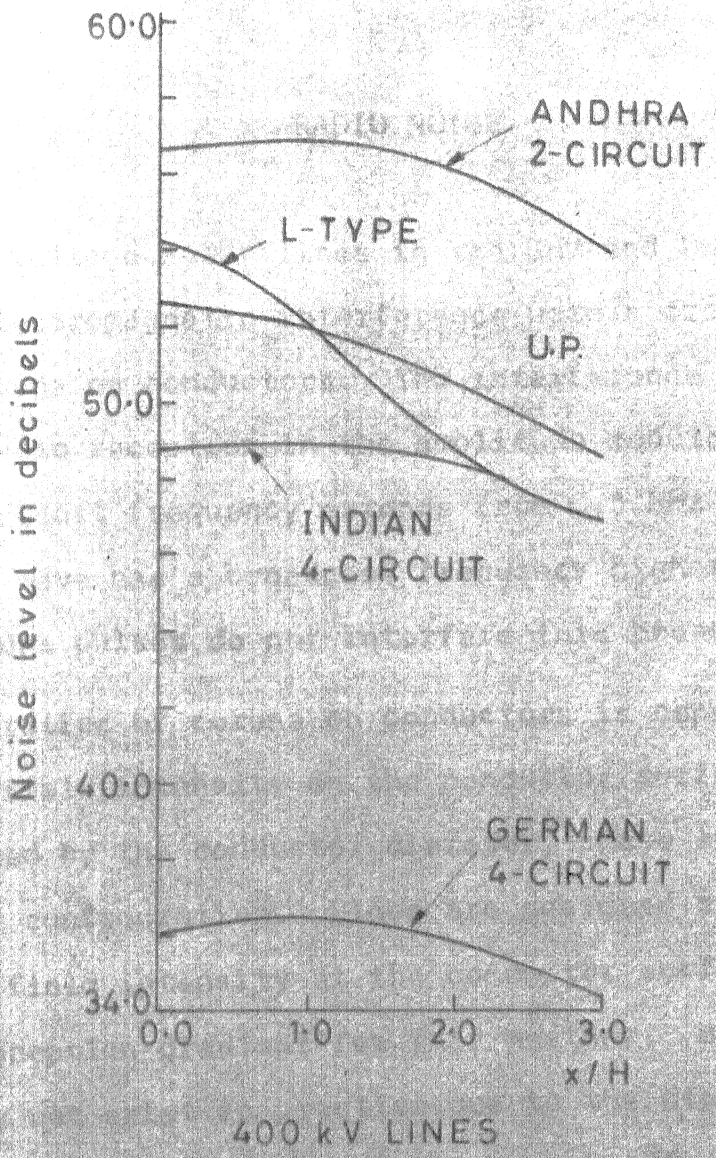

FIG.3·3 AUDIO NOISE PROFILES AT GROUND LEVEL

CHAPTER 4

RADIO NOISE

High Voltage Power lines in the EHV and UHV ranges produce electromagnetic interference upto a frequency of 3 MHz, due to corona on conductors. The interference so generated affects radio reception in the amplitude modulated (AM) range whose broadcast frequency extends from 0.5 MHz to 1.6 MHz. The short wave has a broadcast frequency higher than 3 MHz and hence corona pulses do not interfere this broad cast-frequency.

Generation of corona on conductors is dependent on the electric field intensity on the conductor surface which inturn is affected by the conductor diameter, phase spacing and conductor configuration. Lines are designed such that the electric field intensity at the conductor surface is below the corona inception gradient for fair weather. But such conditions may not exist in practice due to the atmospheric and environmental effects. For ac lines, the RI level will be highest in heavy rain and lowest in fair weather. The main sources of fair weather corona are the atmospheric pollutants.

Corona discharges on the conductors consists of streams pulses of current. These current pulses which are comprised of a large number of sinusoidal components of different

frequencies, propagate along the line and undergo attenuation between the point of generation and the point of measurement.

RI level of a line is measured at a particular frequency. IEEE recommends a standard reference frequency of 1 MHz and a standard location of 15m laterally as measured along the ground from the outermost phase conductor. The radiated interference is called the Radio Interference Field Intensity (RI) and is measured in dB above 1 μV/m.

4.1 MEASUREMENT OF RADIO NOISE

The block diagram of an RI meter is shown in Figure 4.1a.

The instruments which are used to measure the interference to radio reception should itself have the characteristics of radio-receivers. The first stage in an RI meter is an antenna system with a tunable AM radio-receiver in the AM broadcast frequency ranges of 0.5 MHz to 1.6 MHz. The signal at this point is quite weak, having power of the order of pico-watts. The signal received by the antenna is therefore amplified in a radio frequency (RF) amplifier.

The next stage after the RF amplifier is the mixer, which is a nonlinear device utilised in AM. Its function is to mix the signal voltage with a local oscillator voltage wave to generate a new set of sum and difference frequencies which are then passed through the intermediate frequency (IF) amplifier stage and then through the diode detector.

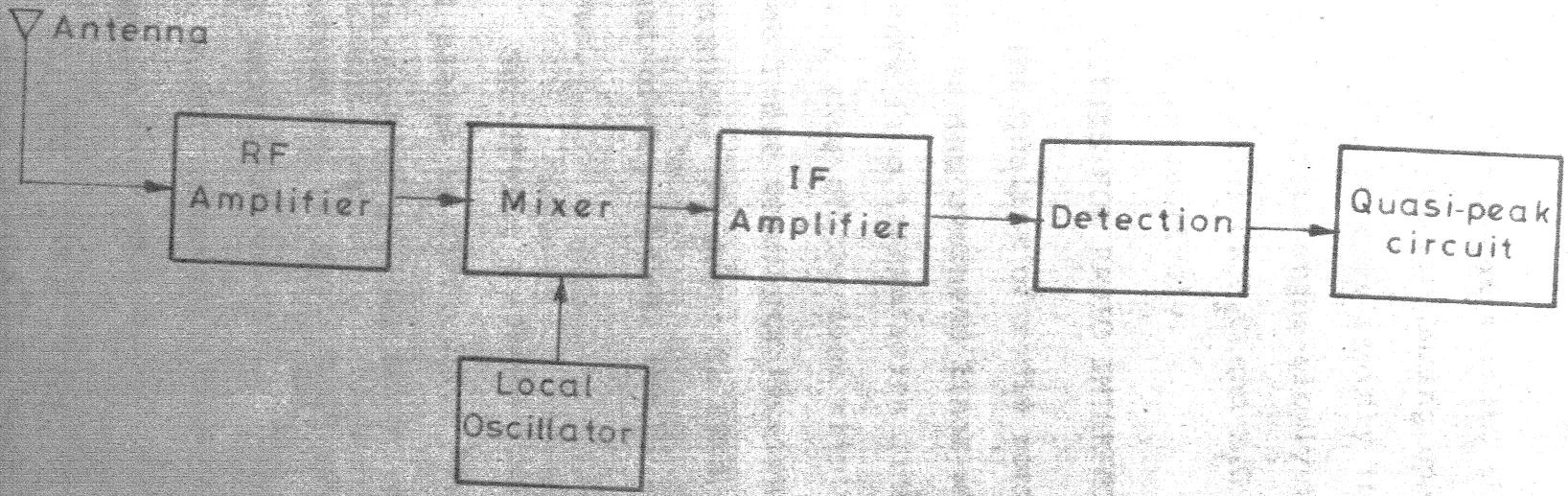

FIG·4·1a RI METER BLOCK DIAGRAM

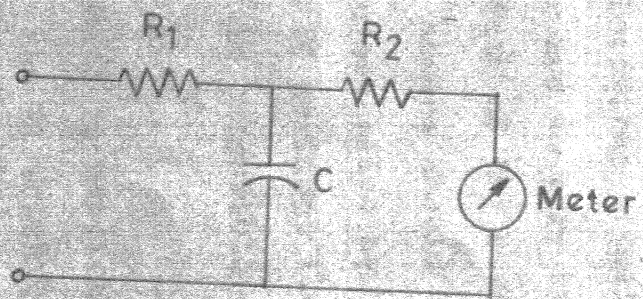

FIG·4·1b QUASI-PEAK CIRCUIT

The quasi-peak circuit shown in Fig. 4.1b is essentially a low-pass filter. During operation of the quasi-peak circuit, capacitor C charges rapidly through R_1 to almost the peak value, and discharges slowly through the high resistance R_2. Typical values of R_1C and R_2C are 1 millisecond and 600 milliseconds respectively.

4.2 LIMITS FOR RADIO INTERFERENCE

The quality of radio reception at locations situated very close to the overhead lines will be poor due to very high interference from transmission lines. The width of the corridor on either side of the line within which no houses should be built or no radio receivers located, should be specified by the power companies. In order to find this width of corridor i.e. the Right-of-Way (R-O-W) the RI limit which is acceptable should be known.

Specifying a single limit for RI which is applicable to all places is difficult. For instance, the RI which can be tolerated at a place which is situated close to the broadcast station may be quite high compared to the RI value at a place far away from the radio transmitter where the radio signals are weak. However, some countries have set limits and these figures have been quoted below :

1. Canada : In Canada, the standard has been developed by the Canadian standards association. The standard specifies

that the fair weather interference field strength, measured at 15m laterally from the outermost conductor of the power line should not exceed 60 dB above 1 μV/m at 0.5 MHz for voltages above 600 kV.

2. USSR : The RI level should be less than 40 dB at 100 metres from the outside phase at 1 MHz.

3. Czechoslovakia : The Czechoslovak standard specifies that the radio interference field under dry weather conditions and at a frequency of 0.5 MHz must not exceed 40 dB at 40m from the outermost conductor for voltages of 750 kV.

4. Poland : As per Polish standards, the interference field strength at a lateral distance of 20m from the outermost phase conductor should not exceed 750 μV/m for air humidity less than 80% and for a frequency of 0.5 MHz.

As can be seen from the values quoted, there is no uniformity of RI limit. However, for design purposes, IEEE has specified in general that the fair weather RI level at 100 feet from the outermost phase conductor should be less than 40 dB [21].

4.3 CALCULATION OF RI

Calculation of RI can be done either by using empirical relations developed on the basis of long term measurements or by using the absolute method [19] which combines in it both analytical as well as experimental work. The analytical methods are flexible because they can be used for lines of any configuration

and for any number of subconductors in a bundle, while the empirical relations for RI prediction have restricted applications.

4.3.1 Absolute Method of RI Calculation

Figure 4.2 shows a single conductor at a height H above the ground and carrying a charge q per unit length.

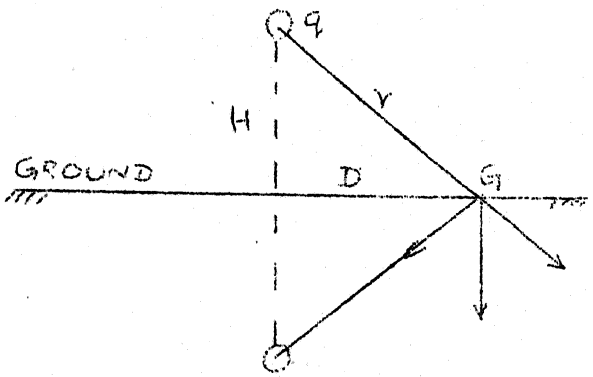

Fig. 4.3 RI due to a line charge

The radio interference field measured on a noise meter placed at the point G at a distance 'D' from the conductor will be the vertical component of the field induced by the charge 'q'.

The total vertical component at G is,

$$RI = \frac{q}{\pi \epsilon_o} \cdot \frac{H}{H^2+D^2} \qquad (4.1)$$

or

$$RI = q \left[\frac{1}{\pi \epsilon_o} \cdot \frac{1}{H} \cdot \frac{1}{1+(\frac{D}{H})^2}\right] \qquad (4.2)$$

i.e., $$RI = q.F_f \qquad (4.3)$$

F_f is called the field factor and represents the quantity within the square bracket in eqn. (4.2).

The relation between the r-f charge per unit length 'q' and the injected current 'I' has been shown in [19] to be,

$$q = I(v)^{-1} (2a)^{-1/2} \tag{4.4}$$

where

a : attenuation factor in nepers per unit length

v : velocity of light .

Combining equations (4.3) and (4.4),

$$RI = I(v)^{-1} (2a)^{-1/2} F_f \tag{4.5}$$

The next stage in RI calculation is the determination of the injected current and this forms the basis of all experimental work.

4.3.1a Computation of the Injected Current

The first step in the determination of the injected current is the establishment of the excitation function

For a multiwire line the relation between excitation function and the injected current has been shown in [25] to be :

$$[I] = \frac{1}{2\pi \epsilon_o} [C] [\tau] \tag{4.6}$$

where [I] is the matrix of injected currents in $A/m^{1/2}$, [τ] is

the matrix of excitation function in $A/m^{1/2}$ and [C] is the line capacitance matrix.

The excitation function of any bundle can be determined by performing experiments on test cages. Trinh et al have carried out such experiments with different bundles and their results have been given in the form of graphs [27]. These graphs have been shown in figure 4.3. From these graphs, the excitation function can be obtained for any bundle characterised by the radius, the number of subconductors and for values of conductor surface gradients within the range of 9kV/cm and 25 kV/cm.

For a line under consideration, the excitation function for each phase can be determined knowing the number of subconductors, the subconductor diameter and its conductor surface gradient. The injected currents can then be calculated using equation (4.6). The calculated injected currents are used to compute the RI by the application of the theory of modes of propagation.

4.3.1b Modes of Propagation

In a multiconductor system, the energy generated on one conductor will be mutually coupled to the other conductors. For 3 conductors, these mutually interacting energies can be split into 3 independent systems. This decoupling, for a perfectly transposed system of conductors, is achieved by using the normalized Clarke transformation which is given below.

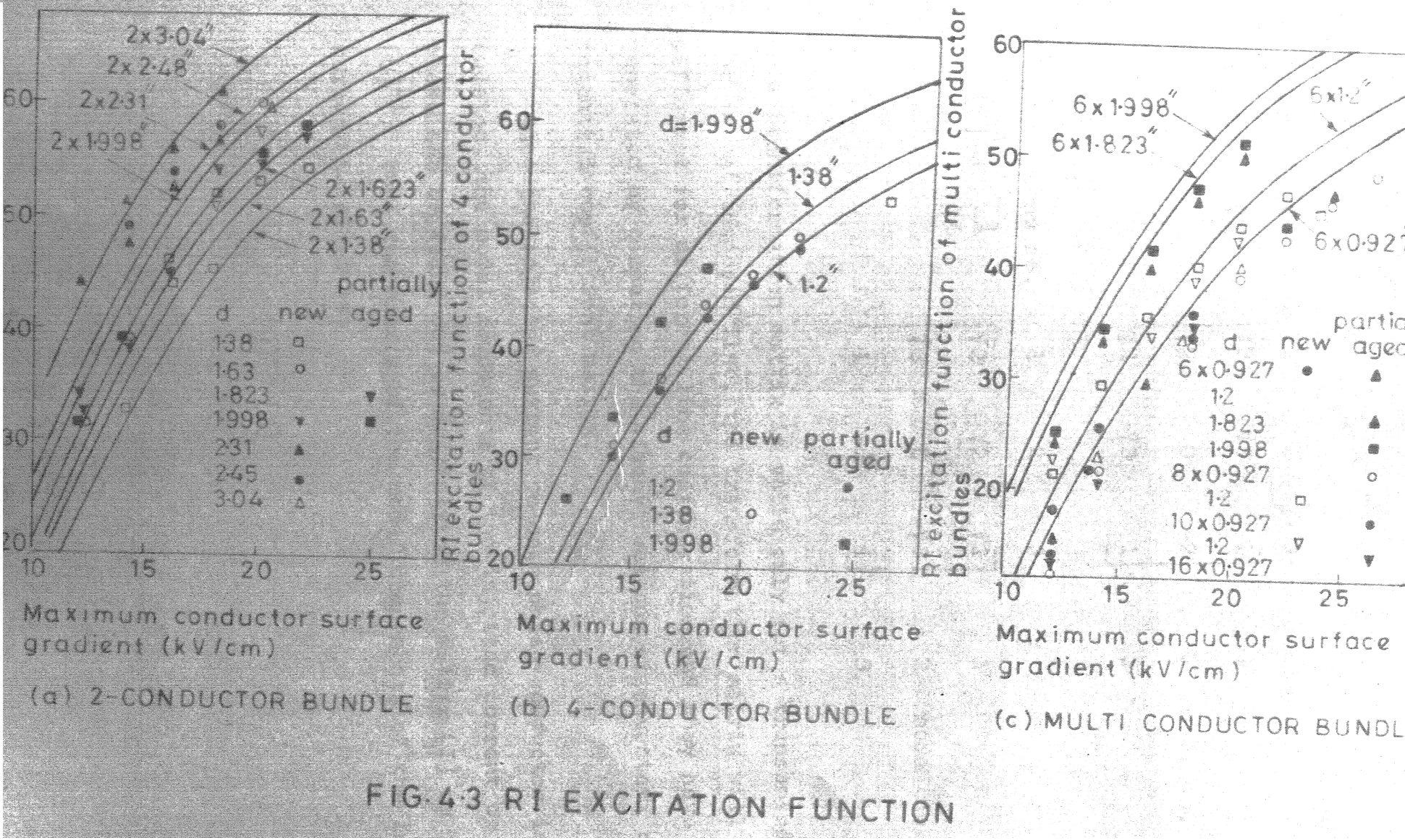

FIG. 4·3 RI EXCITATION FUNCTION

or

$$[I_c] = \begin{array}{c} \text{cond no.1} \quad 2 \quad 3 \\ \begin{bmatrix} I_1^{(1)} & I_2^{(1)} & I_3^{(1)} \\ I_1^{(2)} & I_2^{(2)} & I_3^{(2)} \\ I_1^{(3)} & I_2^{(3)} & I_3^{(3)} \end{bmatrix} \end{array} \begin{array}{l} 1 \\ 2 \text{ mode no.} \\ 3 \end{array} \qquad (4.8)$$

Equation (4.5) can then be used to calculate the RI level. If all the quantities in equation (4.5) are replaced by modal quantities, then the RI contributions due to each of the three modes on conductor 1 are ;

$$\begin{aligned} RI_1^{(1)} &= [2a^{(1)}]^{1/2} [v]^{-1} F_{f1} I_1^{(1)} \\ RI_1^{(2)} &= [2a^{(2)}]^{1/2} [v]^{-1} F_{f1} I_1^{(2)} \\ RI_1^{(3)} &= [2a^{(3)}]^{1/2} [v]^{-1} F_{f1} I_1^{(3)} \end{aligned} \qquad (4.9)$$

where,

$a^{(1)}$, $a^{(2)}$, $a^{(3)}$: attenuation factors in Nepers per unit length for mode 1,2 and 3 respectively.

$I_1^{(1)}$, $I_1^{(2)}$, $I_1^{(3)}$: The three modal components of the injected currents on the phase 1 conductor.

$$F_{f1} = \frac{1}{\pi \epsilon_o} \cdot \frac{1}{H_1} \left[\frac{1}{1+(\frac{D}{H_1})^2}\right] ,$$

and H_1 is the height of conductor 1 above the ground in metres.

The RI at point G due to phase 1 alone is then obtained by the quadratic summation of equations in (4.9).

Thus,

$$RI_1 = \sqrt{[(RI_1^{(1)})^2 + (RI_1^{(2)})^2 + (RI_1^{(3)})^2]}$$

RI_2 and RI_3, the RI's due to phases 2 and 3 respectively can be similarly computed. The summation of RI_1, RI_2 and RI_3 is given in the section below.

4.3.1c Summation of Noise Levels

If one of the fields is atleast 3 dB greater than the others, then this is considered as the RI level.

Otherwise, the two highest among the three, designated as RI_a and RI_b are used and the total RI equals;

$$\frac{RI_a+RI_b}{2} + 1.5 \text{ dB}.$$

A sample calculation, to illustrate the different steps involved, has been given in Appendix E.

4.3.2 RI Calculation Using Empirical Relation

This method of RI calculation is based on the following CIGRE formula :

$$RI_k = 3.5g_{mk} + 12\ \gamma_k - 30 - 33\ \log_{10}\left(\frac{D_k}{20}\right)\ dB \qquad (4.10)$$

$$k = 1,2,3$$

Here, RI_k : RI produced by phase conductor k

g_{mk} : maximum conductor surface gradient in kV/cm on phase k

γ_k : radius of subconductor in cms

D_k : specified in metres, is the aerial distance of the phase K from the point of noise measurement .

The limitations of this formula are :

It applies ,

1) Only in dry weather at a frequency of 0.5 MHz. This does not take into account, climatic conditions which exist in India. Hence, this can be used only for preliminary design of transmission lines and not for representing the RI levels on long term basis.
2) For maximum conductor surface gradients in the range of 12 kV/cm to 20 kV/cm.
3) For subconductor radii ranging from 1 to 2.5 cm.
4) Number of subconductors in a bundle from 1 to 4.
5) Relative subconductor spacing i.e. ratio of distance between two neighbouring subconductors to their diameters from 10 to 20.

Having calculated RI_1, RI_2 and RI_3, the summation of noise levels is done as mentioned in Section 4.3.1c. For a multi-circuit line the summation is given below. Considering for example, a 2-circuit line, there will be 2-conductors belonging to phase A, 2 conductors belonging to phase B and 2 to phase C. Initially, the RI level due to each conductor is calculated. The total RI level due to phase A is then obtained by quadratic summation of the contributions from the individual conductors of that phase. Suppose RI_{A1} and RI_{A2} are the RI levels due to the 2-conductors belonging to phase-A, then the total RI due to phase A is,

$$RI_1 = \sqrt{[(RI_{A1})^2 + (RI_{A2})^2]}$$

Similarly,

$$RI_2 = \sqrt{[(RI_{B1})^2 + (RI_{B2})^2]}$$

$$RI_3 = \sqrt{[(RI_{C1})^2 + (RI_{C2})^2]}$$

Once RI_1, RI_2 and RI_3 are found, the net RI level is calculated by a procedure. Similar to that for a single-phase case given in Section 4.3.1c.

4.4 RESULTS

Lateral profiles of Radio noise, in dB above 1 μV/m have been drawn for transmission lines of voltages ranging from

400 kV to 1300 kV. For voltages upto 750 kV the empirical relation given by CIGRE has been used and for voltages beyond this, the analytical method given in [19] has been used for calculating the RI-profile. The results of calculation have been shown in Figures 4.4 to 4.6.

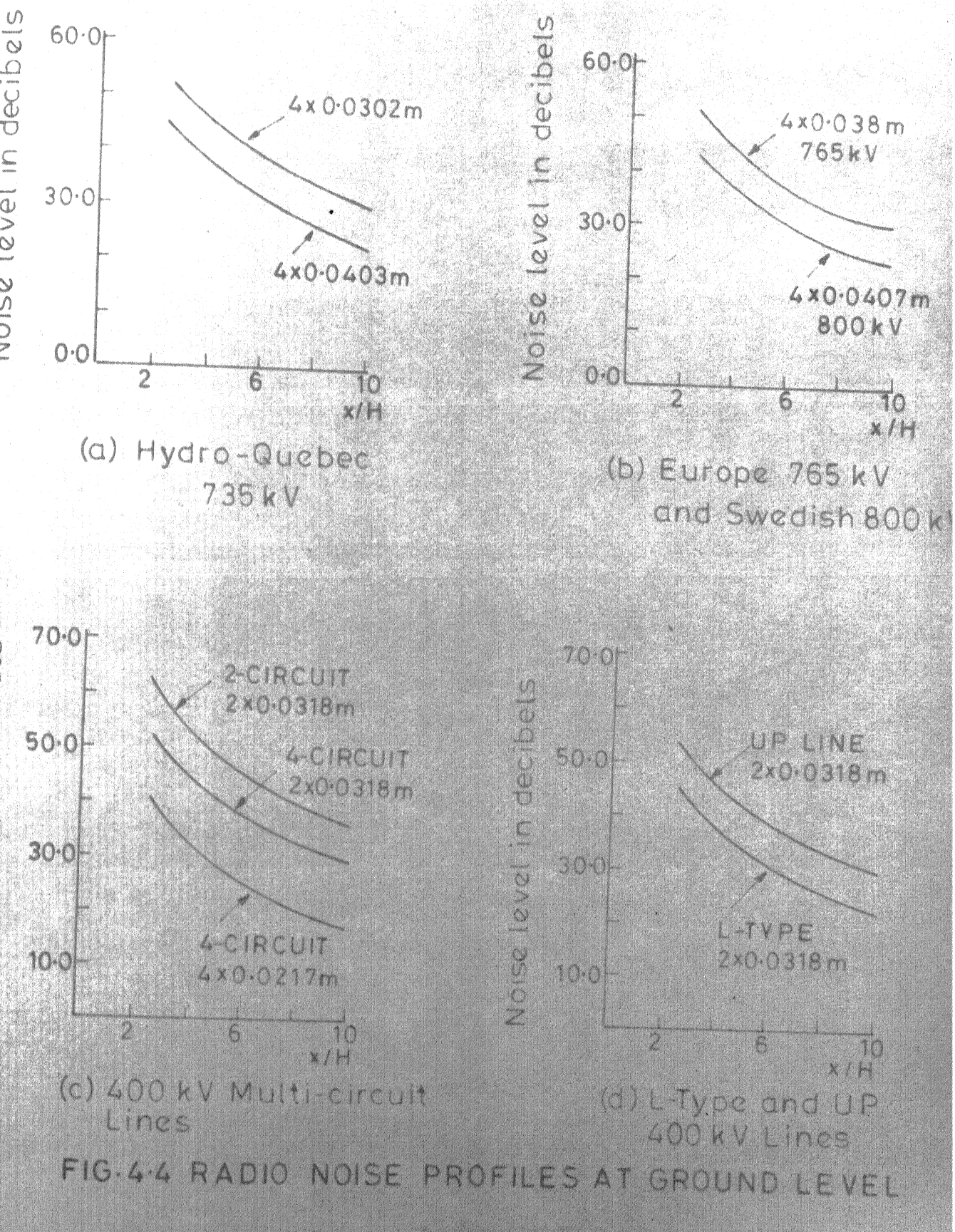

FIG·4·4 RADIO NOISE PROFILES AT GROUND LEVEL

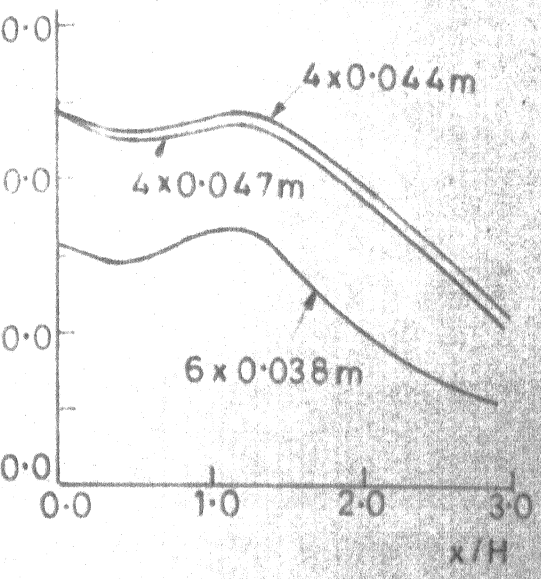

(a) Europe 1000 kV

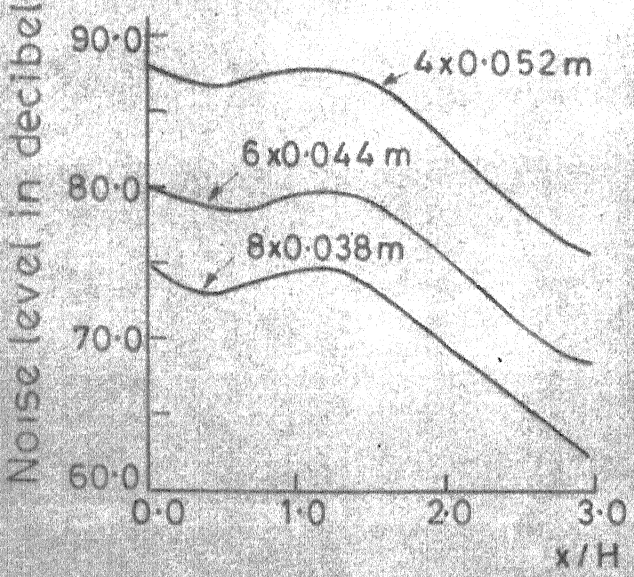

(b) Europe 1300 kV

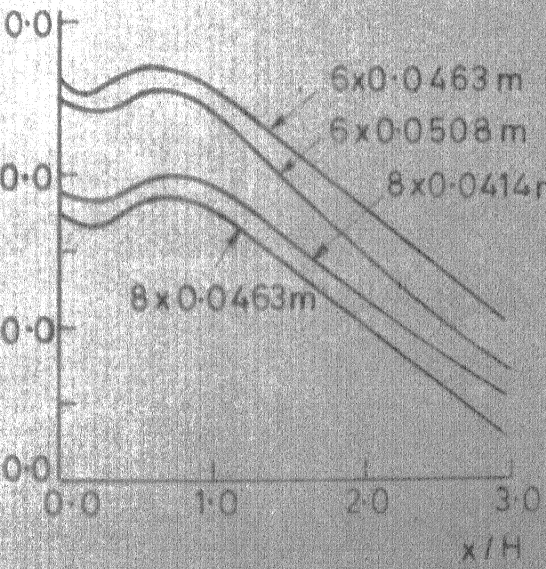

(c) Canadian 1200 kV

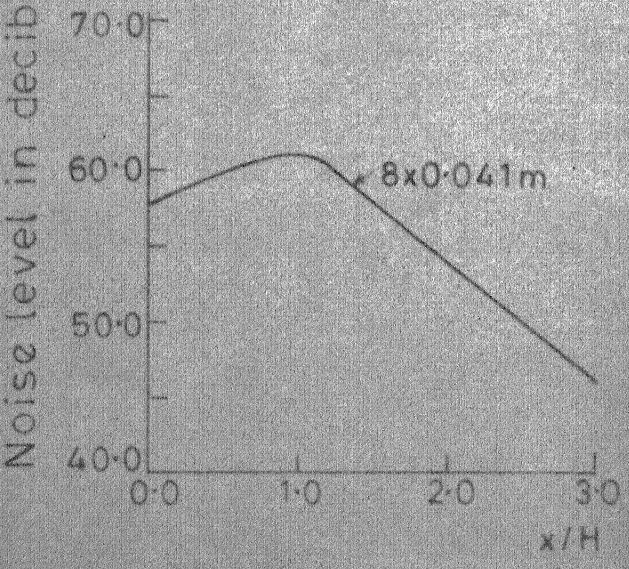

(d) BPA 1150 kV

FIG. 4·5 RADIO NOISE PROFILES AT GROUND LEVEL

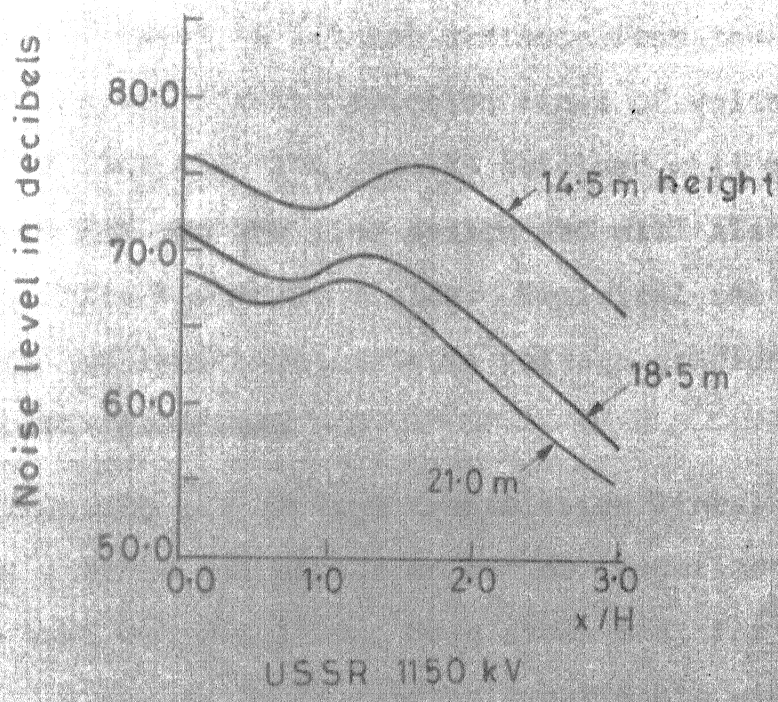

FIG·4·6 RADIO NOISE PROFILES AT GROUND LEVEL

CHAPTER 5

CONCLUSIONS

In this thesis, AN, RI and ES field estimation and their variation with respect to lateral distance from tower centre have been calculated for transmission lines of voltages ranging from 400 kV to 1300 kV. The results obtained will provide guidelines for EHV and UHV line design and will also be useful for setting limits for these fields. Empirical relations for computing the maximum electrostatic voltage gradient at ground level have been developed.

For predicting the AN from transmission lines, experiments are normally carried out either on outdoor experimental lines or by using test cages. It has been shown that for a 3-phase line, it is not necessary to perform experiments with all the three conductors. It is sufficient to carry out the experiments on a single-phase basis and the results can be extrapolated to the three-phase case by using suitable decibel adders.

Limits for AN and RI are difficult to impose on a nation wide basis. However, a value of 50 decibels at a distance of 15m from outer phase can be used for all design purposes. For the ES field, based on the safety considerations to human beings working under the transmission lines, a value of 15 kV/m can be taken as the limit [5].

The present highest transmission voltage in India is 400 kV. But by the end of this century when all regional grids will be interconnected, there will be need for a higher transmission voltage. The next higher voltage likely to be adopted is 750 kV ac. However, it is suggested that a 400 kV, 4-circuit configuration can be adopted instead of a single circuit 750 kV line. The advantage in adopting the 4-circuit configuration being, technology upto 400 kV level is readily available in India and all equipment for this level can be manufactured indigenously. The maximum electrostatic gradient at ground and the AN for the investigated 400 kV, 4-circuit configuration at 15m from the outerphase has been found to be less than the specified limits. However, the RI due to this configuration at the edge of the right-of-way is slightly higher than the limiting value of 50 decibels.

REFERENCES

1. W.V. Inkis, 'Demonstration to Public of EHV Transmission Line effects', IEEE Transactions on Power Apparatus and Systems, vol.97, No.2, March/April 1978, pp 438-443.
2. C.F. Dalziel and W.R. Lee, 'Lethal Electric Currents', IEEE Spectrum, Feb. 1969, pp 44-50.
3. D.W. Deno, 'Transmission Line Fields', IEEE Transactions on Power Apparatus and System, vol. 95, No.5, Sept/Oct.1976, pp 1600-1611.
4. L.O. Barthold et al., 'Electrostatic effects of Overhead Transmission Lines, Part I - Hazards and Effects', IEEE Transactions on Power Apparatus and Power System, vol. 91, No.2, March/April 1972, pp 422-426.
5. R.D. Begamudre, 'Limits for Interference fields from EHV and UHV Transmission Lines.Part II - Audio Noise and Electrostatic Field', CBIP 51st Research Meeting, Vadodara, Jan. 25, 1984.
6. J.W. Bankokse et al., 'Biological Effects of ELF Electric Fields - Some U.S. Research Results', (CIGRE, 1978, No. 36-05).
7. W.T. Kaune et al., 'A method for the exposure of miniature swine to vertical 60 Hz Electric Field', IEEE Transactions on Biomedical Engineering, vol. BME-25, No.3, May 1978, pp 276-283.

8. Working Group 36-07: Measurement of Electric Field in the Vicinity of HV installations - Results and lessons' (CIGRE, 1978, No. 36-07).

9. IEEE Committee Report, 'A comparison of methods for calculating Audible Noise of High Voltage Transmission Lines', IEEE Transactions on Power Apparatus and Systems, vol. PAS 101, No.10, Oct. 1982, pp 4090-4099.

10. V.L. Chartier and R.D. Stearns, 'Formulas for Predicting Audible Noise from Overhead High Voltage ac and dc Lines', IEEE Transactions on Power Apparatus and Systems, vol. PAS-100, No.1, Jan. 1981, pp 121-129.

11. IEEE Committee Report, 'Measurement of Audible Noise from Transmission Lines', IEEE Transactions on Power Apparatus and Systems, vol. PAS-100, No.3, March 1981, pp 1440-1452.

12. C.M. Harris, 'Handbook of Noise Control', (Book), New York: McGraw Hill, 1979.

13. D.N. May, 'Handbook of Noise Assessment', VanNostrand Reinhold Company: 1978.

14. IEEE Committee Report, 'A survey of methods for calculating Transmission Line Conductor Surface Voltage Gradients', IEEE Transactions on Power Apparatus and Systems, vol. PAS-98, No.6, Nov/Dec. 1979, pp 1996-2014.

15. A. Coquard and C. Gary, 'Audible Noise Produced by Electric Power Transmission Lines at Very High Voltage', Paper 36-03, presented at 1972 Session of International Conference on Large High Tension Electric Systems (CIGRE), Aug. 28 - Sept. 6, 1972.

16. IEEE Committee Report, 'CIGRE/IEEE Survey on Extra High Voltage Transmission Line Radio Noise', IEEE Transactions PAS, vol. PAS-92, May/June 1973, pp 1019-1028.

17. IEEE Committee Report, 'Comparison of Radio Noise Prediction Methods with CIGRE/IEEE Survey Results', IEEE Trans. PAS, vol. PAS-92, May/June, 1973, pp 1029-1042.

18. 'Computation of Radio Noise Levels of Existing and proposed EHV Lines in India', CPRI Report No. 101.

19. R.D. Begamudre, 'The Absolute Method of Pre-determination of Radio Noise Levels of E.H.V. A.C. and D.C. Transmission Lines', EHV Transmission Symp. vol.I, April 1980.

20. F.J. Trebby, 'Development of a Square-Law Radio Noise Meter-I', AIEE Transactions, vol.78, Part III A (Power Apparatus and Systems), August 1959, pp 522-528.

21. IEEE Committee Report, 'Radio Noise Design Guide for High Voltage Transmission Lines', IEEE Trans. PAS, vol.PAS-90, March/April 1971, pp 833-842.

22. CIGRE Working Group 36.01, 'Interference produced by Corona effect of Electric Systems', 1974.

23. C.G. Gary and M.R. Moreau, 'Predetermination of the RI Level of H.V. Transmission Lines. Part I - Predetermination of the excitation function', IEEE Trans. Power Apparatus and Systems, 1972, pp 284-91.

24. C.H. Gary and M.R. Moreau, 'Part II of the above' II - Field calculating method', Ibid, pp 292-304.

25. C.H. Gary, 'The Theory of the Excitation Function: A Demonstration of its Physical Meaning', Ibid, pp 305-310.

26. W.E. Pakala, E.R. Taylor Jr., 'A method for analysis of Radio Noise on High-Voltage Transmission Lines', IEEE Transactions on Power Apparatus and Systems, vol. PAS-87, No.2, pp 334-345, Feb. 1968.

27. N. Giao Trinh and P.S. Maruvada, 'A method of Predicting the Corona Performance of Conductor Bundles Based on Cage Test Results', IEEE Transactions on Power Apparatus and Systems, vol. PAS-96, No.1, Jan/Feb. 1977, pp 312-325.

28. IEEE Radio Noise and Corona Subcommittee Report, 'Review of Technical Considerations on limits to interference from Power Lines and Stations', IEEE Trans. Power Apparatus and Systems, vol. PAS-99, No.1, Jan/Feb. 1980.

29. L.V. Blake, 'Prevention Easier than Cure of Radio Interference', Electrical World, vol. 114, Sept. 21, 1941, pp 851-53.

30. P.S. Maruvada, N.G. Trinh, 'A Basis for Setting Limits to Radio Interference from High Voltage Transmission Lines', IEEE Trans. PAS, vol. PAS-94, Sept/Oct. 1975, pp 174-24.

31. A.S. Denholm, 'The Pulses and Radio Influence Voltage of Power Frequency Corona', AIEE Trans. vol. 79, pt-3, 1960, pp 698-707.

2. IEEE Committee Report, 'Transmission System Radio Influence', IEEE Trans. PAS, vol. PAS 1965, pp 714-724.

33. C. Gary and M. Moreau, 'Predetermination of the Radio Noise Level under Rain of an Extra High Voltage Line', IEEE Trans. PAS, vol. PAS-88, pp 653-660, May 1969.

34. O. Nigol, 'Analysis of Radio Noise from High Voltage Lines I - Meter response to Corona Pulses', IEEE Trans. PAS, vol. PAS-83, May 1964, pp 524-33.

APPENDIX A

Referring to Figure 2.1, the electric field intensity at the point P due to the charge Q is,

$$E_1 = \frac{Q}{2\pi \epsilon_o S_1} \qquad (A.1)$$

while the field intensity at P due to the image charge is,

$$E_2 = \frac{Q}{2\pi \epsilon_o S_2} \qquad (A.2)$$

Force E_1 acts in the direction along Pa while E_2 acts along Pb.

a) Derivation of the Horizontal Component

The net horizontal component of the electric field intensity at the point P is;

$$E_H = E_1 \cos\theta - E_2 \cos\alpha \qquad (A.3)$$

θ and α are as defined in the Figure A.1

where

$$\cos\theta = \frac{x-x_i}{S_1} \qquad (A.4)$$

and

$$\cos\alpha = \frac{x-x_i}{S_2}$$

From equations (A.3) and (A.4)

$$E_H = \frac{Q}{2\pi \epsilon_o} \left[\frac{x-x_i}{S_1^2} - \frac{x-x_i}{S_2^2}\right] \tag{A.5}$$

or

$$E_H = \frac{Q}{2\pi \epsilon_o} \left[\frac{x-x_i}{(x-x_i)^2+(y-y_i)^2} - \frac{x-x_i}{(x-x_i)^2+(y+y_i)^2}\right] \tag{A.6}$$

b) Derivation of Vertical Component

Referring to Figure 2.1, the net vertical component of the electric field intensity at the point P is,

$$E_v = E_1 \sin\theta - E_2 \sin\alpha \tag{A.7}$$

where

$$\sin\theta = \frac{y-y_i}{S_1} \tag{A.8}$$

and

$$\sin\alpha = \frac{y+y_i}{S_2}$$

From equations (A.7) and (A.8)

$$E_v = \frac{Q}{2\pi \epsilon_o} \left[\frac{y-y_i}{S_1^2} - \frac{y+y_i}{S_2^2}\right] \tag{A.9}$$

$$E_v = \frac{Q}{2\pi \epsilon_o} \left[\frac{y-y_i}{(x-x_i)^2+(y-y_i)^2} - \frac{y+y_i}{(x-x_i)^2+(y+y_i)^2}\right] \tag{A.10}$$

APPENDIX B

DERIVATION OF E_{Hmax} (MAXIMUM HORIZONTAL COMPONENT)

(a) For 3-Phase Single Circuit Lines

In this case, the number of line conductors, N = 3.

From equation (2.9),

$$E_{Hi} = \frac{Q_i}{2\pi \epsilon_o} \left[\frac{x-x_i}{S_{ai}^2} - \frac{x-x_i}{S_{bi}^2}\right] \qquad (B.1)$$

For the 3-phase single-circuit configuration, i = 1,2,3.

x_1, x_2 and x_3 are the horizontal distances of the line conductors 1,2 and 3 respectively from the chosen reference axes and y_1, y_2, y_3 are the vertical distances of conductors 1,2 and 3 above the ground.

S_{ai} and S_{bi} are defined as,

$$S_{ai}^2 = (x-x_i)^2 + (y-y_i)^2$$

$$S_{bi}^2 = (x-x_i)^2 + (y+y_i)^2 \qquad (B.2)$$

The vector defining the voltage is,

$$[V] = V[\sin\theta \ \sin(\theta - 120) \ \sin(\theta+120)]^t \qquad (B.3)$$

Superscript 't' indicates transpose and V is the RMS line to ground voltage.

$$E_{H1} = \frac{Q_1}{2\pi\epsilon_o}\left[\frac{x-x_1}{s_{a1}^2} - \frac{x-x_1}{s_{b1}^2}\right]$$

$$E_{H2} = \frac{Q_2}{2\pi\epsilon_o}\left[\frac{x-x_2}{s_{a2}^2} - \frac{x-x_2}{s_{b2}^2}\right] \qquad \text{(B.4)}$$

$$E_{H3} = \frac{Q_3}{2\pi\epsilon_o}\left[\frac{x-x_3}{s_{a3}^2} - \frac{x-x_3}{s_{b3}^2}\right]$$

or

$$E_{H1} = \frac{Q_1}{2\pi\epsilon_o} K_{H1}$$

$$E_{H2} = \frac{Q_2}{2\pi\epsilon_o} K_{H2} \qquad \text{(B.5)}$$

$$E_{H3} = \frac{Q_3}{2\pi\epsilon_o} K_{H3}$$

where K_{Hi}, i = 1,2,3 are as defined in equation (2.10b).

$$E_H = E_{H1} + E_{H2} + E_{H3}$$

or

$$E_H = \frac{Q_1}{2\pi\epsilon_o} K_{H1} + \frac{Q_2}{2\pi\epsilon_o} K_{H2} + \frac{Q_3}{2\pi\epsilon_o} K_{H3} \qquad \text{(B.6)}$$

Substituting equation (2.7) into equation (A.6), and re-arranging the terms

$$E_H = [(K_{H1}\, M(1,1) + K_{H2}\, M(2,1) + K_{H3}\, M(3,1))\sin\theta + (K_{H1}\, M(1,2) + K_{H2}\, M(2,2) + K_{H3}\, M(3,2))\, \sin(\theta-120) + (K_{H1}\, M(1,3) + K_{H2}\, M(2,3) + K_{H3}\, M(3,3))\, \sin(\theta+120)]x\ V \qquad (B.7)$$

Define,

$$JH(1) = [K_{H1}\, M(1,1) + K_{H2}\, M(2,1) + K_{H3}\, M(3,1)]x\ V$$

$$JH(2) = [K_{H1}\, M(1,2) + K_{H2}\, M(2,2) + K_{H3}\, M(3,2)]x\ V \qquad (B.8)$$

$$JH(3) = [K_{H1}\, M(1,3) + K_{H2}\, M(2,3) + K_{H3}\, M(3,3)]x\ V$$

Thus,

$$E_H = JH(1)\ \sin\theta + JH(2)\ \sin(\theta-120) + JH(3)\ \sin(\theta+120) \qquad (B.9)$$

By adding and subtracting JH(2) sin(θ+120), the resulting equation is,

$$E_H = JH(1)\ \sin\theta + JH(2)\ \sin(\theta-120) + JH(3)\ \sin(\theta+120) + JH(2)\ \sin(\theta+120) - JH(2)\ \sin(\theta+120)$$

or

$$E_H = [JH(1) - 0.5(JH(2) + JH(3))] \sin\theta + \frac{\sqrt{3}}{2} [JH(3) - JH(2)] \cos\theta \qquad (B.10)$$

Differentiating E_H with respect to θ and setting it equal to zero, θ_{max} is found.

$$\tan \theta_{max} = \sqrt{\frac{2}{3}} \left[\frac{JH(1)-0.5(JH(2)+JH(3))}{JH(3) - JH(2)}\right]$$

or

$$\theta_{max} = \tan^{-1} \left\{ \frac{2}{\sqrt{3}} \left[\frac{JH(1)-0.5(JH(2)+JH(3))}{JH(3)-JH(2)}\right] \right\} \qquad (B.10a)$$

Substituting this value of θ_{max} in equation (B.9),

$$E_{Hmax} = [JH(1) - 0.5(JH(2)+JH(3))] \sin\theta_{max} - \frac{\sqrt{3}}{2} [JH(2) - JH(3)] \cos\theta_{max} \qquad (B.11a)$$

Also,

$$E_{Hmax} = \sqrt{(JH(1)-0.5\ JH(2)-0.5\ JH(3))^2 + \frac{3}{4} (JH(2)-JH(3))^2} \qquad (B.11b)$$

(b) For 3-Phase Double Circuit Lines

Here N = 6 and the vector of voltage is given by,

$$[V] = V[\sin\theta\ \sin\theta\ \sin(\theta-120)\ \sin(\theta-120)\ \sin(\theta+120)\ \sin(\theta+120)]^t \qquad (B.12)$$

Thus,

$$E_H = \frac{Q_1}{2\pi\epsilon_o} K_{H1} + \frac{Q_2}{2\pi\epsilon_o} K_{H2} + \ldots + \frac{Q_6}{2\pi\epsilon_o} K_{H6} \qquad (B.13)$$

Substituting equation (2.7) into equation (B.13),

$$\begin{aligned} E_H = \{ & [M(1,1)\sin\theta + M(1,2)\sin\theta + M(1,3)\sin(\theta-120) + \ldots + \\ & M(1,6)\sin(\theta+120)]K_{H1} + \ldots + M(6,1)\sin\theta + M(6,2)\sin\theta + \\ & M(6,3)\sin(\theta-120) + \ldots M(6,6)\sin(\theta+120)]K_{H6}\} \times V \end{aligned} \qquad (B.14)$$

or

$$E_H = JH(1)\sin\theta + JH(2)\sin(\theta-120) + JH(3)\sin(\theta+120) \qquad (B.15)$$

where JH(1), JH(2) and JH(3) are defined as,

$$\begin{aligned} JH(1) = \{ & [M(1,1)+M(1,2)]K_{H1} + [M(2,1)+M(2,2)]K_{H2} + \\ & [M(3,1)+M(3,2)]K_{H3} + [M(4,1)+M(4,2)]K_{H4} + \\ & [M(5,1)+M(5,2)]K_{H5} + [M(6,1)+M(6,2)]K_{H6}\} \times V \end{aligned}$$

$$\begin{aligned} JH(2) = \{ & [M(1,3)+M(1,4)]K_{H1} + [M(2,3)+M(2,4)]K_{H2} + \\ & [M(3,3)+M(3,4)+K_{H3} + [M(4,3)+M(4,4)]K_{H4} + \\ & [M(5,3)+M(5,4)]K_{H5} + [M(6,3)+M(6,4)]K_{H6}\} \times V \end{aligned} \qquad (B.16)$$

$$\begin{aligned} JH(3) = \{ & [M(1,5)+M(1,6)]K_{H1} + [M(2,5)+M(2,6)]K_{H2} + \\ & [M(3,5)+M(3,6)]K_{H3} + [M(4,5)+M(4,6)]K_{H4} + \\ & [M(5,5)+M(5,6)]K_{H5} + [M(6,5)+M(6,6)]K_{H6}\} \times V \end{aligned}$$

By a similar procedure as outlined for 3-phase single circuit case, θ_{max} can be computed and hence E_{Hmax} found from equation (B.15)

$$E_{Hmax} = \sqrt{(JH(1)-0.5JH(2)-0.5JH(3))^2+ \frac{3}{4} (JH(2)-JH(3))^2} \qquad (B.17)$$

(c) For 3-Phase, 4-Circuit Line

N = 12 and the vector of voltage is,

$$[V] = [V_a \; V_b \; V_c]^t \qquad (B.18)$$

where V_a, V_b and V_c are the vector of voltages of phases a,b and c respectively and are defined as,

$$[V_a] = V[\sin\theta \; \sin\theta \; \sin\theta \; \sin\theta]$$

$$[V_b] = V[\sin(\theta-120) \; \sin(\theta-120) \sin(\theta-120) \; \sin(\theta-120)]$$

and

$$[V_c] = V[\sin(\theta+120) \; \sin(\theta+120) \; \sin(\theta+120) \; \sin(\theta+120)] \qquad (B.19)$$

Thus,

$$E_H = \frac{Q_1}{2\pi\epsilon_o} K_{H1} + \ldots + \frac{Q_{12}}{2\pi\epsilon_o} K_{H12} \qquad (B.20)$$

By substituting equation (2.7) into (B.20) and by suitably rearranging the equation as was done for the earlier case, we

can write E_H in terms of JH(1), JH(2) and JH(3).

$$E_H = JH(1)\sin\theta + JH(2)\sin(\theta-120) + JH(3)\sin(\theta+120) \quad (B.21)$$

where

$$JH(1) = \{[M(1,1)+M(1,2)+M(1,3)+M(1,4)]K_{H1} + \ldots$$

$$\ldots+[M(12,1)+M(12,2)+M(12,3)+M(12,4)]K_{H12}\} \times V \quad (B.22)$$

$$JH(2) = \{[M(1,5)+\ldots+M(1,8)]K_{H1}+[M(12,5)+\ldots+M(12,8)]\} \times V$$

and

$$JH(3) = \{[M(1,9)+\ldots+M(1,12)]K_{H1}+\ldots[M(12,9)+\ldots+M(12,12)]\} \times V$$

From equation (B.21), E_{Hmax} can be found out

$$E_{Hmax} = \sqrt{(JH(1)-0.5JH(2)-0.5JH(3))^2+\frac{3}{4}(JH(2)-JH(3))^2} \quad (B.23)$$

(d) For 6-Phase Lines without Ground Wires

Here N = 6 and the vector of voltages is,

$$[V] = V[\sin\theta \ \sin(\theta-60) \ \sin(\theta-120) \ \sin(\theta-180) \ \sin(\theta-240) \times \sin(\theta-300)]^t \quad (B.24)$$

$$E_H = \frac{Q_1}{2\pi\epsilon_o} K_{H1} + \ldots + \frac{Q_6}{2\pi\epsilon_o} K_{H6} \quad (B.25)$$

Substituting for $\frac{Q}{2\pi\epsilon_o}$ from equation (2.7) into equation (B.25),

$$E_H = \{[M(1,1)\sin\theta + \ldots + M(1,6)\sin(\theta-300)]K_{H1}$$

$$+[M(2,1)\sin\theta + \ldots + M(2,6)\ \sin(\theta-300)]K_{H2} \qquad \text{(B.26)}$$

$$+ \ldots + [M(6,1)\sin\theta + \ldots + M(6,6)\ \sin(\theta-300)]K_{H6}\} \times V$$

or

$$E_H = JH(1)\ \sin\theta + JH(2)\sin(\theta-60) + \ldots + JH(6)\sin(\theta-300) \qquad \text{(B.27)}$$

where

$$JH(1) = [M(1,1)\ K_{H1} + \ldots + M(6,1)\ K_{H6}]V$$

$$JH(2) = [M(1,2)\ K_{H1} + \ldots + M(6,2)\ K_{H6}]V \qquad \text{(B.28)}$$

$$\vdots$$

$$JH(6) = [M(1,6)\ K_{H1} + \ldots + M(6,6)\ K_{H6}]V$$

Differentiating equation (B.27) with respect to θ and equating it to zero, θ_{max} is obtained.

$$\theta_{max} = \tan^{-1}\left[\frac{2(JH(1)-JH(4))+JH(2)+JH(6)-JH(3)-JH(5)}{\sqrt{3}\ (JH(5)+JH(6)-JH(2)-JH(3))}\right] \qquad \text{(B.29)}$$

Substituting the value of θ_{max} in equation (B.27), E_{Hmax} is obtained.

$$E_{Hmax} = JH(1)\sin\theta_{max}+JH(2)\sin(\theta_{max}-60)+ \ldots + JH(6)\sin(\theta_{max}-300) \qquad \text{(B.30)}$$

Also,

$$E_{Hmax} = \sqrt{[(JH(1)-JH(4)+0.5JH(2)+0.5JH(6)-0.5JH(3)-0.5JH(5))^2 + \frac{3}{4}(JH(2)+JH(3)-JH(5)-JH(6))^2]} \quad (B.31)$$

(e) For 6-Phase Lines with Two Ground Wires

In this case, N = 8 and voltage vector is defined as,

$$[V] = V[\sin\theta \ \sin(\theta-60) \ \sin(\theta-120) \ \sin(\theta-240) \ \sin(\theta-300) \ 0 \ 0]^t \quad (B.32)$$

The last two entries in equation (B.32) are zero because the two ground wires are at zero potential.

Again,

$$E_H = \frac{Q_1}{2\pi\epsilon_o} K_{H1} + \ldots + \frac{Q_6}{2\pi\epsilon_o} K_{H6}$$

or

$$E_H = \{[M(1,1)\sin\theta + M(1,2)\sin(\theta-60) + \ldots + M(1,6)\sin(\theta-300)]K_{H1}$$
$$+ M(2,1)\sin\theta + M(2,2)\sin(\theta-60) + \ldots + M(2,6)\sin(\theta-300)]K_{H2}$$
$$+ \ldots + M(8,1)\sin\theta + M(8,2)\sin(\theta-60)$$
$$+ \ldots + M(8,6)\sin(\theta-300)]K_{H8}\}x \ V \quad (B.33)$$

In a compact form, equation (B.33) can be written as

$$E_H = JH(1)\ \sin\theta + \ldots + JH(6)\ \sin(\theta-300) \qquad (B.34)$$

where

$$JH(1) = [M(1,1)K_{H1} + \ldots + M(8,1)\ K_{H8}]\ V$$

$$\vdots$$

$$JH(6) = [M(1,6)K_{H1} + \ldots + M(8,6)\ K_{H8}]V \qquad (B.35)$$

By following the same procedure as outlined for the 6-phase line without ground wire, θ_{max} can be found and E_{Hmax} computed. E_{Hmax} can also be obtained by using equation (B.31).

APPENDIX C

CALCULATION OF VERTICAL COMPONENT (E_{Vmax})

(a) For 3-Phase Single Circuit Lines

N = 3 and the vector of voltages is as defined in equation(B.3).

From equation (2.13),

$$E_{Vi} = \frac{Q_i}{2\pi \epsilon_o} \left[\frac{y-y_i}{S_{ai}^2} - \frac{y+y_i}{S_{bi}^2}\right] \qquad (C.1)$$

S_{ai}^2 and S_{bi}^2 are defined in equations (B.2).

The total vertical component due to all the three line-conductors is,

$$E_V = E_{V1} + E_{V2} + E_{V3}$$

i.e.,

$$E_V = \frac{Q_1}{2\pi \epsilon_o} K_{V1} + \frac{Q_2}{2\pi \epsilon_o} K_{V2} + \frac{Q_3}{2\pi \epsilon_o} K_{V3}$$

$$E_V = \Big\{ [M(1,1)\sin\theta + M(1,2)\sin(\theta-120) + M(1,3)\sin(\theta+120)]K_{V1}$$

$$+[M(2,1)\sin\theta + M(2,2)\sin(\theta-120) + M(2,3)\sin(\theta+120)]K_{V2}$$

$$+[M(3,1)\sin\theta + M(3,2)\sin(\theta-120) + M(3,3)\sin(\theta+120)]K_{V3} \Big\} \text{ V} \qquad (C.2)$$

or

$$E_V = JV(1)\sin\theta + JV(2)\sin(\theta-120) + JV(3)\sin(\theta+120) \qquad (C.3)$$

where

$$JV(1) = [M(1,1)K_{V1} + M(2,1)K_{V2} + M(3,1)K_{V3}]V$$

$$JV(2) = [M(1,2)K_{V1} + M(2,2)K_{V2} + M(3,2)K_{V3}]V \qquad (C.4)$$

$$JV(3) = [M(1,3)KV_1 + M(2,3)K_{V2} + M(3,3)K_{V3}]V$$

Equation (C.3) can be reduced to the form ;

$$E_v = [JV(1)-0.5JV(2)-0.5JV(3)]\sin\theta + \frac{\sqrt{3}}{2}[JV(3)-JV(2)]\cos\theta \qquad (C.5)$$

By differentiating equation (C.5) with respect to θ and equating it to zero, θ_{max} can be found.

$$\theta_{max} = \tan^{-1}\left\{\frac{2}{\sqrt{3}}\left[\frac{JV(1)-0.5JV(2)-0.5JV(3)}{JV(3)-JV(2)}\right]\right\} \qquad (C.6)$$

Substituting equation (C.6) in equation (C.5), E_{vmax} is obtained. Also,

$$E_{vmax} = \sqrt{(JV(1)-0.5JV(2)-0.5JV(3))^2 + \frac{3}{4}(JV(3)-JV(2))^2} \qquad (C.7)$$

(b) For 3-Phase Double Circuit Lines

Here N = 6 and the vector of voltage is as defined by the equation (B.12)

$$E_v = \frac{Q_1}{2\pi\epsilon_o}K_{v1} + \frac{Q_2}{2\pi\epsilon_o}K_{v2} + \ldots + \frac{Q_6}{2\pi\epsilon_o}K_{v6}$$

Hence $E_v = \{[M(1,1)\sin\theta + \ldots + M(1,6)\sin(\theta+120)]K_{v1}$ (C.8)

$+\ldots+[M(6,1)\sin\theta+\ldots+ M(6,6)\sin(\theta+120)]K_{v6}\}\times V$

i.e., $E_v = JV(1)\sin\theta+JV(2)\sin(\theta-120)+JV(3)\sin(\theta+120)$ (C.9)

where,

$$JV(1) = \{[M(1,1)+M(1,2)]K_{v1}+\ldots+[M(6,1)+M(6,2)]K_{v6}\}\ V$$

$$JV(2) = \{[M(1,3)+M(1,4)]K_{v1}+\ldots+[M(6,3)+M(6,4)]K_{v6}\}\ V \quad (C.10)$$

$$JV(3) = \{[M(1,5)+M(1,6)]K_{v1}+\ldots+[M(6,5)+M(6,6)]K_{v6}\}\ V$$

From equation (C.9), θ_{max} can be found and E_{vmax} computed.

$$E_{vmax} = \sqrt{(JV(1)-0.5JV(2)-0.5JV(3))^2 + \frac{3}{4}(JV(3)-JV(2))^2}$$

(c) For 3-Phase, 4-Circuit Line

N = 12 and the vector of voltage is as defined by equations (B.18) and (B.19).

Thus,

$$E_v = \frac{Q_1}{2\pi\epsilon_o} K_{v1} + \ldots + \frac{Q_{12}}{2\pi\epsilon_o} K_{v12} \quad (C.11)$$

Substituting equation (2.7) in equation (C.10),

$$E_v = \{[M(1,1)\sin\theta+M(1,2)\sin\theta + \ldots +M(1,12)\sin(\theta+120)]K_{v1}$$

$$+\ldots+[M(12,1)\sin\theta+\ldots+M(12,12)\sin(\theta+120)]K_{v12}\} V \qquad (C.12)$$

or

$$E_v = JV(1)\sin\theta+JV(2)\sin(\theta-120)+JV(3)\sin(\theta+120) \qquad (C.13)$$

where

$$JV(1) = \{[M(1,1)+M(1,2)+M(1,3)+M(1,4)]K_{v1}$$

$$+\ldots+ [M(12,1)+M(12,2)+M(12,3)+M(12,4)]K_{v12}\} V$$

$$JV(2) = \{[M(1,5)+M(1,6)+M(1,7)+M(1,8)]K_{v1}$$

$$+\ldots+[M(12,5)+M(12,6)+M(12,7)+M(12,8)]K_{v12}\} V \qquad (C.14)$$

$$JV(3) = \{[M(1,9)+M(1,10)+M(1,11)+M(1,12)]K_{v1}$$

$$+\ldots+[M(12,9)+M(12,10)+M(12,11)+M(12,12)]K_{v12}\} V$$

From equation (C.13), θ_{max} and hence E_{vmax} can be computed. Also,

$$E_{vmax} = \sqrt{(JV(1)-0.5JV(2)-0.5JV(3))^2+ \frac{3}{4}(JV(3)-JV(2))^2}$$

(d) 6-Phase Lines Without Ground Wires

Here N = 6 and the vector of voltage is given by equation (B.24)

$$E_v = \frac{Q_1}{2\pi\epsilon_o} K_{v1} + \ldots + \frac{Q_6}{2\pi\epsilon_o} K_{v6}$$

or

$$E_v = \{[M(1,1)\sin\theta+\ldots+M(1,6)\sin(\theta-300)]K_{v1}$$
$$+[M(2,1)\sin\theta+\ldots+M(2,6)\sin(\theta-300)]K_{v2}$$
$$\vdots$$
$$+ M(6,1)\sin\theta+\ldots+M(6,6)\sin(\theta-300)]K_{v6}\} V$$

i.e., $E_v = JV(1)\sin\theta+JV(2)\sin(\theta-60)+\ldots+JV(6)\sin(\theta-300)$ (C.15)

where $JV(1) = [M(1,1)K_{v1}+M(2,1)K_{v2}+\ldots+M(6,1)K_{v6}]V$
$\vdots$
$JV(6) = [M(1,6)K_{v1}+M(2,6)K_{v2}+\ldots+(6,6)K_{v6}]V$ (C.16)

Differentiating equation (C.15) with respect to 'θ' and equating it to zero, θ_{max} is obtained,

$$\theta_{max} = \tan^{-1}\left[\frac{2JV(1)-2JV(4)+JV(2)+JV(6)-JV(3)-JV(5)}{\sqrt{3}(JV(5)+JV(6)-JV(2)-JV(3))}\right] \quad (C.17)$$

Substitution of equation (C.17) in equation (C.15) gives E_{vmax}. E_{vmax} is also given by,

$$E_{vmax} = \sqrt{(JV(1)-JV(4)+0.5JV(2)+0.5JV(6)-0.5JV(3)-0.5JV(5))^2 + \frac{3}{4}(JV(2)+JV(3)-JV(5)-JV(6))^2} \quad (C.18)$$

(e) 6-Phase Lines with Two Ground Wires

N=8 and the voltages are as defined in equation (B.32)

$$E_v = \frac{Q_1}{2\pi \epsilon_o} K_{v1} + \ldots + \frac{Q_6}{2\pi \epsilon_o} K_{v6} \qquad (C.19)$$

Substitution of equation (2.7) in equation (C.19) gives,

$$E_v = \{[M(1,1)\sin\theta + \ldots + M(1,6)\sin(\theta-300)]K_{v1} + \ldots$$

$$+[M(8,1)\sin\theta + \ldots + M(8,6)\sin(\theta-300)]K_{v8}\} V$$

or

$$E_v = JV(1)\ \sin\theta + \ldots + JV(6)\ \sin(\theta-300) \qquad (C.20)$$

where

$$\begin{aligned} JV(1) &= [M(1,1)K_{v1} + \ldots + M(8,1)K_{v8}]V \\ &\vdots \\ JV(6) &= [M(1,6)K_{v1} + \ldots + M(8,6)K_{v8}]V \end{aligned} \qquad (C.21)$$

From equation (C.20), θ_{max} and hence E_{vmax} can be obtained. E_{vmax} is also given by equation (C.18). However, JV's for this case are as defined in equations(C.21).

APPENDIX D

DERIVATION OF E_{Tmax} (maximum Total Component)

The total component E_T is given by,

$$E_T^2 = E_H^2 + E_V^2 \qquad (D.1)$$

(a) 3-Phase Lines

For 3-Phase (Single, Double and four-circuit) lines, E_H and E_V can be written as,

$$E_H = [JH(1)-0.5JH(2)-0.5JH(3)]\sin\theta + \frac{\sqrt{3}}{2}[JH(3)-JH(2)]\cos\theta$$

and

$$E_V = [JV(1)-0.5JV(2)-0.5JV(3)]\sin\theta + \frac{\sqrt{3}}{2}[JV(3)-JV(2)]\cos\theta$$

or

$$E_V = A\sin\theta + B\cos\theta$$

and

$$E_H = D\sin\theta + E\cos\theta$$

where

$$A = [JV(1)-0.5JV(2)-0.5JV(3)]$$

$$B = [JV(3)-JV(2)]\frac{\sqrt{3}}{2} \qquad (D.2)$$

$$D = [JH(1)-0.5JH(2)-0.5JH(3)]$$

$$E = [JH(3)-JH(2)]\frac{\sqrt{3}}{2}$$

(b) 6-Phase Lines

For 6-Phase lines (with and without ground wires), E_V and E_H can be written as,

$$E_V = JV(1)\sin\theta+JV(2)\sin(\theta-60)+JV(3)\sin(\theta-120)+JV(4)\sin(\theta-180)$$
$$+ JV(5)\sin(\theta-240)+JV(6)\sin(\theta-300)$$

i.e.,

$$E_V = [JV(1)\sin\theta+JV(2)(0.5\sin\theta - \frac{\sqrt{3}}{2}\cos\theta)+JV(3)(-0.5\sin\theta- \frac{\sqrt{3}}{2}\cos\theta)$$
$$+ JV(4)(-\sin\theta)+JV(5)(-0.5\sin\theta+ \frac{\sqrt{3}}{2}\cos\theta)$$
$$+ JV(6)(0.5\sin\theta+ \frac{\sqrt{3}}{2}\cos\theta)]$$

i.e.,

$$E_V = [JV(1)+ \frac{JV(2)}{2} - \frac{JV(3)}{2} - JV(4) - \frac{JV(5)}{2} + \frac{JV(6)}{2}]\sin\theta$$
$$+ \frac{\sqrt{3}}{2}[JV(5)+JV(6)-JV(2)-JV(3)]\cos\theta \qquad (D.3)$$

Similarly, it can be shown that

$$E_H = [JH(1)+ \frac{JH(2)}{2} - \frac{JH(3)}{2} - JH(4) - \frac{JH(5)}{2} + \frac{JH(6)}{2}]\sin\theta$$
$$+ \frac{\sqrt{3}}{2}[JH(5)+JH(6)-JH(2)-JH(3)]\cos\theta \qquad (D.4)$$

Equations (D.3) and (D.4) can be written as,

$$E_V = A\sin\theta + B\cos\theta$$

$$E_H = D\sin\theta + E\cos\theta$$

where

$$A = [JV(1) + \frac{JV(2)}{2} - \frac{JV(3)}{2} - JV(4) - \frac{JV(5)}{2} + \frac{JV(6)}{2}]$$

$$B = \frac{\sqrt{3}}{2} [JV(5) + JV(6) - JV(2) - JV(3)]$$

$$D = [JH(1) + \frac{JH(2)}{2} - \frac{JH(3)}{2} - JH(4) - \frac{JH(5)}{2} + \frac{JH(6)}{2}] \qquad (D.5)$$

$$E = \frac{\sqrt{3}}{2} [JH(5) + JH(6) - JH(2) - JH(3)]$$

Thus, for any line configuration, E_V and E_H can in general be written as,

$$E_V = A\sin\theta + B\cos\theta$$

$$E_H = D\sin\theta + E\cos\theta \qquad (D.6)$$

Substituting equations (D.6) in (D.1),

$$E_T^2 = A^2\sin^2\theta + B^2\cos^2\theta + 2AB\sin\theta\cos\theta + D^2\sin^2\theta + E^2\cos^2\theta + 2DE \sin\theta \cos\theta$$

or

$$E_T^2 = (A^2+D^2-B^2-E^2)\sin^2\theta + (AB+DE)\sin 2\theta + (B^2+E^2) \qquad (D.7)$$

When E_T is maximum, it is evident that E_T^2 is also maximum. Differentiating equation (D.7) with respect to θ and equating it to zero,

$$\frac{d}{d\theta}(E_T^2) = 2(A^2+D^2-B^2-E^2)\sin\theta\cos\theta+2(AB+DE)\cos2\theta = 0$$

This gives:

$$\tan2\theta_{max} = \left[\frac{2(AB + DE)}{(B^2+E^2)-(A^2+D^2)}\right]$$

or

$$\theta_{max} = 0.5 \tan^{-1}\left[\frac{2(AB + DE)}{(B^2+E^2)-(A^2+D^2)}\right] \qquad (D.8)$$

Knowing θ_{max}, E_{Tmax} can be found from equation (D.7)

$$E_{Tmax}^2 = (A^2+D^2-B^2-E^2)\sin^2\theta_{max}+(AB+DE)\sin2\theta_{max}+(B^2+E^2) \qquad (D.9)$$

Equation (D.8) holds for any line configuration, however, the values of A,B,D and E will be different for different cases as given below.

(i) For 3-Phase Single Circuit Lines

JH(1), JH(2), JH(3) and JV(1), JV(2), JV(3) can be calculated from equations (B.8) and (C.4) respectively. Knowing JH's and JV's, A,B,D and E can be found. θ_{max} is then calculated using equation (D.8) and E_{Tmax} is computed using equation (D.9).

(ii) For 3-Phase Double Circuit Lines

In this case, JH's and JV's are defined by equations (B.16) and (C.10) respectively. Values of A,B,D and E can then

APPENDIX E

A sample calculation, to illustrate the computation of RI using the analytical method has been given below.

The line considered is the single circuit, 3-phase 400 kV. The line configuration and the dimension are shown in Figure E.1.

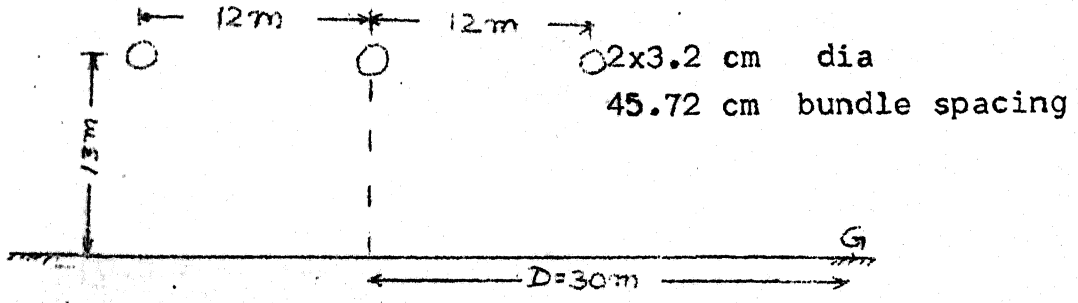

Figure E.1 Line dimension for sample RI calculation

The ground level RI has been computed at the point G, 30 metres from the line centre.

The potential coefficient matrix is,

$$[P] = \begin{bmatrix} 3.41 & 0.87 & 0.39 \\ 0.87 & 3.41 & 0.87 \\ 0.39 & 0.87 & 3.41 \end{bmatrix} \qquad \text{(E.1)}$$

and the inverse of the potential coefficient matrix,

$$[M] = \frac{1}{34.56}\begin{bmatrix} 10.87 & -2.63 & -0.57 \\ -2.63 & 11.48 & -2.63 \\ -0.57 & -2.63 & 10.87 \end{bmatrix}$$

or

$$[M] = \begin{bmatrix} 0.31 & -0.08 & -0.02 \\ -0.08 & 0.33 & -0.08 \\ -0.02 & -0.08 & 0.31 \end{bmatrix} \qquad \text{(E.2)}$$

The eigenvalues and the corresponding eigenvectors of the potential coefficient matrix is then obtained.

The matrix of eigenvectors is denoted by [U]

$$[U] = \begin{bmatrix} 0.538 & 0.707 & 0.459 \\ 0.650 & 0 & -0.760 \\ 0.538 & -0.707 & 0.459 \end{bmatrix}$$

and

$$[U]^{-1} = \begin{bmatrix} 0.538 & 0.650 & 0.538 \\ 0.707 & 0 & -0.707 \\ 0.459 & -0.760 & 0.459 \end{bmatrix} \qquad \text{(E.3)}$$

(E.3) is the transformation matrix which will decompose the mutually interacting energies of a 3-phase system into 3-independent systems.

The excitation functions τ_1, τ_2 and τ_3 for phases 1,2 and 3 respectively at 1 MHz are then obtained from the graphs given in [27]. The system matrix of the excitation function is,

$$[\tau] = \begin{bmatrix} \tau_1 & 0 & 0 \\ 0 & \tau_2 & 0 \\ 0 & 0 & \tau_3 \end{bmatrix}$$

For the configuration shown in Figure E.1, the [ ] matrix is,

$$[\tau] = \begin{bmatrix} 39.5 & 0 & 0 \\ 0 & 41.9 & 0 \\ 0 & 0 & 39.5 \end{bmatrix}$$

The injected current is related to the excitation function by the relation,

$$[I] = \frac{1}{2\pi\epsilon_o} [C] [\tau]$$

or

$$[I] = [M] [\tau]$$

$$[I] = \begin{bmatrix} 10.87 & -2.63 & -0.57 \\ -2.63 & 11.48 & -2.63 \\ -0.57 & -2.63 & 10.87 \end{bmatrix} \begin{bmatrix} 39.5 & 0 & 0 \\ 0 & 41.9 & 0 \\ 0 & 0 & 39.5 \end{bmatrix} \frac{1}{34.56}$$

$$[I] = \begin{bmatrix} 12.25 & -3.35 & -0.79 \\ -3.16 & 13.83 & -3.16 \\ -0.79 & -3.35 & 12.25 \end{bmatrix}$$

The modal components of the injected current is then obtained as,

$$[I_c] = [U]^{-1}\,[I]$$

Thus,

$$[I_c] = \begin{array}{c} \text{cond no.} \\ \\ \end{array} \begin{array}{ccc} 1 & 2 & 3 \\ \hline \end{array}$$

$$\left[\begin{array}{ccc} 4.11 & 5.38 & 4.11 \\ 9.22 & 0 & -9.22 \\ 7.66 & -13.59 & 7.66 \end{array}\right] \begin{array}{l} 1 \\ 2 \\ 3 \end{array} \quad \text{mode no.}$$

The modal components of the RI due to phase 1 alone are,

$$RI_1^{(1)} = (2\times\frac{2}{1000})^{-1/2} \times (3\times10^8)^{-1} \times \frac{1}{\pi\epsilon_o} \times \frac{1}{13} \times \frac{4.11}{[1+(\frac{12+30}{13})^2]}$$

or

$$RI_1^{(1)} = 1.66 \times \sqrt{1000}$$

$$RI_1^{(2)} = (\frac{2\times1.019}{1000})^{-1/2} \times (3\times10^8)^{-1} \times \frac{1}{\pi\epsilon_o} \times \frac{1}{13} \times \frac{9.22}{[1+(\frac{12+30}{13})^2}$$

or

$$RI_1^{(2)} = 5.21 \times \sqrt{1000}$$

and

$$RI_1^{(3)} = (\frac{2\times2}{1000})^{-1/2} \times (3\times10^8)^{-1} \times \frac{1}{\pi\epsilon_o} \times \frac{1}{13} \times \frac{7.66}{[1+(\frac{12+30}{13})^2]}$$

or

$$RI_1^{(3)} = 3.09 \times \sqrt{1000}$$

The net RI due to phase 1 alone is,

$$RI_1 = \sqrt{(RI_1^{(1)})^2 + (RI_1^{(2)})^2 + (RI_1^{(3)})^2}$$

or

$$RI_1 \text{ in dB} = 46.$$

Similarly,

$$RI_2^{(1)} = \left(\frac{2x2}{1000}\right)^{-1/2} x (3x10^8)^{-1} x \frac{1}{\pi \epsilon_o} x \frac{1}{13} x \frac{5.38}{[1+(\frac{30}{13})^2]}$$

$$= 3.93x\sqrt{1000}$$

$$RI_2^{(2)} = 0$$

$$RI_2^{(3)} = \left(\frac{2x2}{1000}\right)^{-1/2} x (3x10^8)^{-1} x \frac{1}{\pi \epsilon_o} x \frac{1}{13} x \frac{(-13.59)}{[1 + (\frac{30}{13})^2]}$$

$$= -9.92x\sqrt{1000}$$

The net RI due to phase 2 is,

$$RI_2 = 50.6 \text{ dB}.$$

Similarly,

$$RI_3^{(1)} = \left(\frac{2x2}{1000}\right)^{-1/2} x (3x10^8)^{-1} x \frac{1}{\pi \epsilon_o} x \frac{1}{13} x \frac{4.11}{[1+(\frac{18}{13})^2]}$$

$$RI_3^{(2)} = \left(\frac{2\times1.019}{1000}\right)^{-1/2}\times(3\times10^8)^{-1}\times\frac{1}{\pi\epsilon_o}\times\frac{1}{13}\times\frac{(-9.22)}{\left[1+\left(\frac{18}{13}\right)^2\right]}$$

$$RI_3^{(3)} = \left(\frac{2\times2}{1000}\right)^{-1/2}\times(3\times10^8)^{-1}\times\frac{1}{\pi\epsilon_o}\times\frac{1}{13}\times\frac{(7.66)}{\left[1+\left(\frac{18}{13}\right)^2\right]}$$

Thus, the net RI due to phase 3 is,

$$RI_3 = 57.8 \text{ dB}$$

The overall RI at the point G, due to phases 1,2 and 3 is 57.8 dB.

EE-1984-M-SEN-ANA.